

Thèse

pour obtenir le grade de

Docteur de l'Université de Grenoble

Spécialité : Matériaux, Mécanique, Génie civil, Électrochimie

Arrêté ministériel : 7 août 2006

et de

Dottore di Ricerca dell'Università di Roma "Tor Vergata"

XXIV ciclo del Dottorato di Ricerca in **Ingegneria delle Strutture e Geotecnica**

Coordinatore del corso: Prof. Ing. Franco MACERI

Présentée par **Fabrizio GEMELLI**

UNIVERSITÉ
FRANCO
ITALIENNE

Modélisation de l'endommagement pour les milieux poreux saturés: une approche multi-échelle

Thèse soutenue publiquement à **Grenoble** le **5 décembre 2012** devant le jury
composé de :

M. Luigi GAMBAROTTA

Président, Professeur, Università di Genova.

M. Djimédo KONDO

Rapporteur, Professeur, Université "Pierre et Marie Curie" Paris VI.

M^{me} Jolanta LEWANDOWSKA

Rapporteur, Professeur, Université Montpellier 2.

M. Elio SACCO

Examinateur, Professeur, Università di Cassino e del Lazio Meridionale.

M. Denis CAILLERIE

Directeur de thèse, Professeur, Grenoble Institut National Polytechnique.

M. Cristian DASCALU

Directeur de thèse, Professeur, Université "Pierre et Marie Curie" Paris VI.

M. Carlo CALLARI

Directeur de thèse, Professeur, Università del Molise.

Università di Roma



Thèse préparée au sein du

Laboratoire "Sols, Solides, Structures – Risques" (3S-R)

dans le cadre de l'**École Doctorale "Ingénierie - Matériaux, Mécanique, Environnement, Énergétique, Procédés, Production" (I-MEP2)**

et au sein du

Dipartimento d'Ingegneria Civile dans le cadre de la **Scuola di Dottorato dell'Università di Roma "Tor Vergata"**

Dissertation

submitted in partial fulfillment of the requirements for the degree of

Doctor of Philosophy of the University of Grenoble

Specialty: Materials, **Mechanics, Civil Engineering**, Electrochemistry

Ministerial decree: August 7th 2006

and of

Doctor of Philosophy of the University of Rome “Tor Vergata”

XXIV course of Philosophy Doctorate in **Structural and Geotechnical Engineering**

Course coordinator: Prof. Ing. Franco MACERI

by

Fabrizio GEMELLI

Damage modeling for saturated porous media: a multi-scale approach

Public defense in **Grenoble** on **December 5th 2012** in front of the Committee composed by:

Mr. Luigi GAMBAROTTA

President, Professor, Università di Genova.

Mr. Djimédo KONDO

Reviewer, Professor, Université “Pierre et Marie Curie” Paris VI.

Mrs. Jolanta LEWANDOWSKA

Reviewer, Professor, Université Montpellier 2.

Mr. Elio SACCO

Examinator, Professor, Università di Cassino e del Lazio Meridionale.

Mr. Denis CAILLERIE

Thesis Director, Professor, Grenoble Institut National Polytechnique.

Mr. Cristian DASCALU

Thesis Director, Professor, Université “Pierre et Marie Curie” Paris VI.

Mr. Carlo CALLARI

Thesis Director, Professor, Università del Molise.

Dissertation carried out at

Laboratoire “Sols, Solides, Structures – Risques” (3S-R)

within the framework of the **École Doctorale “Ingénierie - Matériaux, Mécanique, Environnement, Énergétique, Procédés, Production” (I-MEP2)**

and at

Dipartimento d’Ingegneria Civile within the framework of the **Scuola di Dottorato dell’Università di Roma “Tor Vergata”**

*I have no special talents.
I am only passionately curious.*

— Albert Einstein

Gutta cavat lapidem

— P. Ovidius Naso

A mia madre

Foreword

This PhD Thesis was developed in the framework of a joint PhD agreement reached between the University of Grenoble and the University of Rome “Tor Vergata”, and signed by the Presidents of the two establishments, the three Thesis Directors and myself.

According to such agreement, the work presented in this dissertation started in March 2009 and was carried out at the Laboratory 3S-R of Grenoble under the supervision of Professor Denis Caillerie and Professor Cristian Dascalu, and at the Department of Civil Engineering of Rome “Tor Vergata” where it was supervised by Professor Carlo Callari.

Furthermore, this agreement prescribes the present manuscript to be written in english and to embody both a short and an extended abstract in the official languages of the two establishments.

Lastly, in May 2009, this research project was declared to be a winner of the public contest “Vinci Program 2009 (Chapter II)” announced by the Franco-Italian University.

Grenoble, October 26th, 2012

Abstract

This work presents the constitutive modeling of a geomaterial consisting of a deformable and saturated porous matrix including a periodic distribution of evolving fluid-filled cavities. The homogenization method based on two-scale asymptotic developments is used in order to deduce a model able to describe the macroscopic hydro-mechanical coupling. By taking into account the cavity growth and without any phenomenological assumption, it is proposed a mesoscopic energy analysis coupled with the homogenization scheme which provides a damage evolution law. In this way, a direct link between the meso-structural fracture phenomena and the corresponding macroscopic damage is established.

Lastly, a numerical study of the local macroscopic hydro-mechanical damage behaviour is presented.

Keywords: homogenization; meso-fracture; damage; porous media; hydro-mechanical coupling.

Resumé

Le présent travail montre la modélisation constitutive d'un géomatériau composé d'une matrice poreuse saturée et déformable contenant une distribution périodique de fissures évolutives remplies de fluide. La méthode d'homogénéisation des développements asymptotiques est utilisée afin de déduire un modèle capable de décrire le couplage hydro-mécanique macroscopique.

Prenant en considération l'évolution de fissures et sans faire des hypothèses phénoménologiques, un'analyse énergétique mésoscopique couplé avec un schéma d'homogénéisation a été développée et elle fournit une loi d'évolution d'endommagement macroscopique. De cette façon, un lien direct entre les phénomènes de rupture de la structure mésoscopique et l'endommagement macroscopique correspondant est établie. Finalement, on présente une étude numérique du comportement macroscopique d'endommagement hydro-mécanique.

Mots clés: homogénéisation; méso-fissuration; endommagement; milieux poreux; couplage hydro-mécanique.

Sommario

In questa tesi si presenta la modellazione costitutiva di un geomateriale composto da una matrice porosa satura, deformabile e contenente una distribuzione periodica di cavità riempite da fluido che si propagano. Il metodo di omogeneizzazione basato sugli sviluppi asintotici a doppia scala viene utilizzato con l'obiettivo di dedurre un modello capace di descrivere l'accoppiamento idro-meccanico macroscopico.

Prendendo in considerazione la propagazione delle cavità e senza nessuna ipotesi fenomenologica, si propone un'analisi energetica mesoscopica accoppiata ad uno schema di omogeneizzazione che fornisce una legge di evoluzione del danno.

In questo modo, una relazione diretta tra i fenomeni di frattura meso-strutturali ed il corrispondente danno macroscopico viene stabilita. Infine, uno studio numerico del comportamento macroscopico locale di danno idro-meccanico viene presentato.

Parole chiave: omogeneizzazione; meso-frattura; danno; mezzi porosi; accoppiamento idro-meccanico.

Contents

Foreword	iii
Acknowledgements	vii
Notation	xv
General introduction	1
Objectives	1
Upscaling Techniques	2
Dissertation overview	3
1 From mesoscopic to macroscopic porosity	5
1.1 Introduction	5
1.2 Assumptions and nomenclature	6
1.3 Mesoscopic porosity	6
1.3.1 Definitions	6
1.3.2 Mesoscopic porosity rate	8
1.3.3 Small transformation framework	8
1.3.3.1 Expansion of the mesoscopic porosity	9
1.3.3.2 Expansion of the mesoscopic porosity rate	10
1.4 Macroscopic porosity	10
1.4.1 Definitions and symbols	10
1.4.2 Small transformation framework	12
1.4.2.1 Expansion of the macroscopic porosity	13
1.5 Conclusions	16
2 From mesoscale to macroscale	17
2.1 Introduction	17
2.2 Mesoscopic description	18
2.2.1 Linear momentum balance	19
2.2.2 Fluid mass balance	19
2.2.2.1 Eulerian description	19
2.2.2.2 Lagrangian description	20
2.2.2.3 Small transformation framework	21

2.2.3	Constitutive relations	23
2.2.3.1	Porous matrix	23
2.2.3.2	Cavities and cavity fluid	23
2.2.3.3	Variation of the mesoscopic porosities	24
2.2.4	Darcy's law	25
2.2.5	Conditions at cavity boundary	25
2.2.5.1	Stress continuity	25
2.2.5.2	Fluid pressure continuity	26
2.2.5.3	Fluid mass balance	27
2.2.6	Synopsis of mesoscopic description	27
2.3	Homogenization	28
2.3.1	Method of double-scale asymptotic expansions	28
2.3.2	Double-scale asymptotic expansions	29
2.3.3	Asymptotic expansions of the governing equations	31
2.3.3.1	Constitutive Relations	31
2.3.3.2	Linear momentum balance	32
2.3.3.3	Fluid mass balance	32
2.3.3.4	Darcy's law	33
2.3.3.5	Conditions at the cavity boundary	33
2.3.4	Unit cell problems	35
2.3.4.1	BVP for $\mathbf{u}^{pm(0)}$	35
2.3.4.2	36
2.3.4.3	BVP for $\mathbf{u}^{pm(1)}$	37
2.3.4.4	BVP for $p^{pm(1)}$, $\mathbf{v}^{pm(0)}$ and $\mathbf{v}^{cf(0)}$	39
2.3.5	Synopsis of asymptotic expansions	42
2.4	Macroscopic description	43
2.4.1	Linear momentum balance	43
2.4.2	Constitutive law	43
2.4.2.1	Homogenized coefficients.	44
2.4.3	Variation of macro-porosities	44
2.4.3.1	Homogenized coefficients.	45
2.4.3.2	Constitutive relations.	46
2.4.3.3	A proof	46
2.4.4	Fluid mass balance	47
2.4.5	Darcy's law	49
2.4.6	Synopsis of macroscopic description	50
2.5	Numerical solution of unit cell problems	51
2.6	Conclusions	54
3	Energy analysis and damage evolution law	55
3.1	Introduction	55
3.2	From micro- to meso-energy terms	56
3.2.1	Strain energy	56
3.2.2	Dissipation in the pore fluid	59

3.3	Global energy analysis at the mesoscale	61
3.3.1	Weak formulation of linear momentum balance	62
3.3.2	Weak formulation of fluid mass balance	62
3.3.3	Weak formulation of cavity fluid incompressibility	63
3.3.4	Energy rate balance	63
3.3.4.1	Stationary cavities	63
3.3.4.2	Evolving cavities and fracture energy release rate	65
3.3.5	Modeling of cavity propagation	66
3.3.6	Fracture criteria	66
3.4	Cell energy analysis at the mesoscale	68
3.4.1	From meso- to macro-energy terms	68
3.4.1.1	Strain energy	68
3.4.1.2	Dissipation in the fluid	69
3.4.2	Energy rate balance	70
3.4.2.1	Stationary cavity	71
3.4.2.2	Evolving cavity	72
3.4.2.3	Damage energy release rate	73
3.4.2.4	Approximation due to small thickness of the cavity	74
3.4.2.5	Asymptotic expansion of the fracture energy release rate	74
3.4.3	Modeling of cavity propagation	75
3.5	Damage laws	76
3.6	Conclusions	77
4	Numerical study of macroscopic local behaviour	79
4.1	Employed poroelastic damage model	79
4.2	Homogenized parameters and their derivatives	80
4.3	Incremental resolution algorithm	80
4.4	Numerical examples	81
5	Conclusions and perspectives	93
5.1	General conclusions	93
5.2	Perspectives	94
A	Porosity rate and volumetric strain	97
B	From microscale to mesoscale	101
C	Useful Taylor developments	105
D	Reynolds transport theorem	109
	Bibliography	111

List of Figures

1	Macroscopic, mesoscopic and microscopic scales of observation and corresponding periodic distributions of fluid-filled mesoscopic cavities and microscopic pores. . .	1
1.1	Macroscopic body, mesoscopic and microscopic REV. The double-scale heterogeneities are empty and randomly distributed. The condition of separation of scales is satisfied: $L \gg l_\varepsilon \gg l_e$	5
1.2	Mesoscopic structure of the body and microscopic REV.	6
1.3	Macroscopic body and mesoscopic REV.	11
2.1	At the macroscopic observation scale the body Ω appears as a continuum. The mesoscopic REV \mathcal{B} shows the fluid-filled cavities surrounded by the porous matrix and its size is much smaller than the characteristic dimension of Ω , that is, $L \gg l_\varepsilon$. . .	17
2.2	Mesoscopic structure of the whole body Ω : the porous matrix Ω^{pm} with the set Ω^{cf} of fluid-filled cavities. \mathcal{N}^{pm} is a generic subset volume of Ω^{pm} , while \mathcal{M} is a subset volume of Ω which intersects a single cavity.	18
2.3	The volume subset \mathcal{M} of Ω^{pm} contains a portion of a fluid-filled cavity.	26
2.4	The macroscopic continuum and its locally periodic mesoscopic structure.	28
2.5	Resizing the mesoscopic periodic cell $\mathcal{B}_\varepsilon = [0, \varepsilon] \times [0, \varepsilon]$ to the unit cell, $Y = [0, 1] \times [0, 1]$	29
2.6	Physical meaning of the asymptotic expansions of the displacement field $\mathbf{u}^{pm(\varepsilon)}$. . .	30
2.7	Notation in the periodic unit cell Y . Orientation of the unit normal vector \mathbf{n} : outward with respect to Y^{pm}	35
2.8	Numerical solution of unit cell problems: unstructured mesh (left), plots of the deformed configuration and of the norm of $\boldsymbol{\xi}^{22}$ (center) and $\boldsymbol{\xi}^{12}$ (right).	51
2.9	Terms of the homogenized elasticity tensor appearing in constitutive equation (2.175) as a function of cavity length.	52
2.10	Terms of the homogenized Biot's tensors appearing in constitutive equations (2.175, 2.179) as a function of cavity length	53
2.11	Homogenized storage modulus S appearing in constitutive equations (2.179) as a function of cavity length d	53
3.1	Geometrical assumption about the propagation of the mesoscopic fluid-filled cavity. Periodic cell \mathcal{B}_ε with cavity length l . Resized unit cell Y with cavity length d	55

3.2	Mesoscopic and microscopic periodic structures. \mathcal{B}_ε and \mathcal{B}_e are the periodic cells, their sizes are such that: $\varepsilon \gg e$. Rescaling of \mathcal{B}_ε in $Y = Y^{pm} \cup Y^{cf}$, and of \mathcal{B}_e in $Z = Z^s \cup Z^{pf}$	57
3.3	The body Ω with its mesoscopic and locally periodic structure. The unit vector \mathbf{n} is the outward normal of the porous matrix Ω^{pm} and it is denoted as \mathbf{n}_α on the boundary of the α th cavity.	61
3.4	Nomenclature in the α th periodic cell: ∂c_α^{fr} is the set of the two cavity fronts; \mathbf{n}_α is the inward normal unit vector to the cavity boundary; \mathbf{m}_α is the unit vector in the direction of the propagation.	65
3.5	Nomenclature in the α th periodic cell and in the corresponding unit cell.	68
3.6	Nomenclature in the α th periodic cell and in the corresponding unit cell.	75
4.1	Orientation of the axes 1 and 2 in the periodic unit cell Y	82
4.2	Quasi-brittle damage (Test 1): stress Σ_{22} (top) and damage variable d (bottom) versus the imposed macroscopic pressure P and for different values of imposed constant strain: $E_{x22} = 0.0000$ (magenta), $E_{x22} = 0.0010$ (black), $E_{x22} = 0.0025$ (red), $E_{x22} = 0.0050$ (blue) and $E_{x22} = 0.0075$ (green).	84
4.3	Brittle damage (Test 1): stress Σ_{22} (top) and damage variable d (bottom) as functions of imposed macroscopic pressure P and for different values of imposed constant strain: $E_{x22} = 0.0000$ (magenta), $E_{x22} = 0.0001$ (black), $E_{x22} = 0.0002$ (red), $E_{x22} = 0.0003$ (blue).	85
4.4	Brittle damage (Test 1): stress Σ_{22} (top) and damage variable d (bottom) as functions of imposed macroscopic pressure P and for different values of constant fracture energy: $\mathcal{G}_c = 400 J/m^2$ (magenta), $\mathcal{G}_c = 200 J/m^2$ (black), $\mathcal{G}_c = 100 J/m^2$ (red), $\mathcal{G}_c = 50 J/m^2$ (blue) and $\mathcal{G}_c = 10 J/m^2$ (green).	86
4.5	Quasi-brittle damage (Test 2): stress Σ_{22} (top) and damage variable d (bottom) as functions of imposed macroscopic strain E_{x22} and for different values of constant pressure: $P = 0.0$ MPa (magenta), $P = 1$ MPa (black), $P = 2.5$ MPa (red), $P = 5$ MPa (blue) and $P = 7.5$ MPa (green).	87
4.6	Brittle damage (Test 2): stress Σ_{22} (top) and damage variable d (bottom) as functions of imposed macroscopic strain E_{x22} and for different values of constant pressure: $P = 0.0$ MPa (magenta), $P = 0.1$ MPa (black), $P = 0.3$ MPa (red) and $P = 0.5$ MPa (blue).	88
4.7	Quasi-brittle damage (Test 2): stress Σ_{22} (top) and damage variable d (bottom) as functions of imposed macroscopic strain E_{x22} and for different values of constant fracture energy: $\mathcal{G}_c = 400 J/m^2$ (magenta), $\mathcal{G}_c = 200 J/m^2$ (black), $\mathcal{G}_c = 100 J/m^2$ (red), $\mathcal{G}_c = 50 J/m^2$ (blue) and $\mathcal{G}_c = 10 J/m^2$ (green).	89
4.8	Quasi-brittle damage (Test 2): stress Σ_{22} (top) and damage variable d (bottom) as functions of imposed macroscopic strain E_{x22} and for different values of the size of fracture process zone: $c_f = 1.0 \cdot 10^{-3}$ m (green), $c_f = 0.8 \cdot 10^{-3}$ m (blue), $c_f = 0.6 \cdot 10^{-3}$ m (red), $c_f = 0.4 \cdot 10^{-3}$ m (black), $c_f = 0.2 \cdot 10^{-3}$ m (magenta) . . .	90

4.9	Quasi-brittle damage (Test 2): porosity variation Φ_u (top) and damage variable d (bottom) as functions of imposed macroscopic strain E_{x22} and for different values of constant pressure: $P = 0.0$ MPa (magenta), $P = 1$ MPa (black), $P = 2.5$ MPa (red), $P = 5$ MPa (blue) and $P = 7.5$ MPa (green).	91
B.1	Mesosopic and microscopic scales of observation. Condition of scale separation satisfied: $l_\varepsilon \gg l_e$. Random distributions of saturated microscopic pores.	101
B.2	Periodic distributions of saturated microscopic pores. Periodic cell \mathcal{B}_e of size e	102
B.3	Microscopic periodic cell \mathcal{B}_e and corresponding resized unit cell Z	103

Notation

In this dissertation, the analytical developments follow the notation employed by Caillerie (2011) and described below.

Let \mathcal{E} be a three-dimensional Euclidean space, and let \mathcal{V} be the associated vector space. Let $\mathcal{L}(\mathcal{V})$ denote the set of all the linear transformations of \mathcal{V} into itself, that is, the space of all second-order tensors.

The inner product between two elements $\mathbf{a}, \mathbf{b} \in \mathcal{V}$ is denoted by $\mathbf{a} \cdot \mathbf{b}$.

Let $\mathbf{A} \otimes \mathbf{a} = A_{ij}a_j$ be the image of the vector \mathbf{a} by means of the linear transformation \mathbf{A} . The transpose of $\mathbf{A} \in \mathcal{L}(\mathcal{V})$ is a linear transformation as well and it is denoted by \mathbf{A}^t ; its definition $\forall \mathbf{a}, \mathbf{b} \in \mathcal{V}$ reads:

$$(\mathbf{A} \otimes \mathbf{a}) \cdot \mathbf{b} = (\mathbf{A}^t \otimes \mathbf{b}) \cdot \mathbf{a} \quad (A_{ij}a_j)b_i = (A_{ji}b_i)a_j$$

The composition of two elements $\mathbf{A}, \mathbf{B} \in \mathcal{L}(\mathcal{V})$ is denoted by $\mathbf{A} \circ \mathbf{B} = A_{ik}B_{kj}$ and defined as follows $\forall \mathbf{a} \in \mathcal{V}$:

$$(\mathbf{A} \circ \mathbf{B}) \otimes \mathbf{a} = \mathbf{A} \otimes (\mathbf{B} \otimes \mathbf{a}) \quad (A_{ik}B_{kj})a_j = A_{ik}(B_{kj}a_j)$$

The symmetric and anti-symmetric parts of $\mathbf{A} \in \mathcal{L}(\mathcal{V})$ are denoted by \mathbf{A}^S and \mathbf{A}^A respectively; their definitions read:

$$\mathbf{A}^S := \frac{1}{2}(\mathbf{A} + \mathbf{A}^t), \quad \mathbf{A}^A := \frac{1}{2}(\mathbf{A} - \mathbf{A}^t) \quad A_{ij}^S := \frac{1}{2}(A_{ij} + A_{ji}), \quad A_{ij}^A := \frac{1}{2}(A_{ij} - A_{ji})$$

A linear transformation \mathbf{A} is symmetric if $\mathbf{A} = \mathbf{A}^t$, that is if $\mathbf{A}^A = 0$. On the contrary, \mathbf{A} is anti-symmetric if $\mathbf{A} = -\mathbf{A}^t$, that is if $\mathbf{A}^S = 0$.

Let $\mathcal{L}(\mathcal{V})$ be endowed with a Euclidean structure by defining the inner product $\mathbf{A} : \mathbf{B}$ as follows:

$$\mathbf{A} : \mathbf{B} := \text{tr}(\mathbf{A} \circ \mathbf{B}^t) \quad A_{ij}B_{ij} := \text{tr}(A_{ik}B_{kj}) = A_{ik}B_{kj}\delta_{ij}$$

where the trace of a linear transformation \mathbf{A} is denoted by $\text{tr}\mathbf{A}$ and its definition reads:

$$\text{tr}(\mathbf{A}) := \mathbf{A} : \mathbf{I} = A_{ij}\delta_{ij}$$

with \mathbf{I} denoting the identity of \mathcal{V} , that is, \mathbf{I} satisfies the equality $\mathbf{I} \otimes \mathbf{a} = \mathbf{a}$.

It is easily proved that the inner product between a symmetric linear transformation \mathbf{A} and an anti-symmetric one \mathbf{B} is equal to zero: $\mathbf{A} : \mathbf{B} = 0$

The tensor product of two elements $\mathbf{a}, \mathbf{b} \in \mathcal{V}$ is an element of $\mathcal{L}(\mathcal{V})$ denoted by $\mathbf{a} \otimes \mathbf{b}$ and defined as follows $\forall \mathbf{x} \in \mathcal{V}$:

$$(\mathbf{a} \otimes \mathbf{b}) @ \mathbf{x} = (\mathbf{b} . \mathbf{x}) \mathbf{a} \qquad (\mathbf{a} \otimes \mathbf{b})_{ij} x_j = (b_j x_j) a_i = (a_i b_j) x_j$$

General introduction

Objectives

In this work, the macroscopic behaviour of a geomaterial consisting of a saturated and deformable porous matrix with a (quasi-)periodic distribution of fluid-filled cavities is investigated.

The first objective is to deduce, by means of a upscaling technique, the description of a macroscopic continuous medium which is equivalent to the finely heterogenous medium of the smaller scale. It is worth precising that the chosen upscaling technique is the method of homogenization based on the double-scale asymptotic developments (Bensoussan, Lions and Papanicolaou 1978; Sanchez-Palencia 1974, 1980), and that the observation scales of interest are three (fig. 1): the microscopic or pore scale, the mesoscopic or cavity scale and the macroscopic scale. Despite that, the upscaling is performed only between the mesoscopic scale and the macroscopic one: in fact, the porous matrix is already considered as a continuum by means of the classic poroelastic model proposed by Biot (1941). The interest in the microscopic scale is due, firstly, to the choice to make some minor modifications to the mesoscopic description of the porous matrix provided in the work by Auriault and Sanchez-Palencia (1977) where the Biot's model is reobtained by means of asymptotic homogenization, and then also to understand the physical meaning of some energy terms appearing in the energy balance at larger scales.

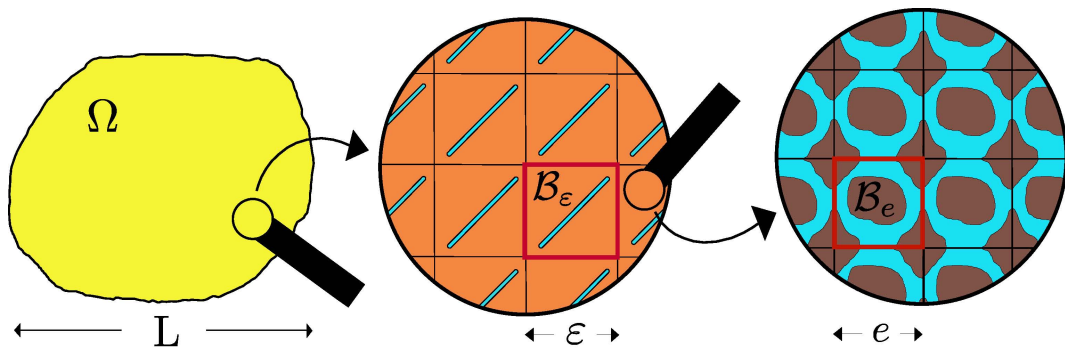


Figure 1: Macroscopic, mesoscopic and microscopic scales of observation and corresponding periodic distributions of fluid-filled mesoscopic cavities and microscopic pores.

The second objective is to enrich the macroscopic description, previously obtained, by taking into account the damage evolution, that is, by considering that the mesoscopic cavities may propagate. In order to model the hydro-mechanical damage, a mesoscopic energy analysis coupled with the homogenization scheme is performed and a damage evolution law is obtained. The main advantage of this approach is that the modeling does not require any phenomenological assumption.

The final objective is the understanding of how, according to the damage evolution law previously deduced, the fluid pressure influences the damage evolution. With such an aim, a numerical time-integration analysis of the local macroscopic hydro-mechanical damage behaviour is performed.

Upscaling Techniques

In the modeling of heterogeneous media, a description which takes into account every single heterogeneity would yield to intractable boundary value problems and to extremely expensive computations. Then, it is necessary to deduce a overall behaviour which is valid at a very large scale with respect to the heterogeneity scale. There are mainly two ways of deriving this macroscopic description:

- i. The phenomenological approach which is a directly macroscopic technique and it is often associated with experiments. For instance, the Biot's constitutive equations have been derived in this way (Biot 1941).
- ii. The upscaling techniques which are continuous approaches and require the description at the heterogeneity scale only over a representative elementary volume (REV).

In this thesis work, the second approach is adopted.

Therefore, the definition and the existence of the REV are issues which deserve a special attention. For what concerns the choice of the REV size, even if it is a subject of various discussions (see for instance Dormieux, Kondo and Ulm (2006b)), it can be said that the REV is a volume subdomain that needs to be small with respect to the macroscopic structure, but it also needs to be able to consider enough heterogeneities. Then, it is fundamental to ensure its existence by imposing the condition of separation between the length scales which characterize the heterogeneities. With referring to the object studied in this work (fig. 1), the separation condition reads:

$$L \gg \varepsilon \gg e \quad (1)$$

where L is the characteristic dimension of the whole body, while e and ε are the characteristic lengths of the microscopic and mesoscopic scale respectively. And it is worth remarking that, even if the form of this condition intuitively calls up only a geometrical

meaning, this fundamental condition has to be satisfied also in terms of the physical process as explained in Auriault (2002).

Different upscaling techniques are available for both random and periodic heterogeneous media, and most analytical or semi-analytical homogenization methods are based on the computation of the homogenized (effective) coefficients using various methods shortly summarized below:

- based on averaging theory. This is the simplest homogenization method and consists of the computation of global properties of a heterogeneous material using the averaging technique on each composant weighted by its volume. This method is used and/or enriched by different researchers, such as Eshelby (1957) or Mori and Tanaka (1973).
- “self-consistent” method developed by Hill (1965) or Christensen and Lo (1979). In this case, global properties of the material are obtained by analytical solving of a boundary value problem on a micro-structure composed of a first phase of constituting the matrix and a second phase of a spherical or ellipsoidal inclusion. This homogenization technique works very well in the case of linear problems, but much more difficult in non-linear cases, even if interesting results were obtained by Guery (2007) using an elasto-plastic damage model on Callovo-Oxfordian argillites, or, in more general works like Deudé, Dormieux, Kondo and Maghous (2002); Dormieux and Kondo (2005); Dormieux, Kondo and Ulm (2006b);
- asymptotic developments based method of displacement and stress fields with respect to a natural material length defined as the ratio between heterogeneities length and macroscopic characteristic length (Bakhvalov and Panasenko 1989; Bensoussan, Lions and Papanicolaou 1978; Sanchez-Palencia 1980).

In this thesis work, the homogenization method based on double-scale asymptotic expansion is used for upscaling the mesoscopic structure.

Besides analytical homogenization methods, one can find also numerical improvements (Geers, Kouznetsova and Brekelmans 2001; Guedes and Kikuchi 1990; S. Lee and Moorthy 1995; Terada and Kikuchi 1995). The weak point of a purely numerical homogenization technique is the computational time. Indeed, in this process, for each time increment, in each macroscopic integration (Gauss) point, a full computation on the micro-structure is necessary.

Dissertation overview

An outline of this thesis is as follows.

Chapter 1: Mesoscopic and macroscopic porosity. Both in the framework of large and small deformations, and with the aim of determining the expressions of the porosity variation induced by the motion of the solid-skeleton, both the porosities at the different observation scales and in Lagrangian and Eulerian descriptions are studied.

Chapter 2: From the mesoscopic scale to the macroscopic scale. In this chapter, the starting scale of observation is the mesoscopic one. It means that the heterogeneous microscopic structure, composed by a solid-skeleton within a network of fluid-saturated pores, is here replaced by a porous and deformable saturated solid.

Notwithstanding that, because of the set of mesoscopic fluid-filled cavities included in the porous matrix, the medium here investigated is still heterogeneous. Then, a further equivalent and macroscopic continuum is required in order to have governing equations and hydro-mechanical properties defined in every single point of the whole body.

The targeted macroscopic description is searched by applying the method of the asymptotic homogenization to the mesoscopic description. The main developments of the analytical calculus which leads to the homogenized equations and also provides the effective poroelastic coefficients are presented.

Lastly, in order to evaluate numerically the homogenized coefficients, the solutions of some boundary value problems defined in the periodic cell are required and they are obtained by means of the FEM software Comsol Multiphysics. Then, the numerical values of the homogenized coefficients is obtained by evaluating the integrals appearing in their definitions. Even if the problems are quasi-static, this procedure is repeated for several values of the cavity length and, by polynomial interpolation of the sampling points, continuous functions are obtained.

Chapter 3: Energy analysis and damage evolution law. The mesoscopic energy analysis is the tool which provides the macroscopic damage evolution law. Actually, both a global and a cell energy analysis are performed at the mesoscopic scale. From the first one the energy release rate is identified. Moreover, a cell energy analysis is developed also at the microscopic scale in order to interpret properly some energetic terms at the larger scales.

Chapter 4: Numerical study of the macroscopic local behaviour. The hydro-mechanical damage model presented in the previous chapters is here exploited from a numerical point of view in order to investigate his constitutive behaviour in a single Gauss point. The objective is to understand how the fluid pressure influences the damage evolution.

Lastly, conclusions and perspectives are reported in the final chapter.

Chapter 1

From mesoscopic to macroscopic porosity

1.1 Introduction

In this chapter, both in the framework of large and small deformations, and with the aim of determining the expressions of the porosity variations induced by the motion of the solid-skeleton, the porosities at the two observation scales and their rates are studied. Furthermore, following Coussy (2004), both the Eulerian and the Lagrangian porosities are defined and then investigated in order to determine their mutual relations and their induced variation rates.

All the relations here presented are useful in the following chapters.

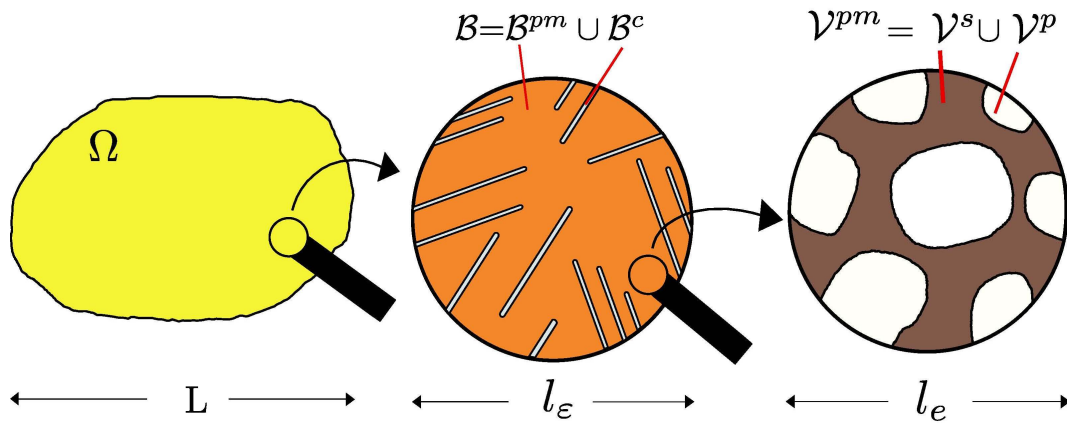


Figure 1.1: Macroscopic body, mesoscopic and microscopic REV. The double-scale heterogeneities are empty and randomly distributed. The condition of separation of scales is satisfied: $L \gg l_\epsilon \gg l_e$.

1.2 Assumptions and nomenclature

In this chapter, the attention is focused on the geometry, then the whole body Ω , that is the porous solid with the cavities, is considered to be dry: in fact, both the microscopic pores and the mesoscopic cavities are assumed to be empty (Fig. 1.1). In terms of nomenclature, it implies that the superscripts p and c , standing for empty pores and empty cavities respectively, are here used. On the contrary, in all the following chapters, it is assumed that the pores are fluid-saturated and the cavities are fluid-filled; then, the superscripts pf and cf will replace the corresponding ones.

Moreover, let the subscript r denote the reference configuration; while the subscript t denotes the current configuration but, in order to simplify the notation, it will be omitted as much as possible.

Lastly, in this chapter, the distributions of the two-scales heterogeneities are assumed to be random (Fig. 1.1). On the contrary, the relations here presented hold for both random and periodic heterogeneous media.

1.3 Mesoscopic porosity

1.3.1 Definitions

At the microscopic observation level and in the reference configuration, the porous domain Ω_r^{pm} is the union of two disjoint subdomains: the solid phase subdomain, denoted by Ω_r^s , and the set of empty pores, denoted by Ω_r^p , that is, $\Omega_r^{pm} = \Omega_r^s \cup \Omega_r^p$ and $\emptyset = \Omega_r^s \cap \Omega_r^p$.

The microscopic displacement field \mathbf{u}^s of the solid phase is prolonged by continuity to the empty pores, that is, this field is assumed to be continuous at the interface between the solid phase and the void.

Then, being \mathbf{u}^s defined in Ω_r^{pm} , for the corresponding deformation function φ^s it reads:

$$\mathbf{X} \in \Omega_r^{pm} \rightarrow \mathbf{x} = \varphi^s(\mathbf{X}, t) = \mathbf{X} + \mathbf{u}^s(\mathbf{X}, t) \quad (1.1)$$

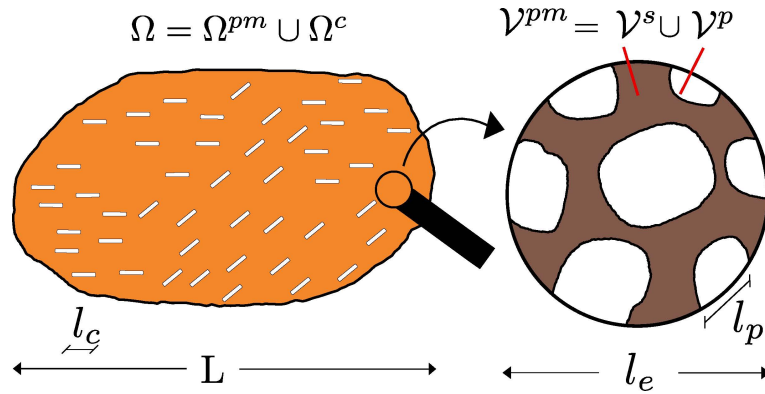


Figure 1.2: Mesoscopic structure of the body and microscopic REV.

where \mathbf{X} and \mathbf{x} are the material particle positions in the reference and in the current configuration respectively.

Let \mathcal{V}_r^{pm} denote the representative elementary volume (REV) of the porous matrix around the point $\mathbf{X} \in \Omega_r^{pm}$, that is, the microscopic REV. It is a special subset of the porous matrix domain and his size l_e is such that only the heterogeneities of the microscopic scale are visible (Fig. 1.2):

$$l_p < l_e \ll l_c \quad (1.2)$$

with l_p and l_c being the characteristic dimensions of the microscopic pores and of the mesoscopic cavities respectively. Let the disjoint subdomains \mathcal{V}_r^s and \mathcal{V}_r^p be the solid phase domain and the empty pores domain included in the microscopic REV respectively, that is $\mathcal{V}_r^{pm} = \mathcal{V}_r^s \cup \mathcal{V}_r^p$ and $\emptyset = \mathcal{V}_r^s \cap \mathcal{V}_r^p$. Then, the corresponding quantities in the current configuration read:

$$\mathcal{V}^s := \varphi^s(\mathcal{V}_r^s, t) \quad (1.3a)$$

$$\mathcal{V}^p := \varphi^s(\mathcal{V}_r^p, t) \quad (1.3b)$$

$$\mathcal{V}^{pm} := \varphi^s(\mathcal{V}_r^{pm}, t) \quad (1.3c)$$

Moreover, in the following the measures of the volume subdomains \mathcal{V}^{pm} , \mathcal{V}^s and \mathcal{V}^p will be denoted by V^{pm} , V^s and V^p respectively.

Following Coussy (2004), let ϕ denote the Lagrangian mesoscopic porosity which, at the time t and around the material point $\mathbf{x} \in \mathcal{V}^{pm}$, is defined as the ratio between the current volume of the pores V^p and the initial total volume V_r^{pm} :

$$\phi := \frac{V^p}{V_r^{pm}} = \frac{V^{pm} - V^s}{V_r^{pm}} \quad (1.4)$$

Let η denote the Eulerian mesoscopic porosity which, at the time t and around the material point $\mathbf{x} \in \mathcal{V}^{pm}$, is defined as the ratio between the current volume of the pores V^p and the current total volume V^{pm} :

$$\eta := \frac{V^p}{V^{pm}} = 1 - \frac{V^s}{V^{pm}} \quad (1.5)$$

Let \mathbf{F}^s and J^s be the gradient and the Jacobian of the deformation function φ^s respectively; their definitions read:

$$\mathbf{F}^s := \nabla_X \varphi^s \quad J^s := \det \mathbf{F}^s \quad (1.6)$$

The measures V^α are evaluated through simple integrals:

$$V^\alpha = \int_{\mathcal{V}^\alpha} dv_x \quad \text{with } \alpha = pm, s \quad (1.7)$$

which, by using the change of variables $\mathbf{X} \leftrightarrow \mathbf{x} = \varphi^s(\mathbf{X}, t)$, become:

$$V^\alpha = \int_{\mathcal{V}_r^\alpha} J^s dV_X \quad \text{with } \alpha = pm, s \quad (1.8)$$

Then, the relation (1.5) is rewritten as follows:

$$\eta = 1 - \frac{\int_{\mathcal{V}_r^s} J^s dV_X}{\int_{\mathcal{V}_r^{pm}} J^s dV_X} \quad (1.9)$$

1.3.2 Mesoscopic porosity rate

From the definition (1.5) of the Eulerian mesoscopic porosity, it follows also that:

$$V^s = (1 - \eta) V^{pm} \quad (1.10)$$

the material time derivative of which reads:

$$\dot{V}^s = (1 - \eta) \dot{V}^{pm} - \dot{\eta} V^{pm} \quad (1.11)$$

or equivalently:

$$\dot{\eta} = (1 - \eta) \left(\frac{\dot{V}^{pm}}{V^{pm}} - \frac{\dot{V}^s}{V^s} \right) \quad (1.12)$$

By using the relation (1.8) and the Taylor's development (C.16), the time derivative of V^α with respect to the motion of the solid phase reads:

$$\dot{V}^\alpha = \int_{\mathcal{V}_r^\alpha} \text{tr}(\dot{\mathbf{F}}^s \circ (\mathbf{F}^s)^{-1}) J^s dV_X \quad \text{with } \alpha = pm, s \quad (1.13)$$

where the symbol “ \circ ” denotes the composition of linear transformations, as shown in the initial pages dedicated to the notation. So, the Eulerian mesoscopic porosity rate $\dot{\eta}$ is rewritten as follows:

$$\dot{\eta} = (1 - \eta) \left(\frac{1}{V^{pm}} \int_{\mathcal{V}_r^{pm}} \text{tr}(\dot{\mathbf{F}}^s \circ (\mathbf{F}^s)^{-1}) J^s dV_X - \frac{1}{V^s} \int_{\mathcal{V}_r^s} \text{tr}(\dot{\mathbf{F}}^s \circ (\mathbf{F}^s)^{-1}) J^s dV_X \right) \quad (1.14)$$

1.3.3 Small transformation framework

Being \mathbf{u}^s the displacement field of the solid phase extended by continuity to the microscopic pores, it reads:

$$\mathbf{u}^s(\mathbf{X}, t) = \boldsymbol{\varphi}^s(\mathbf{X}, t) - \mathbf{X} \quad (1.15)$$

Then, the gradient \mathbf{F}^s of the deformation function $\boldsymbol{\varphi}^s$ reads:

$$\mathbf{F}^s = \mathbb{I} + \nabla_X \mathbf{u}^s \quad (1.16)$$

In the framework of the small transformations approximation, the inverse of the gradient of the deformation function is expanded by using the Taylor's development (C.19) and it reads:

$$(\mathbf{F}^s)^{-1} = \mathbb{I} - \nabla_X \mathbf{u}^s + \dots \quad (1.17)$$

In the same way, by using the Taylor's development (C.11), the Jacobian J^s of the transformation reads:

$$J^s = \det(\mathbb{I} + \nabla_X \mathbf{u}^s) = 1 + \text{tr}(\nabla_X \mathbf{u}^s) + \dots = 1 + \text{div}_X \mathbf{u}^s + \dots \quad (1.18)$$

1.3.3.1 Expansion of the mesoscopic porosity

By using the expansion (1.18) of J^s , the expression (1.8) of V^α is expanded as follows:

$$V^\alpha = \int_{\mathcal{V}_r^\alpha} J^s dV_X = \int_{\mathcal{V}_r^\alpha} (1 + \text{div}_X \mathbf{u}^s + \dots) dV_X \quad \text{with } \alpha = pm, s \quad (1.19)$$

which, by regrouping, becomes:

$$V^\alpha = V_r^\alpha \left(1 + \frac{1}{V_r^\alpha} \int_{\mathcal{V}_r^\alpha} \text{div}_X \mathbf{u}^s dV_X + \dots \right) \quad \text{with } \alpha = pm, s \quad (1.20)$$

By using the expansions above, definition(1.5) of the Eulerian mesoscopic porosity η is expanded as well by means of the Taylor's development (C.6) and it reads:

$$\begin{aligned} \eta &= 1 - \frac{V_r^s}{V_r^{pm}} \left(1 + \frac{1}{V_r^s} \int_{\mathcal{V}_r^s} \text{div}_X \mathbf{u}^s dV_X + \dots \right) \left(1 - \frac{1}{V_r^{pm}} \int_{\mathcal{V}_r^{pm}} \text{div}_X \mathbf{u}^s dV_X + \dots \right) \\ &= 1 - \frac{V_r^s}{V_r^{pm}} \left(1 + \frac{1}{V_r^s} \int_{\mathcal{V}_r^s} \text{div}_X \mathbf{u}^s dV_X - \frac{1}{V_r^{pm}} \int_{\mathcal{V}_r^{pm}} \text{div}_X \mathbf{u}^s dV_X + \dots \right) \end{aligned} \quad (1.21)$$

or it can be rewritten in a more compact form as follows:

$$\eta = \eta_r + \eta_u \quad (1.22)$$

where η_r denotes the Eulerian mesoscopic porosity in the reference configuration and η_u denotes the variation of the Eulerian mesoscopic porosity induced by the motion of the solid-skeleton:

$$\eta_r = \frac{V_r^p}{V_r^{pm}} = 1 - \frac{V_r^s}{V_r^{pm}} \quad (1.23a)$$

$$\eta_u = (1 - \eta_r) \left(\frac{1}{V_r^{pm}} \int_{\mathcal{V}_r^{pm}} \text{div}_X \mathbf{u}^s dV_X - \frac{1}{V_r^s} \int_{\mathcal{V}_r^s} \text{div}_X \mathbf{u}^s dV_X \right) \quad (1.23b)$$

Therefore, in this approximated framework, the mesoscopic porosity η of the deformed porous matrix is described as the sum of two terms written in the reference configuration. But, whereas η_r is a data of the problem, η_u is an unknown which depends on the displacements. It is worth remarking that the smallness of the displacement gradients implies the smallness of η_u with respect to η_r .

1.3.3.2 Expansion of the mesoscopic porosity rate

From the definitions (1.15) of the displacement field \mathbf{u}^s and (1.6) of the gradient of the deformation function \mathbf{F}^s , it follows that:

$$\dot{\mathbf{u}}^s(\mathbf{X}, t) = \dot{\boldsymbol{\varphi}}^s(\mathbf{X}, t) \implies \dot{\mathbf{F}}^s = \nabla_X \dot{\mathbf{u}}^s \quad (1.24)$$

Given the expansions (1.17) of \mathbf{F}^{s-1} and (1.18) of the Jacobian of the deformation function J^s , it reads:

$$\text{tr}(\dot{\mathbf{F}}^s \circ \mathbf{F}^{s-1}) J^s = \text{tr}(\nabla_X \dot{\mathbf{u}}^s \circ (\mathbb{I} - \nabla_X \mathbf{u}^s + \dots)) (1 + \text{div}_X \mathbf{u}^s + \dots) = \text{div}_X \dot{\mathbf{u}}^s + \dots \quad (1.25)$$

Therefore, the expansion (1.14) of the Eulerian mesoscopic porosity rate $\dot{\eta}$ becomes:

$$\dot{\eta} = (1 - \eta_r) \left(\frac{1}{V_r^{pm}} \int_{\mathcal{V}_r^{pm}} \text{div}_X \dot{\mathbf{u}}^s dV_X - \frac{1}{V_r^s} \int_{\mathcal{V}_r^s} \text{div}_X \dot{\mathbf{u}}^s dV_X + \dots \right) \quad (1.26)$$

which corresponds exactly to the relation (A.19) provided in Callari and Abati (2011) and which could have been obtained directly by deriving the expansion (1.22) of the Eulerian mesoscopic porosity η .

Remark 1.3.1. *In this approximated framework, given the expressions (1.23, 1.22) about the Eulerian mesoscopic porosity, it is apparent that η is of order zero in terms of the displacement \mathbf{u}^s . While, the expression (1.26) makes clear that $\dot{\eta}$ is of order one. In reason of the assumed smallness of \mathbf{u}^s , the material time derivative can be approximated by the partial time derivative:*

$$\dot{\eta} = \partial_t \eta + \nabla_x \eta \cdot \dot{\mathbf{u}}^s = \partial_t \eta + \dots \quad (1.27)$$

Moreover, given the decomposition (1.22) of the Eulerian mesoscopic porosity η and being η_r a constant, it follows that:

$$\dot{\eta} = \dot{\eta}_u \quad (1.28)$$

1.4 Macroscopic porosity

1.4.1 Definitions and symbols

At the mesoscopic observation level and in the reference configuration, the whole body Ω_r is the union of two disjoint subdomains: the porous matrix subdomain Ω_r^{pm} and the set of empty cavities Ω_r^c , that is, $\Omega_r = \Omega_r^{pm} \cup \Omega_r^c$ and $\emptyset = \Omega_r^{pm} \cap \Omega_r^c$.

The mesoscopic displacement field \mathbf{u}^{pm} of the porous matrix is prolonged by continuity to the empty cavities, that is, this field is assumed to be continuous at the interface between the porous matrix and the void.

Then, being \mathbf{u}^{pm} defined in Ω_r , for the corresponding deformation function $\boldsymbol{\varphi}^{pm}$ it reads:

$$\mathbf{X} \in \Omega_r \rightarrow \mathbf{x} = \boldsymbol{\varphi}^{pm}(\mathbf{X}, t) = \mathbf{X} + \mathbf{u}^{pm}(\mathbf{X}, t) \quad (1.29)$$

where \mathbf{X} and \mathbf{x} are the material particle positions in the reference and in the current configuration respectively.

Let \mathcal{B}_r denote the REV of the whole body around the point $\mathbf{X} \in \Omega_r$, that is, the mesoscopic REV. It is a special subset of the porous solid with the cavities and his size l_ε is such that only the heterogeneities of the mesoscopic scale are visible (Fig. 1.3), that is:

$$l_c < l_\varepsilon \ll L \quad (1.30)$$

with l_c and L being the characteristic dimensions of the mesoscopic cavities and of the whole body respectively. Let the disjoint subdomains \mathcal{B}_r^{pm} and \mathcal{B}_r^c be the porous matrix domain and the empty cavities domain included in the mesoscopic REV respectively, that is $\mathcal{B}_r = \mathcal{B}_r^{pm} \cup \mathcal{B}_r^c$ and $\emptyset = \mathcal{B}_r^{pm} \cap \mathcal{B}_r^c$. Then, the corresponding quantities in the current configuration read:

$$\mathcal{B}^{pm} := \boldsymbol{\varphi}^{pm}(\mathcal{B}_r^{pm}, t) \quad (1.31a)$$

$$\mathcal{B}^c := \boldsymbol{\varphi}^{pm}(\mathcal{B}_r^c, t) \quad (1.31b)$$

$$\mathcal{B} := \boldsymbol{\varphi}^{pm}(\mathcal{B}_r, t) \quad (1.31c)$$

In the following, the measure of the subdomains \mathcal{B} and \mathcal{B}^c will be denoted, respectively, by V and V^c . While, in order to distinguish with the corresponding quantities of the microscopic REV, the measure of \mathcal{B}^{pm} is denoted by V_B^{pm} . In the same way, the measure of the set of all the microscopic pores contained in \mathcal{B}^{pm} is denoted by V_B^p and reads:

$$V_B^p = \int_{\mathcal{B}^{pm}} \eta \, dv_x \quad (1.32)$$

where η is the Eulerian mesoscopic porosity already defined in (1.5).

Let Φ denote the Lagrangian macroscopic porosity which, at the time t and around the material point $\mathbf{x} \in \mathcal{B}^{pm}$, is defined as the ratio between the current volume of all the

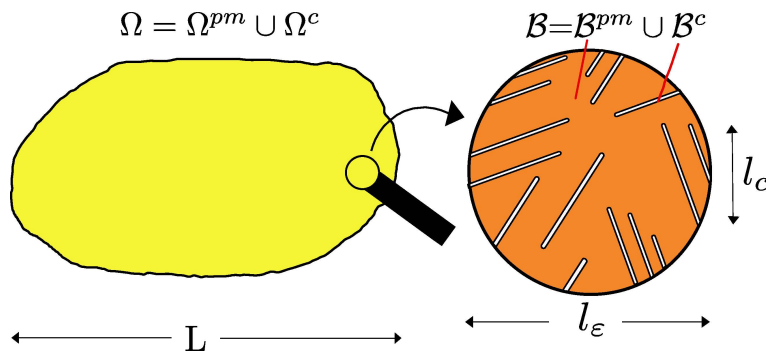


Figure 1.3: Macroscopic body and mesoscopic REV.

multi-scale voids, microscopic pores and mesoscopic cavities, and the initial total volume, V_r :

$$\Phi := \frac{V^c + V_B^p}{V_r} \quad (1.33)$$

Let H denote the Eulerian macroscopic porosity which, at the time t and around the material point $\mathbf{x} \in \mathcal{B}^{pm}$, is defined as the ratio between the current volume of all the multi-scale voids, and the current total volume V :

$$H := \frac{V^c + V_B^p}{V} \quad (1.34)$$

Let \mathbf{F}^{pm} and J^{pm} be the gradient and the Jacobian of the deformation function $\boldsymbol{\varphi}$ of the porous matrix respectively; their definitions read:

$$\mathbf{F}^{pm} := \nabla_X \boldsymbol{\varphi}^{pm} \quad J^{pm} := \det \mathbf{F}^{pm} = \frac{V^{pm}}{V_r^{pm}} \quad (1.35)$$

By using the change of variables $\mathbf{X} \leftrightarrow \mathbf{x} = \boldsymbol{\varphi}^{pm}(\mathbf{X}, t)$ in the (1.32), the relation (1.34) becomes:

$$H = \frac{V^c + \int_{\mathcal{B}_r^{pm}} \eta J^{pm} dv_X}{V} \quad (1.36)$$

Remark 1.4.1. *Given the definition of the Jacobian J^{pm} as ratio of the measures of volume subdomains of the porous matrix (1.35b), the following relation between the mesoscopic porosities η and ϕ , the Eulerian and the Lagrangian one respectively, follows:*

$$\phi = J^{pm} \eta \quad (1.37)$$

1.4.2 Small transformation framework

Being \mathbf{u}^{pm} the displacement field of the porous matrix extended by continuity to the mesoscopic cavities, it reads:

$$\mathbf{u}^{pm}(\mathbf{X}, t) = \boldsymbol{\varphi}^{pm}(\mathbf{X}, t) - \mathbf{X} \quad (1.38)$$

Then, the gradient \mathbf{F}^{pm} of the deformation function $\boldsymbol{\varphi}$ reads:

$$\mathbf{F}^{pm} = \mathbb{I} + \nabla_X \mathbf{u}^{pm} \quad (1.39)$$

In the framework of the small transformations approximation, the inverse of the deformation gradient is expanded by using the Taylor's development (C.19) and it reads:

$$(\mathbf{F}^{pm})^{-1} = \mathbb{I} - \nabla_X \mathbf{u}^{pm} + \dots \quad (1.40)$$

In the same way, by using the Taylor's development (C.11), the Jacobian J^{pm} of the transformation reads:

$$J^{pm} = \det(\mathbb{I} + \nabla_X \mathbf{u}^{pm}) = 1 + \text{tr}(\nabla_X \mathbf{u}^{pm}) + \dots = 1 + \text{div}_X \mathbf{u}^{pm} + \dots \quad (1.41)$$

Remark 1.4.2. Given expansion (1.41) of the Jacobian J^{pm} and relation (1.22) of the Eulerian mesoscopic porosity η , in this framework, the relation (1.37) between the mesoscopic porosities is expanded as well and it reads:

$$\phi = J^{pm} \eta = (1 + \text{div}_X \mathbf{u}^{pm} + \dots)(\eta_r + \eta_u) = \eta_r + \eta_u + \eta_r \text{div}_X \mathbf{u}^{pm} + \dots \quad (1.42)$$

then, the Lagrangian mesoscopic porosity ϕ reads:

$$\phi = \phi_r + \phi_u \quad (1.43)$$

where ϕ_r denotes the Lagrangian mesoscopic porosity in the reference configuration and ϕ_u denotes the variation of the Lagrangian mesoscopic porosity induced by the motion of the solid-skeleton:

$$\phi_r = \eta_r \quad (1.44a)$$

$$\phi_u = \eta_u + \eta_r \text{div}_X \mathbf{u}^{pm} \quad (1.44b)$$

Given the relations (1.27, 1.28) about $\dot{\eta}$, and the relations (1.43, 1.44b) about ϕ and ϕ_u , for the Lagrangian mesoscopic porosity rate $\dot{\phi}$ the following relations hold:

$$\dot{\phi} = \partial_t \phi + \dots \quad (1.45a)$$

$$\dot{\phi} = \dot{\phi}_u \quad (1.45b)$$

$$\dot{\phi}_u = \dot{\eta}_u + \eta_r \text{div}_X \dot{\mathbf{u}}^{pm} \quad (1.45c)$$

1.4.2.1 Expansion of the macroscopic porosity

By using the expansion (1.41) of J^{pm} , the volume V^c is expanded as follows:

$$V^c = \int_{\mathcal{B}_r^c} J^{pm} dV_X = \int_{\mathcal{B}_r^c} (1 + \text{div}_X \mathbf{u}^{pm} + \dots) dV_X \quad (1.46)$$

and, in the same way, the volume V is expanded as well. While, given the expression (1.42), the expansion of the expression (1.32) of the volume V_B^p reads:

$$V_B^p = \int_{\mathcal{B}_r^{pm}} \left(\eta_u + \eta_r (1 + \text{div}_X \mathbf{u}^{pm}) \right) dV_X + \dots \quad (1.47)$$

Therefore, the relation (1.36) is expanded as follows:

$$H = \frac{V_r^c + \int_{\mathcal{B}_r^c} \text{div}_X \mathbf{u}^{pm} dV_X + \int_{\mathcal{B}_r^{pm}} \left(\eta_u + \eta_r (1 + \text{div}_X \mathbf{u}^{pm}) \right) dV_X + \dots}{V_r \left(1 + \frac{1}{V_r} \int_{\mathcal{B}_r^c} \text{div}_X \mathbf{u}^{pm} dV_X + \dots \right)} \quad (1.48)$$

which is expanded as well by using the Taylor's development (C.6) and it becomes:

$$H = \left(\frac{V_r^c + \int_{\mathcal{B}_r^c} \operatorname{div}_X \mathbf{u}^{pm} dV_X + \dots}{V_r} \right) \left(1 - \frac{1}{V_r} \int_{\mathcal{B}_r} \operatorname{div}_X \mathbf{u}^{pm} dV_X + \dots \right) \\ + \left(\frac{\int_{\mathcal{B}_r^{pm}} (\eta_u + \eta_r (1 + \operatorname{div}_X \mathbf{u}^{pm})) dV_X + \dots}{V_r} \right) \left(1 - \frac{1}{V_r} \int_{\mathcal{B}_r} \operatorname{div}_X \mathbf{u}^{pm} dV_X + \dots \right) \quad (1.49)$$

that is also:

$$H = \left(\frac{V_r^c + \int_{\mathcal{B}_r^{pm}} \eta_r dV_X}{V_r} \right) \left(1 - \frac{1}{V_r} \int_{\mathcal{B}_r} \operatorname{div}_X \mathbf{u}^{pm} dV_X + \dots \right) \\ + \frac{\int_{\mathcal{B}_r^c} \operatorname{div}_X \mathbf{u}^{pm} dV_X + \int_{\mathcal{B}_r^{pm}} (\eta_u + \eta_r \operatorname{div}_X \mathbf{u}^{pm} dV_X)}{V_r} \quad (1.50)$$

or in a more compact form:

$$H = H_r + H_u \quad (1.51)$$

where H_r is the Eulerian macroscopic porosity in the reference configuration and H_u is the variation of the Eulerian macroscopic porosity induced by the motion of the porous matrix:

$$H_r = \frac{V_r^c + V_{\mathcal{B}_r}^p}{V_r} = \frac{V_r^c + \eta_r V_{\mathcal{B}_r}^{pm}}{V_r} \quad (1.52a)$$

$$H_u = \frac{-H_r \int_{\mathcal{B}_r} \operatorname{div}_X \mathbf{u}^{pm} dV_X + \int_{\mathcal{B}_r^c} \operatorname{div}_X \mathbf{u}^{pm} dV_X + \int_{\mathcal{B}_r^{pm}} (\eta_u + \eta_r \operatorname{div}_X \mathbf{u}^{pm}) dV_X}{V_r} + \dots \quad (1.52b)$$

Moreover, given that $\mathcal{B}_r = \mathcal{B}_r^{pm} \cup \mathcal{B}_r^c$, the variation H_u of the Eulerian macroscopic porosity reads also:

$$H_u = \frac{\int_{\mathcal{B}_r^{pm}} \eta_u dV_X + (\eta_r - 1) \int_{\mathcal{B}_r^{pm}} \operatorname{div}_X \mathbf{u}^{pm} dV_X + (1 - H_r) \int_{\mathcal{B}_r} \operatorname{div}_X \mathbf{u}^{pm} dV_X}{V_r} + \dots \quad (1.53)$$

or:

$$H_u = \frac{\int_{\mathcal{B}_r^{pm}} \eta_u dV_X + (\eta_r - H_r) \int_{\mathcal{B}_r^{pm}} \operatorname{div}_X \mathbf{u}^{pm} dV_X + (1 - H_r) \int_{\mathcal{B}_r^c} \operatorname{div}_X \mathbf{u}^{pm} dV_X}{V_r} + \dots \quad (1.54)$$

Remark 1.4.3. By analogy with the relations (1.44, 1.45) about the Lagrangian mesoscopic porosity, the corresponding relations at the macroscopic scale can be deduced by means of the concept of macroscopic displacement field $\mathbf{u}^{pm(0)}$ which is properly explained in the chapter 2 (section 2.3.4.2). Actually, in order to write the relation between the macroscopic Eulerian and Lagrangian porosities H and Φ , it is necessary to define the deformation function $\varphi^{(0)}$ of the homogenized body as follows:

$$\mathbf{X} \in \Omega_r \rightarrow \mathbf{x} = \varphi^{(0)}(\mathbf{X}, t) = \mathbf{X} + \mathbf{u}^{pm(0)}(\mathbf{X}, t) \quad (1.55)$$

and its Jacobian $J^{(0)}$, that is the macroscopic Jacobian:

$$J^{(0)} := \det \mathbf{F}^{(0)} = \det \nabla_{\mathbf{X}} \varphi^{(0)} = \frac{V}{V_r} \quad (1.56)$$

where V denotes a small subset of the whole body Ω in the current configuration. So, the searched relation between the Lagrangian and the Eulerian macroscopic porosities reads:

$$\Phi = J^{(0)} H \quad (1.57)$$

Moreover, in the small transformation framework, its expansion reads:

$$\Phi = J^{(0)} H = (1 + \operatorname{div}_{\mathbf{X}} \mathbf{u}^{pm(0)} + \dots)(H_r + H_u) = H_u + H_r(1 + \operatorname{div}_{\mathbf{X}} \mathbf{u}^{pm(0)}) + \dots \quad (1.58)$$

So, the Lagrangian macroscopic porosity reads:

$$\Phi = \Phi_r + \Phi_u \quad (1.59)$$

where Φ_r is the Lagrangian mesoscopic porosity in the reference configuration and Φ_u is the variation of the Lagrangian mesoscopic porosity induced by the motion of the porous matrix:

$$\Phi_r = H_r \quad (1.60a)$$

$$\Phi_u = H_u + H_r \operatorname{div}_{\mathbf{X}} \mathbf{u}^{pm(0)} \quad (1.60b)$$

And the time derivative of the latter one yields:

$$\dot{\Phi}_u = \dot{H}_u + H_r \operatorname{div}_{\mathbf{X}} \dot{\mathbf{u}}^{pm(0)} \quad (1.61)$$

Remark 1.4.4. With referring to the asymptotic developments (2.51a) that are introduced in the section 2.3, it is worth pointing out that, just like the macroscopic displacement field $\mathbf{u}^{pm(0)}$ is the term of order zero in the asymptotic expansion of the mesoscopic displacement field \mathbf{u}^{pm} of the porous matrix, this latter one is the term of order zero of the microscopic displacement field \mathbf{u}^s of the solid phase.

1.5 Conclusions

In this chapter, different useful relations about the porosities have been deduced. At both the mesoscopic scale and the macroscopic one, the relations (1.37, 1.57) between the Eulerian porosity and the Lagrangian one are deduced.

In the small transformation framework, both in the Eulerian definition and in the Lagrangian one, both the mesoscopic porosity and the macroscopic one can be described as the sum of two terms (1.22, 1.43, 1.51, 1.59): the first one is written in the reference configuration and it is a data of the problem, while the second one depends on the displacement field and it is an unknown.

By means of the Taylor's expansions shown and proved in the appendix C, at both the scales, the relations between the Eulerian porosities variation, η_u and H_u , and the Lagrangian ones, ϕ_u and Φ_u , are provided (1.44b, 1.60b).

Moreover, the relation (1.26) which describes the Eulerian microscopic porosity rate $\dot{\eta}$ is deduced and then validated by comparison with the relation (A.19) provided in Callari and Abati (2011).

Lastly, the relation (1.45c) between the variation of the Eulerian microscopic porosity rate $\dot{\eta}_u$ and the corresponding Lagrangian quantity $\dot{\phi}_u$ is determined.

In the following chapter, all the relations here presented are useful for writing the fluid mass balance (sections 2.2.2 and 2.4.4) and the constitutive law for the variation of the porosity at both the mesoscopic scale and the macroscopic one (sections 2.2.3.3 and 2.4.3).

Chapter 2

From mesoscale to macroscale

2.1 Introduction

In this chapter, the starting scale of observation is the mesoscopic one. It means that the heterogeneous microscopic structure, composed by a solid-skeleton within a network of fluid-saturated pores, is here replaced by a porous saturated and deformable matrix, that is, the equivalent continuum whose description is given by the equations of poroelasticity obtained by Biot (1941) using a phenomenologic approach, and re-obtained also by means of upscaling techniques in (Auriault 2004; Auriault and Sanchez-Palencia 1977). Notwithstanding that, because of the set of mesoscopic fluid-filled cavities included in the porous matrix, the medium here investigated is still heterogeneous (fig. 2.1). Therefore, a further equivalent and macroscopic continuum is required in order to have governing equations and hydro-mechanical properties defined in every single point of the whole body Ω .

The aimed macroscopic description is searched by applying the method of the asymptotic homogenization to the mesoscopic description and without any phenomenological

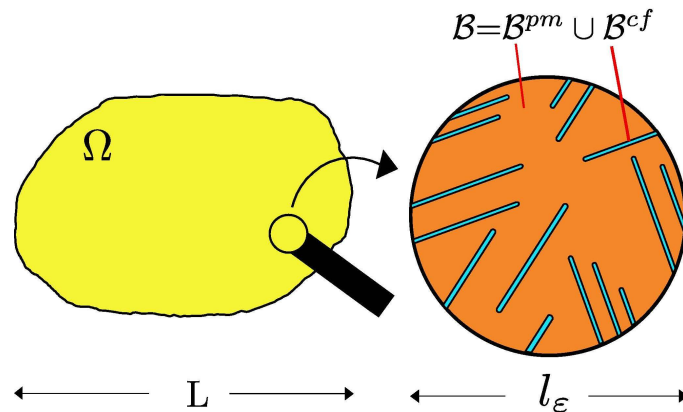


Figure 2.1: At the macroscopic observation scale the body Ω appears as a continuum. The mesoscopic REV \mathcal{B} shows the fluid-filled cavities surrounded by the porous matrix and its size is much smaller than the characteristic dimension of Ω , that is, $L \gg l_\epsilon$.

assumptions. The main developments of the analytical calculus which leads to the homogenized equations and also provides the effective poroelastic coefficients are presented in this chapter.

2.2 Mesoscopic description

In this section, the mesoscopic description of the whole body Ω is provided. It is composed by the linear momentum balance and the fluid mass balance, the constitutive relations and the conditions at the cavity boundary.

Even if in (Auriault 2004; Auriault and Sanchez-Palencia 1977) an equivalent form of the Biot's equations is already obtained by means of the method of the asymptotic homogenization, in this thesis a further formulation of them is proposed and adopted. Actually, in the appendix B, a look to the microscopic scale is taken by recalling the Auriault's analytical calculus, very likely the most instructive example available in the literature about the application of the method to the porous media; but then it is also enriched by splitting the fluid mass balance from the II Biot's equation, and by changing the definition of the mean value of the pore fluid absolute velocity.

As said above, at the mesoscopic scale of observation, the whole body Ω appears as a porous solid which contains a distribution of fluid-filled cavities. So, it can be described as the union of two disjoint subdomains: the porous matrix subdomain Ω^{pm} and the set of fluid-filled cavities Ω^{cf} ; that is, $\Omega = \Omega^{pm} \cup \Omega^{cf}$ and $\emptyset = \Omega^{pm} \cap \Omega^{cf}$ (fig. 2.2).

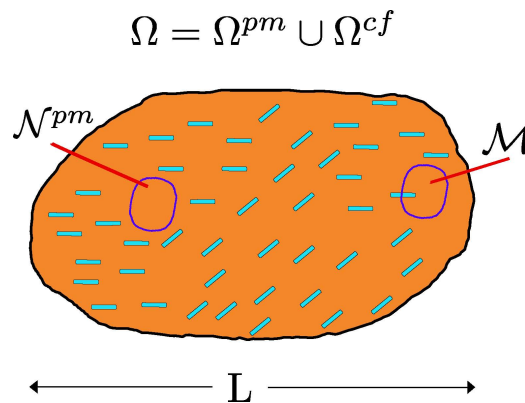


Figure 2.2: Mesoscopic structure of the whole body Ω : the porous matrix Ω^{pm} with the set Ω^{cf} of fluid-filled cavities. \mathcal{N}^{pm} is a generic subset volume of Ω^{pm} , while \mathcal{M} is a subset volume of Ω which intersects a single cavity.

2.2.1 Linear momentum balance

The equilibrium in the whole body Ω reads: $\forall \mathbf{x} \in \Omega$,

$$\operatorname{div}_x \boldsymbol{\sigma} = 0 \quad (2.1)$$

where the body forces are not taken into account and $\boldsymbol{\sigma}$ is the Cauchy stress tensor defined as follows:

$$\boldsymbol{\sigma} = \begin{cases} \boldsymbol{\sigma}^{pm} & \text{in } \Omega^{pm} \\ \boldsymbol{\sigma}^{cf} & \text{in } \Omega^{cf} \end{cases} \quad (2.2)$$

so, $\boldsymbol{\sigma}^{pm}$ is the Cauchy stress tensor in the porous matrix and $\boldsymbol{\sigma}^{cf}$ is the Cauchy stress tensor of the cavity fluid .

2.2.2 Fluid mass balance

In this section, both in the framework of large and small deformations, it is shown how to write the local form of the conservation of the fluid mass in the porous matrix Ω^{pm} . Both the Lagrangian and the Eulerian formulations of this balance are provided.

2.2.2.1 Eulerian description

Let \mathcal{N}^{pm} denote a generic subset volume of Ω^{pm} (fig. 2.2). A fluid volume is identified with the set of fluid particles which occupy the pores of \mathcal{N}^{pm} at the time t and, by means of a Lagrangian approach, these particles are followed in their motion. Let \mathcal{N}_{t+dt}^{pm} denote the special volume subset of the porous matrix Ω_{t+dt}^{pm} whose pores, at the time $t + dt$, host the selected fluid particles. It is worth remarking that \mathcal{N}_{t+dt}^{pm} is not the deformed configuration of \mathcal{N}^{pm} due to the motion of the solid-skeleton.

By definition, the mass of a material volume is constant and, by assuming the fluid to be incompressible, its volume is constant as well. Then, the conservation of the fluid volume reads:

$$\int_{\mathcal{N}_{t+dt}^{pm}} \eta(\tilde{\mathbf{x}}, t + dt) dv_{\tilde{x}} = \int_{\mathcal{N}^{pm}} \eta(\mathbf{x}, t) dv_x \quad (2.3)$$

where η is the Eulerian mesoscopic porosity, already defined in (1.5), and $\tilde{\mathbf{x}}$ denotes the position vector at the time $t + dt$ of the fluid particle labeled as \mathbf{x} .

From the (2.3) it is clear that if $\eta(\mathbf{x}, t) = \eta(\tilde{\mathbf{x}}, t + dt)$, then even the volumes of \mathcal{N}^{pm} and of \mathcal{N}_{t+dt}^{pm} would be equal.

Let $\mathbf{v}^{pm}(\mathbf{x}, t)$ denote the average fluid velocity field of the pore fluid in \mathcal{N}^{pm} such that:

$$\tilde{\mathbf{x}} = \mathbf{x} + \mathbf{v}^{pm}(\mathbf{x}, t)dt \quad (2.4)$$

Then, by using the change of variables $\mathbf{x} \leftrightarrow \tilde{\mathbf{x}}$, the left member of the equality (2.3) reads:

$$\int_{\mathcal{N}^{pm}} \eta(\mathbf{x} + \mathbf{v}^{pm}(\mathbf{x}, t) dt, t + dt) \det(\mathbb{I} + \nabla_x \mathbf{v}^{pm} dt) dv_x \quad (2.5)$$

and, by means of the Taylor's expansions (C.4, C.11), its expansion reads:

$$\begin{aligned} & \int_{\mathcal{N}^{pm}} (\eta(\mathbf{x}, t) + \nabla_x \eta \cdot \mathbf{v}^{pm} dt + \partial_t \eta dt + \dots) (1 + \operatorname{div}_x \mathbf{v}^{pm} dt + \dots) dv_x \\ &= \int_{\mathcal{N}^{pm}} \eta(\mathbf{x}, t) dv_x + \int_{\mathcal{N}^{pm}} (\nabla_x \eta \cdot \mathbf{v}^{pm} + \partial_t \eta + \eta \operatorname{div}_x \mathbf{v}^{pm}) dv_x dt + \dots \end{aligned} \quad (2.6)$$

So, the equality (2.3) can be rewritten as follows:

$$\int_{\mathcal{N}^{pm}} (\nabla_x \eta \cdot \mathbf{v}^{pm} + \partial_t \eta + \eta \operatorname{div}_x \mathbf{v}^{pm}) dt dv_x = 0 \quad (2.7)$$

which, in view of the arbitrariness of $\mathcal{N}^{pm} \subseteq \Omega^{pm}$, is equivalent to: $\forall \mathbf{x} \in \Omega^{pm}$,

$$\operatorname{div}_x(\eta \mathbf{v}^{pm}) + \partial_t \eta = 0 \quad (2.8)$$

which is the Eulerian form of the fluid mass balance in terms of porosity for the particular case of an incompressible pore fluid.

2.2.2.2 Lagrangian description

The material time derivative of the Eulerian mesoscopic porosity η with respect to the motion of the porous medium reads:

$$\dot{\eta} = \partial_t \eta + \nabla_x \eta \cdot \dot{\mathbf{u}}^{pm} \quad (2.9)$$

where $\dot{\mathbf{u}}^{pm}$ is the velocity field of the porous medium. Then, by substituting the (2.9) in the balance (2.8), it yields:

$$\dot{\eta} + \eta \operatorname{div}_x \dot{\mathbf{u}}^{pm} + \operatorname{div}_x (\eta (\mathbf{v}^{pm} - \dot{\mathbf{u}}^{pm})) = 0 \quad (2.10)$$

Taking into account the relation (1.37) between the Lagrangian and the Eulerian mesoscopic porosities, $\phi = J^{pm} \eta$, and writing the time derivative of the Jacobian J as follows:

$$\dot{J}^{pm} = J^{pm} \operatorname{div}_x \dot{\mathbf{u}}^{pm} \quad (2.11)$$

the balance (2.10) can be rewritten in a more compact form as:

$$\dot{\phi} + J^{pm} \operatorname{div}_x (\eta (\mathbf{v}^{pm} - \dot{\mathbf{u}}^{pm})) = 0 \quad (2.12)$$

In the change of variables $\mathbf{X} \leftrightarrow \mathbf{x} = \boldsymbol{\varphi}^{pm}(\mathbf{X}, t)$, that is to say from the reference configuration to the current one, the following relations hold for a generic vector $\mathbf{a}(x)$ and a generic scalar function $f(x)$:

$$\nabla_X \mathbf{a} = \nabla_x \mathbf{a} \circ \mathbf{F}^{pm} \implies \nabla_x \mathbf{a} = \nabla_X \mathbf{a} \circ (\mathbf{F}^{pm})^{-1} \implies \operatorname{div}_x \mathbf{a} = \operatorname{tr}(\nabla_X \mathbf{a} \circ (\mathbf{F}^{pm})^{-1}) \quad (2.13)$$

and

$$\nabla_x f = (\mathbf{F}^{pm})^{-t} \circ \nabla_X f \quad (2.14)$$

where, as shown in the initial pages dedicated to the notation, the symbol “ \circ ” denotes the composition of two linear transformations, while “ \circ ” provides the image of a vector by a linear transformation. Therefore, the Lagrangian formulations (2.10, 2.12), with respect to the motion of the porous medium, of the fluid volume balance read:

$$\dot{\eta} + \eta \operatorname{tr}(\nabla_X \dot{\mathbf{u}}^{pm} \circ (\mathbf{F}^{pm})^{-1}) + \operatorname{tr}\left(\nabla_X (\eta(\mathbf{v}^{pm} - \dot{\mathbf{u}}^{pm})) \circ (\mathbf{F}^{pm})^{-1}\right) = 0 \quad (2.15)$$

and

$$\dot{\phi} + J^{pm} \operatorname{tr}\left(\nabla_X (\eta(\mathbf{v}^{pm} - \dot{\mathbf{u}}^{pm})) \circ (\mathbf{F}^{pm})^{-1}\right) = 0 \quad (2.16)$$

respectively.

2.2.2.3 Small transformation framework

In this approximated framework, the Eulerian microscopic porosity η is described by the relations (1.22, 1.23), while the Lagrangian one ϕ by the relations (1.43, 1.44): clearly, η_r and ϕ_r does not depend on time. Moreover, in the Lagrangian representation, as already shown in (1.27), the material time derivative can be approximated by the partial time derivative. So, the formulations (2.15, 2.16) are rewritten as:

$$\partial_t \eta_u + (\eta_r + \eta_u) \operatorname{tr}(\nabla_X \dot{\mathbf{u}}^{pm} \circ (\mathbf{F}^{pm})^{-1}) + \operatorname{tr}\left(\nabla_X ((\eta_r + \eta_u)(\mathbf{v}^{pm} - \dot{\mathbf{u}}^{pm})) \circ (\mathbf{F}^{pm})^{-1}\right) = 0 \quad (2.17)$$

and

$$\partial_t \phi_u + J^{pm} \operatorname{tr}\left(\nabla_X ((\eta_r + \eta_u)(\mathbf{v}^{pm} - \dot{\mathbf{u}}^{pm})) \circ (\mathbf{F}^{pm})^{-1}\right) = 0 \quad (2.18)$$

respectively. It is taken into account that the displacement \mathbf{u}^{pm} and its gradient are small. Then, it is assumed that the velocity $\dot{\mathbf{u}}^{pm}$ is small as well and that the fluid velocity field \mathbf{v}^{pm} is of the same order. So, by using the expansions (1.17) of $(F^{pm})^{-1}$ and (1.18) of J^{pm} , the formulations (2.17, 2.18) become:

$$\partial_t \eta_u + \eta_r \operatorname{div}_X \dot{\mathbf{u}}^{pm} = -\operatorname{div}_X \mathbf{q}^{pm} \quad (2.19)$$

and

$$\partial_t \phi_u = -\operatorname{div}_X \mathbf{q}^{pm} \quad (2.20)$$

where \mathbf{q}^{pm} denotes the Lagrangian relative flow vector of fluid volume, that is, the fluid volume which flows through a unit surface of the porous matrix during the unit time, and it is defined as follows:

$$\mathbf{q}^{pm} := \eta_r (\mathbf{v}^{pm} - \dot{\mathbf{u}}^{pm}) \quad (2.21)$$

It is worth remarking that:

- i. clearly, the formulations (2.19) and (2.20) have to be identical and the proof is given by the relation (1.45c) between $\dot{\eta}_u$ and $\dot{\phi}_u$;
- ii. it is worth remarking that, being in the framework of the small transformations and by taking into account the definition (2.21) of \mathbf{q}^{pm} , the balance (2.19) can be rewritten in terms of the absolute pore fluid velocity \mathbf{v}^{pm} as follows:

$$\partial_t \eta_u = -\operatorname{div}_X (\eta_r \mathbf{v}^{pm}) \quad (2.22)$$

- iii. the Lagrangian relative flow vector of fluid mass, that is, the fluid mass which flows through a unit surface of the porous matrix during the unit time, is denoted by \mathbf{q}_m and defined as follows:

$$\mathbf{q}_m^{pm} := \rho^{pf} \eta_r (\mathbf{v}^{pm} - \dot{\mathbf{u}}^{pm}) \quad (2.23)$$

where ρ^{pf} is the density of the fluid. It is obvious that the relation between \mathbf{q}^{pm} and \mathbf{q}_m^{pm} , defined in the (2.21, 2.23), reads:

$$\mathbf{q}_m^{pm} := \rho^{pf} \mathbf{q}^{pm} \quad (2.24)$$

Then, let m^{pm} denote the mesoscopic current Lagrangian fluid mass content per unit of the initial volume of the porous medium; following Biot (1941), it can be defined as a variation:

$$m^{pm} := \frac{(V^{pf} - V_r^{pf}) \rho^{pf}}{V_r^{pm}} = \phi_u \rho^{pf} \quad (2.25)$$

where, as already done in the section 1.3.1 for the mesoscopic porosities in the dry case, V^{pm} and V^{pf} are the measures of the microscopic REV and of the set of fluid-saturated microscopic pores included in the microscopic REV respectively. Taking into account the assumed incompressibility of the fluid, the balance (2.20) is, as expected, a particular case of the following fluid mass balance written in terms of fluid mass content (Biot 1941; Coussy 2004):

$$\partial_t m^{pm} = -\operatorname{div}_X \mathbf{q}_m^{pm} \quad (2.26)$$

In the following, among all the aforementioned formulations of the fluid volume balance, the relation (2.20) will be mainly used.

2.2.3 Constitutive relations

2.2.3.1 Porous matrix

The deformable and saturated porous matrix Ω^{pm} is assumed to be elastic and its hydro-mechanical behaviour is described by the Biot's equation:

$$\boldsymbol{\sigma}^{pm} = \mathbf{c} @ \mathbf{e}_x(\mathbf{u}^{pm}) - \mathbf{b} p^{pm} \quad (2.27)$$

where $\boldsymbol{\sigma}^{pm}$ is the Cauchy (total) stress tensor; p^{pm} is the pressure of the pore fluid, that is the fluid which saturates the pores; \mathbf{c} and \mathbf{b} are the solid-skeleton elasticity tensor and the Biot's tensor respectively; $\mathbf{e}_x(\mathbf{u}^{pm})$ is the infinitesimal strain tensor defined as the symmetric part of the gradient of the displacement field, that is:

$$\mathbf{e}_x(\mathbf{u}^{pm}) := (\nabla_x \mathbf{u}^{pm})^S \quad (2.28)$$

2.2.3.2 Cavities and cavity fluid

The set of cavities Ω^{cf} is assumed to be fluid-filled. With the aim of understanding how to model the cavity fluid, that is the fluid which fills the cavities, it is worth having a look at the microscopic scale (appendix B, Auriault 2004, Auriault and Sanchez-Palencia 1977): the pore fluid was assumed to be viscous Newtonian and, in order to have a homogenized diphasic behaviour, that is in order to have a fluid motion through the small pores not requiring extremely high fluid pressures, it is imposed a constant viscosity μ^{pf} of order two in the power of the separation scale parameter e , which is very small (fig. B.2). Then, the constitutive law for the pore fluid in Auriault (2004) reads:

$$\boldsymbol{\sigma}^{pf} = 2 \mu^{pf} e^2 \mathbf{D} - p^{pf} \mathbf{I} \quad (2.29)$$

where \mathbf{D} denotes the strain rate tensor, that is the symmetric part of the gradient of the velocity field \mathbf{v}^{pf} of the pore fluid, that is $\mathbf{D} := (\nabla_x \mathbf{v}^{pf})^S$. Clearly, in reason of the upscaling approach, at the mesoscopic scale only the terms of order zero in the power of e are kept, then the pore fluid is considered inviscid. So, from this remark about the microscopic structure and in order to have a consistent set of constitutive hypothesis, also the cavity fluid is modelled as inviscid. So, its constitutive hypothesis is isotropic and reads:

$$\boldsymbol{\sigma}^{cf} = -p^{cf} \mathbf{I} \quad (2.30)$$

where p^{cf} is the fluid pressure in the cavities.

Moreover, the cavity fluid is assumed to be incompressible:

$$\operatorname{div}_x \mathbf{v}^{cf} = 0 \quad (2.31)$$

where \mathbf{v}^{cf} is the absolute velocity of the cavity fluid.

For what concerns the cavities, it is worth remarking that if they would be connected in a network, then the fluid flux through the connecting channels would be significant and the assumption of inviscid fluid would not be suitable anymore and some boundary conditions at the interface which separates the channel flow and the porous matrix should be determined and imposed, e.g. as proposed by Beavers and Joseph (1967).

So, in this work, it is assumed that the cavities are not connected in a network, that is, the cavity fluid is not exchanged among the cavities but only between the single cavity and the surrounding matrix. In such a way the consistency with the assumption of inviscid cavity fluid is ensured: in fact, it is reasonable to assume that the velocity \mathbf{v}^{cf} of the cavity fluid is very small or, equivalently, that it is of the same order of the pore fluid velocity \mathbf{v}^{pf} in the Auriault's problem quoted above.

Lastly, it is worth remarking that:

- i. given the governing equations for the cavity fluid, its velocity \mathbf{v}^{cf} is indeterminate;
- ii. given the linear momentum balance (2.1) in \mathcal{B}^{cf} , the pressure of the cavity fluid is homogeneous in a single cavity:

$$\operatorname{div}_x(p^{cf}\mathbf{I}) = 0 \quad \implies \quad \nabla_x p^{cf} = \mathbf{0} \quad (2.32)$$

Notwithstanding that, in every cavity the pressure has a different value.

2.2.3.3 Variation of the mesoscopic porosities

The Biot's constitutive law for the fluid mass content m_f , defined by (2.25), is particularized to the case of incompressible fluid and rewritten in terms of the variation of the Lagrangian mesoscopic porosity ϕ_u , defined in (1.44b), as follows:

$$\phi_u = \frac{m^{pm}}{\rho^{pf}} = s p^{pm} + \mathbf{b} : \mathbf{e}_x(\mathbf{u}^{pm}) \quad (2.33)$$

or, as in (appendix B, Auriault (2004)), rewritten in terms of the variation of the Eulerian mesoscopic porosity η_u , defined in (1.23b), as:

$$\eta_u = s p^{pm} + (\mathbf{b} - \eta_r \mathbf{I}) : \mathbf{e}_x(\mathbf{u}^{pm}) \quad (2.34)$$

In both the cases s denotes the Biot's modulus and the equivalence of the (2.33, 2.34) is easily proven by taking into account the relation (1.44b) between ϕ_u and η_u .

2.2.4 Darcy's law

In the porous matrix Ω^{pm} , the motion of the fluid is described by the Darcy's law:

$$\mathbf{q}^{pm} = -\mathbf{k}_@ \nabla_x p^{pm} \quad (2.35)$$

where \mathbf{k} is the permeability tensor.

2.2.5 Conditions at cavity boundary

In the present section, it is useful to define more precisely the fluid-filled cavity volume subdomain as follows:

$$\Omega^{cf} = \bigcup_{\alpha=1}^A c_\alpha \quad (2.36)$$

where c_α is the α -th cavity out of A . The boundary $\partial\Omega^{pm}$ of the porous matrix is composed by an external part $\partial\Omega$ and an internal one $\partial\Omega^{cf}$:

$$\partial\Omega^{cf} = \bigcup_{\alpha=1}^A \partial c_\alpha \quad (2.37)$$

where ∂c_α is the boundary of the α -th cavity, that is, the interface between a single cavity and the surrounding porous matrix. Being this latter deformable, ∂c_α is a moving interface with velocity $\dot{\mathbf{u}}^{pm}$. And, it reads: $\partial\Omega^{pm} = \partial\Omega \cup \partial\Omega^{cf}$.

With the aim of writing a well-posed mesoscopic boundary value problem, the proper interface conditions are introduced below.

2.2.5.1 Stress continuity

Let \mathcal{M} denote a subdomain of Ω which intersects a single fluid-filled cavity (fig. 2.2). It is composed by the union of the porous subpart, denoted by \mathcal{M}^{pm} , and a portion of the fluid-filled cavity which is embodied, denoted by \mathcal{M}^{cf} , that is $\mathcal{M} = \mathcal{M}^{pm} + \mathcal{M}^{cf}$ (fig. 2.3).

The boundaries of \mathcal{M}^{pm} and \mathcal{M}^{cf} are denoted by $\partial\mathcal{M}^{pm}$ and $\partial\mathcal{M}^{cf}$ respectively. While, the interface separating \mathcal{M}^{pm} from \mathcal{M}^{cf} is denoted by \mathcal{S}^{int} . Then, it reads:

$$\partial\mathcal{M}^{pm} = \mathcal{S}^{pm} \cup \mathcal{S}^{int} \quad (2.38a)$$

$$\partial\mathcal{M}^{cf} = \mathcal{S}^{cf} \cup \mathcal{S}^{int} \quad (2.38b)$$

$$\partial\mathcal{M} = \mathcal{M}^{pm} \cup \mathcal{M}^{cf} \quad (2.38c)$$

The equilibria in \mathcal{M}^{pm} and of \mathcal{M}^{cf} read respectively:

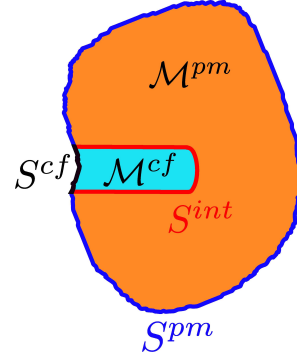


Figure 2.3: The volume subset \mathcal{M} of Ω^{pm} contains a portion of a fluid-filled cavity.

$$\int_{S^{int}} \boldsymbol{\sigma}^{pm} \otimes \mathbf{n} \, ds + \int_{S^{pm}} \boldsymbol{\sigma}^{pm} \otimes \mathbf{n} \, ds = 0 \quad (2.39a)$$

$$- \int_{S^{int}} \boldsymbol{\sigma}^{cf} \otimes \mathbf{n} \, ds + \int_{S^{cf}} \boldsymbol{\sigma}^{cf} \otimes \mathbf{n} \, ds = 0 \quad (2.39b)$$

where the sign minus is due to the inward orientation of the normal unit vector \mathbf{n} to ∂c_α with respect to \mathcal{M}^{pm} . The equilibrium of \mathcal{M} reads:

$$\int_{S^{pm}} \boldsymbol{\sigma}^{pm} \otimes \mathbf{n} \, ds + \int_{S^{cf}} \boldsymbol{\sigma}^{cf} \otimes \mathbf{n} \, ds = 0 \quad (2.40)$$

then, by comparison, it follows that:

$$\int_{S^{int}} \boldsymbol{\sigma}^{pm} \otimes \mathbf{n} \, ds - \int_{S^{int}} \boldsymbol{\sigma}^{cf} \otimes \mathbf{n} \, ds = 0 \quad (2.41)$$

In the end, as S^{int} is an arbitrary portion of ∂c_α , it follows that:

$$\boldsymbol{\sigma}^{pm} \otimes \mathbf{n} = \boldsymbol{\sigma}^{cf} \otimes \mathbf{n} \quad (2.42)$$

and, by taking into account the constitutive hypothesis (2.30) for the cavity fluid, it reads:

$$\boldsymbol{\sigma}^{pm} \otimes \mathbf{n} = -p^{cf} \otimes \mathbf{n} \quad (2.43)$$

2.2.5.2 Fluid pressure continuity

The cavity fluid and the pore fluid are in contact at interface $\partial \Omega^{cf}$, then:

$$p^{pm} = p^{cf} \quad (2.44)$$

Moreover, by taking into account the homogeneity (2.32) of the fluid pressure in each cavity, it follows that the pore fluid pressure is homogeneous too at each interface ∂c_α .

2.2.5.3 Fluid mass balance

The interface is moving with the same velocity of the porous matrix, then the local fluid volume conservation through ∂c_α reads:

$$\mathbf{q}^{pm} \cdot \mathbf{n} = (\mathbf{v}^{cf} - \dot{\mathbf{u}}^{pm}) \cdot \mathbf{n} \quad (2.45)$$

and it is worth remarking that it does not imply that the velocity of the fluid is discontinuous at the interface: in fact, as already said, \mathbf{v}^{pm} is the average velocity of the pore fluid and not the true velocity of the fluid in the pores.

Moreover, by taking into account the incompressibility of the cavity fluid, a global conservation condition is easily deduced:

$$\int_{\partial c_\alpha} \mathbf{q}^{pm} \cdot \mathbf{n} ds = - \int_{\partial c_\alpha} \dot{\mathbf{u}}^{pm} \cdot \mathbf{n} ds \quad (2.46)$$

2.2.6 Synopsis of mesoscopic description

The mesoscopic equations governing the hydro-mechanical behaviour of the porous solid with fluid-filled cavities are listed below.

$$\mathbf{0} = \text{div}_x \boldsymbol{\sigma} \quad \text{Linear momentum balance in } \Omega \quad (2.47a)$$

$$0 = \text{div}_x \mathbf{v}^{cf} \quad \text{Fluid incompressibility in } \Omega^{cf} \quad (2.47b)$$

$$\dot{\phi}_u = -\text{div}_x \mathbf{q}^{pm} \quad \text{Fluid mass balance in } \Omega^{pm} \quad (2.47c)$$

$$\mathbf{q}^{pm} = -\mathbf{k} @ \nabla_x p^{pm} \quad \text{Darcy law in } \Omega^{pm} \quad (2.47d)$$

$$\boldsymbol{\sigma}^{pm} = \mathbf{c} @ \mathbf{e}_x(\mathbf{u}^{pm}) - \mathbf{b} p^{pm} \quad \text{I Biot's constitutive relation in } \Omega^{pm} \quad (2.47e)$$

$$\boldsymbol{\sigma}^{cf} = -p^{cf} \mathbf{I} \quad \text{Constitutive hypothesis in } \Omega^{cf} \quad (2.47f)$$

$$\phi_u = \mathbf{b} : \mathbf{e}_x(\mathbf{u}^{pm}) + s p^{pm} \quad \text{II Biot's constitutive relation in } \Omega^{pm} \quad (2.47g)$$

$$p^{pm} = p^{cf} \quad \text{Fluid pressure continuity on } \partial \Omega^{cf} \quad (2.47h)$$

$$\boldsymbol{\sigma}^{pm} @ \mathbf{n} = \boldsymbol{\sigma}^{cf} @ \mathbf{n} \quad \text{Stress continuity on } \partial \Omega^{cf} \quad (2.47i)$$

$$\mathbf{q}^{pm} \cdot \mathbf{n} = (\mathbf{v}^{cf} - \dot{\mathbf{u}}^{pm}) \cdot \mathbf{n} \quad \text{Fluid mass balance on } \partial \Omega^{cf} \quad (2.47j)$$

where \mathbf{n} is the outward normal to Ω^{pm} .

The relative flow vector of fluid volume \mathbf{q}^{pm} is defined in Ω^{pm} as:

$$\mathbf{q}^{pm} := \eta_r (\mathbf{v}^{pm} - \dot{\mathbf{u}}^{pm}) \quad (2.48)$$

2.3 Homogenization

In this section the upscaling of the mesoscopic structure is presented. The upscaling technique chosen is the method of double-scale asymptotic expansions. It is applied to the mesoscopic description obtained in the previous section.

2.3.1 Method of double-scale asymptotic expansions

The method has been introduced by (Bensoussan, Lions and Papanicolaou 1978; Keller 1977; Sanchez-Palencia 1974, 1980). More recently, a more physical methodology based on dimensionless analysis has been introduced by Auriault (1991).

As usual in micromechanical approaches, the fields are split into the contributions corresponding to the different length scales which are assumed to be well separated. With this aim, two different space variables are introduced :

- i. let \mathbf{x} denote the “slow” space variable which describes the macroscopic variations;
- ii. let \mathbf{y} denote the “fast” space variable which describes the fluctuations at the small length scale of the heterogeneities;

They are related by means of the scaling parameter ε in the following change of variable (fig. 2.5):

$$\mathbf{y} = \frac{\mathbf{x}}{\varepsilon} \quad (2.49)$$

which may be viewed as a zooming-in of the macroscale in order to make the heterogeneity scale comparable with. By assuming a macroscopic point of view, any space dependent quantity $f = f(\mathbf{x})$ appears as a function of the two variables, $f = f(\mathbf{x}, \mathbf{y})$. While, by using the chain rule, the total derivative with respect to \mathbf{x} reads:

$$\frac{d}{d\mathbf{x}} = \frac{\partial}{\partial \mathbf{x}} + \frac{1}{\varepsilon} \frac{\partial}{\partial \mathbf{y}} \quad (2.50)$$

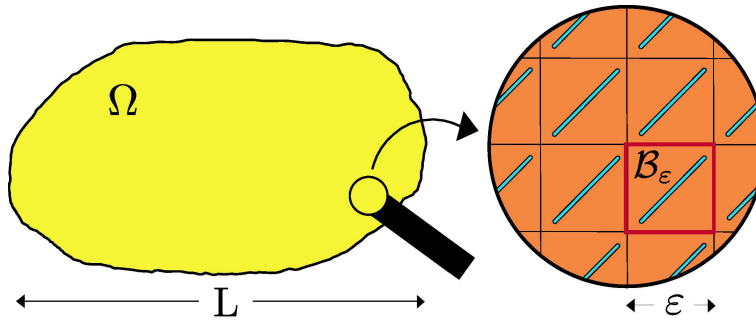


Figure 2.4: The macroscopic continuum and its locally periodic mesoscopic structure.

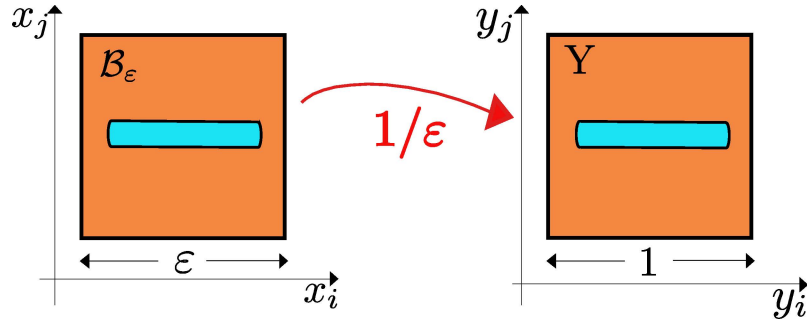


Figure 2.5: Resizing the mesoscopic periodic cell $\mathcal{B}_\varepsilon = [0, \varepsilon] \times [0, \varepsilon]$ to the unit cell, $Y = [0, 1] \times [0, 1]$.

The distribution of fluid-filled cavities is assumed to be periodic (fig. 2.4). Then, a mesoscopic periodic cell \mathcal{B}_ε is identified and it is rescaled by the small parameter ε , to a unit cell $Y = [0, 1] \times [0, 1]$, such that the period of the material is εY . In this way, the parameter ε appears, naturally, as a characteristic length of the mesostructure.

2.3.2 Double-scale asymptotic expansions

The primary variables of the problem $\mathbf{u}^{pm(\varepsilon)}$, $p^{pm(\varepsilon)}$ and $\mathbf{v}^{cf(\varepsilon)}$ are looked for in the form of asymptotic expansions with respect to the powers of ε as follows (Bensoussan, Lions and Papanicolaou 1978; Sanchez-Palencia 1980):

$$\mathbf{u}^{pm(\varepsilon)}(\mathbf{x}) = \mathbf{u}^{pm(0)}\left(\mathbf{x}, \frac{\mathbf{x}}{\varepsilon}\right) + \varepsilon \mathbf{u}^{pm(1)}\left(\mathbf{x}, \frac{\mathbf{x}}{\varepsilon}\right) + \dots \quad (2.51a)$$

$$p^{pm(\varepsilon)}(\mathbf{x}) = p^{pm(0)}\left(\mathbf{x}, \frac{\mathbf{x}}{\varepsilon}\right) + \varepsilon p^{pm(1)}\left(\mathbf{x}, \frac{\mathbf{x}}{\varepsilon}\right) + \dots \quad (2.51b)$$

$$\mathbf{v}^{cf(\varepsilon)}(\mathbf{x}) = \mathbf{v}^{cf(0)}\left(\mathbf{x}, \frac{\mathbf{x}}{\varepsilon}\right) + \varepsilon \mathbf{v}^{cf(1)}\left(\mathbf{x}, \frac{\mathbf{x}}{\varepsilon}\right) + \dots \quad (2.51c)$$

and, as shown in the section 2.3.4.1 for the displacement field, the physical meaning of which is the following (fig. 2.6): $\mathbf{u}^{pm(0)}$ usually denotes the effective or macroscopic displacement field and $\mathbf{u}^{pm(1)}$ stands for the first order displacement perturbations due to the smaller scale structure. This latter one is assumed to be periodic and the size of the periodic cell is denoted by ε . Moreover, a serie of finely heterogeneous materials with $\varepsilon \rightarrow 0$ is considered; it implies that all the fields depend on ε and that is the meaning of the superscript (ε) for all the exact fields, for instance $\mathbf{u}^{pm(\varepsilon)}$. Only the first order terms in the powers of ε are retained because this order of approximation is judged to be appropriate for the studied problem. As a consequence of (2.51) the following expansions are deduced for the infinitesimal strain tensor defined by (2.28) and for the pore pressure

gradient respectively:

$$\mathbf{e}_x(\mathbf{u}^{pm(\varepsilon)}) = \varepsilon^{-1} \mathbf{e}_y(\mathbf{u}^{pm(0)}) + \left(\mathbf{e}_x(\mathbf{u}^{pm(0)}) + \mathbf{e}_y(\mathbf{u}^{pm(1)}) \right) + \varepsilon \mathbf{e}_x(\mathbf{u}^{pm(1)}) + \dots \quad (2.52a)$$

$$\nabla_x(p^{pm(\varepsilon)}) = \varepsilon^{-1} \nabla_y(p^{pm(0)}) + \left(\nabla_x(p^{pm(0)}) + \nabla_y(p^{pm(1)}) \right) + \varepsilon \nabla_x(p^{pm(1)}) + \dots \quad (2.52b)$$

In the expansions of $\boldsymbol{\sigma}^{pm(\varepsilon)}$, $\boldsymbol{\sigma}^{cf(\varepsilon)}$, $\phi_u^{(\varepsilon)}$ and $\mathbf{v}^{pm(\varepsilon)}$ the order in the powers of ε of the first term depends on the constitutive relations (2.27, 2.30, 2.33), and on the Darcy's law (2.35), respectively, leading to:

$$\boldsymbol{\sigma}^{cf(\varepsilon)}(\mathbf{x}) = \boldsymbol{\sigma}^{cf(0)}\left(\mathbf{x}, \frac{\mathbf{x}}{\varepsilon}\right) + \varepsilon \boldsymbol{\sigma}^{cf(1)}\left(\mathbf{x}, \frac{\mathbf{x}}{\varepsilon}\right) + \dots \quad (2.53a)$$

$$\boldsymbol{\sigma}^{pm(\varepsilon)}(\mathbf{x}) = \varepsilon^{-1} \boldsymbol{\sigma}^{pm(-1)}\left(\mathbf{x}, \frac{\mathbf{x}}{\varepsilon}\right) + \boldsymbol{\sigma}^{pm(0)}\left(\mathbf{x}, \frac{\mathbf{x}}{\varepsilon}\right) + \varepsilon \boldsymbol{\sigma}^{pm(1)}\left(\mathbf{x}, \frac{\mathbf{x}}{\varepsilon}\right) + \dots \quad (2.53b)$$

$$\phi_u^{(\varepsilon)}(\mathbf{x}) = \varepsilon^{-1} \phi_u^{(-1)}\left(\mathbf{x}, \frac{\mathbf{x}}{\varepsilon}\right) + \phi_u^{(0)}\left(\mathbf{x}, \frac{\mathbf{x}}{\varepsilon}\right) + \varepsilon \phi_u^{(1)}\left(\mathbf{x}, \frac{\mathbf{x}}{\varepsilon}\right) + \dots \quad (2.53c)$$

$$\mathbf{v}^{pm(\varepsilon)}(\mathbf{x}) = \varepsilon^{-1} \mathbf{v}^{pm(-1)}\left(\mathbf{x}, \frac{\mathbf{x}}{\varepsilon}\right) + \mathbf{v}^{pm(0)}\left(\mathbf{x}, \frac{\mathbf{x}}{\varepsilon}\right) + \varepsilon \mathbf{v}^{pm(1)}\left(\mathbf{x}, \frac{\mathbf{x}}{\varepsilon}\right) + \dots \quad (2.53d)$$

Given these expansions, the following ones are deduced:

$$\operatorname{div}_x(\boldsymbol{\sigma}^{pm(\varepsilon)}) = \varepsilon^{-1} \operatorname{div}_y(\boldsymbol{\sigma}^{pm(0)}) + \left(\operatorname{div}_x(\boldsymbol{\sigma}^{pm(0)}) + \operatorname{div}_y(\boldsymbol{\sigma}^{pm(1)}) \right) + \varepsilon \operatorname{div}_x(\boldsymbol{\sigma}^{pm(1)}) + \dots \quad (2.54a)$$

$$\operatorname{div}_x(\mathbf{v}^{pm(\varepsilon)}) = \varepsilon^{-1} \operatorname{div}_y(\mathbf{v}^{pm(0)}) + \left(\operatorname{div}_x(\mathbf{v}^{pm(0)}) + \operatorname{div}_y(\mathbf{v}^{pm(1)}) \right) + \varepsilon \operatorname{div}_x(\mathbf{v}^{pm(1)}) + \dots \quad (2.54b)$$

Moreover, in view of the asymptotic expansions (2.53d, 2.51a, 2.53c) of $\mathbf{v}^{pm(\varepsilon)}$, $\mathbf{u}^{pm(\varepsilon)}$ and $\phi_u^{(\varepsilon)}$, the form of the expansions of $\mathbf{q}^{pm(\varepsilon)}$ and $\eta_u^{(\varepsilon)}$ is deduced from definitions (1.44b, 2.21) as follows:

$$\mathbf{q}^{pm(\varepsilon)}(\mathbf{x}) = \varepsilon^{-1} \mathbf{q}^{pm(-1)}\left(\mathbf{x}, \frac{\mathbf{x}}{\varepsilon}\right) + \mathbf{q}^{pm(0)}\left(\mathbf{x}, \frac{\mathbf{x}}{\varepsilon}\right) + \varepsilon \mathbf{q}^{pm(1)}\left(\mathbf{x}, \frac{\mathbf{x}}{\varepsilon}\right) + \dots \quad (2.55a)$$

$$\eta_u^{(\varepsilon)}(\mathbf{x}) = \varepsilon^{-1} \eta_u^{(-1)}\left(\mathbf{x}, \frac{\mathbf{x}}{\varepsilon}\right) + \eta_u^{(0)}\left(\mathbf{x}, \frac{\mathbf{x}}{\varepsilon}\right) + \varepsilon \eta_u^{(1)}\left(\mathbf{x}, \frac{\mathbf{x}}{\varepsilon}\right) + \dots \quad (2.55b)$$

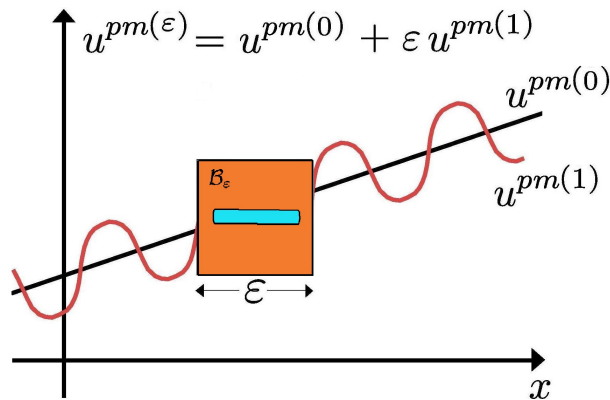


Figure 2.6: Physical meaning of the asymptotic expansions of the displacement field $\mathbf{u}^{pm(\varepsilon)}$.

Finally, it is worth remarking that the functions $\mathbf{u}^{pm(i)}$, $p^{pm(i)}$, $\mathbf{v}^{cf(i)}$, $\boldsymbol{\sigma}^{(i)}$, $\mathbf{v}^{pm(i)}$, $\phi_u^{(i)}$, $\mathbf{q}^{pm(i)}$ and $\eta_u^{(i)}$ are smooth and \mathbf{y} -periodic functions in \mathbf{y} , with period Y .

2.3.3 Asymptotic expansions of the governing equations

The asymptotically expanded variables above, from the (2.51a) to the (2.55b), are substituted in the mesoscopic governing equations recalled at section 2.2 and then, taking into account that $\varepsilon \rightarrow 0$, the relations below are deduced by identification of the like powers of ε .

2.3.3.1 Constitutive Relations

Porous matrix The constitutive law (2.27) in the powers -1 , 0 and 1 of ε respectively reads:

$$\boldsymbol{\sigma}^{pm(-1)} = \mathbf{c}_{@} \mathbf{e}_y(\mathbf{u}^{pm(0)}) \quad (2.56a)$$

$$\boldsymbol{\sigma}^{pm(0)} = \mathbf{c}_{@} \left(\mathbf{e}_x(\mathbf{u}^{pm(0)}) + \mathbf{e}_y(\mathbf{u}^{pm(1)}) \right) - \mathbf{b} p^{pm(0)} \quad (2.56b)$$

$$\boldsymbol{\sigma}^{pm(1)} = \mathbf{c}_{@} \mathbf{e}_x(\mathbf{u}^{pm(1)}) - \mathbf{b} p^{pm(1)} \quad (2.56c)$$

Cavity fluid. The constitutive hypothesis (2.30) in the powers 0 and 1 of ε respectively reads:

$$\boldsymbol{\sigma}^{cf(0)} = -p^{cf(0)} \mathbf{I}, \quad \boldsymbol{\sigma}^{cf(1)} = -p^{cf(1)} \mathbf{I} \quad (2.57)$$

while the incompressibility condition (2.31) in the powers -1 , 0 and 1 of ε respectively reads:

$$0 = \operatorname{div}_y(\mathbf{v}^{cf(0)}), \quad 0 = \operatorname{div}_x(\mathbf{v}^{cf(0)}) + \operatorname{div}_y(\mathbf{v}^{cf(1)}), \quad 0 = \operatorname{div}_x(\mathbf{v}^{cf(1)}) \quad (2.58)$$

Variation of the mesoscopic porosities. The constitutive relations (2.33, 2.34) for the variation of the mesoscopic porosities in the powers -1 , 0 and 1 of ε respectively read:

$$\phi_u^{(-1)} = \mathbf{b} : \mathbf{e}_y(\mathbf{u}^{pm(0)}) \quad (2.59a)$$

$$\phi_u^{(0)} = \mathbf{b} : (\mathbf{e}_y(\mathbf{u}^{pm(1)}) + \mathbf{e}_x(\mathbf{u}^{pm(0)})) + s p^{pm(0)} \quad (2.59b)$$

$$\phi_u^{(1)} = \mathbf{b} : \mathbf{e}_x(\mathbf{u}^{pm(1)}) + s p^{pm(1)} \quad (2.59c)$$

and

$$\eta_u^{(-1)} = (\mathbf{b} - \eta_r \mathbf{I}) : \mathbf{e}_y(\mathbf{u}^{pm(0)}) \quad (2.60a)$$

$$\eta_u^{(0)} = (\mathbf{b} - \eta_r \mathbf{I}) : (\mathbf{e}_y(\mathbf{u}^{pm(1)}) + \mathbf{e}_x(\mathbf{u}^{pm(0)})) + s p^{pm(0)} \quad (2.60b)$$

$$\eta_u^{(1)} = (\mathbf{b} - \eta_r \mathbf{I}) : \mathbf{e}_x(\mathbf{u}^{pm(1)}) + s p^{pm(1)} \quad (2.60c)$$

Moreover, it is useful to write the corresponding expressions for the relation (1.44b) between $\phi_u^{(\varepsilon)}$ and $\eta_u^{(\varepsilon)}$ which in the powers -1 , 0 and 1 of ε reads respectively:

$$\phi_u^{(-1)} = \eta_u^{(-1)} + \eta_r \mathbf{I} : \mathbf{e}_y(\mathbf{u}^{pm(0)}) \quad (2.61a)$$

$$\phi_u^{(0)} = \eta_u^{(0)} + \eta_r \mathbf{I} : (\mathbf{e}_y(\mathbf{u}^{pm(1)}) + \mathbf{e}_x(\mathbf{u}^{pm(0)})) \quad (2.61b)$$

$$\phi_u^{(1)} = \eta_u^{(1)} + \eta_r \mathbf{I} : \mathbf{e}_x(\mathbf{u}^{pm(1)}) \quad (2.61c)$$

2.3.3.2 Linear momentum balance

Both in Ω^{pm} and in Ω^{cf} , the equilibrium (2.1) in the powers -2 , -1 , 0 and 1 of ε reads respectively:

$$0 = \text{div}_y(\boldsymbol{\sigma}^{(-1)}) \quad (2.62a)$$

$$0 = \text{div}_x(\boldsymbol{\sigma}^{(-1)}) + \text{div}_y(\boldsymbol{\sigma}^{(0)}) \quad (2.62b)$$

$$0 = \text{div}_x(\boldsymbol{\sigma}^{(0)}) + \text{div}_y(\boldsymbol{\sigma}^{(1)}) \quad (2.62c)$$

$$0 = \text{div}_x(\boldsymbol{\sigma}^{(1)}) \quad (2.62d)$$

Given that the cavity fluid is assumed to be inviscid, in Ω^{cf} the equilibrium (2.62a) in the powers -1 , 0 and 1 of ε reads respectively:

$$0 = \nabla_y(p^{cf(0)}), \quad 0 = \nabla_x(p^{cf(0)}) + \nabla_y(p^{cf(1)}), \quad 0 = \nabla_x(p^{cf(1)}) \quad (2.63)$$

which, by integration, yield:

$$p^{cf(0)} = p^{cf(0)}(\mathbf{x}, t), \quad p^{cf(1)} = -\nabla_x(p^{cf(0)}) \cdot \mathbf{y} + \tilde{p}^{cf(1)} \quad (2.64)$$

where $p^{cf(0)}$ is homogeneous in every single cavity; while $p^{cf(1)}$ represents the oscillation of the pressure of the cavity fluid which can be observed only from a mesoscopic point of view and $\tilde{p}^{cf(1)}$ is an integration constant.

2.3.3.3 Fluid mass balance

The balance (2.20) in the powers -2 , -1 , 0 and 1 of ε reads respectively:

$$0 = \text{div}_y(\mathbf{q}^{pm(-1)}) \quad (2.65a)$$

$$-\dot{\phi}_u^{(-1)} = \text{div}_y(\mathbf{q}^{pm(0)}) + \text{div}_x(\mathbf{q}^{pm(-1)}) \quad (2.65b)$$

$$-\dot{\phi}_u^{(0)} = \text{div}_y(\mathbf{q}^{pm(1)}) + \text{div}_x(\mathbf{q}^{pm(0)}) \quad (2.65c)$$

$$-\dot{\phi}_u^{(1)} = \text{div}_x(\mathbf{q}^{pm(1)}) \quad (2.65d)$$

where

$$\mathbf{q}^{pm(-1)} = \eta_r \mathbf{v}^{pm(-1)} \quad (2.66a)$$

$$\mathbf{q}^{pm(0)} = \eta_r (\mathbf{v}^{pm(0)} - \dot{\mathbf{u}}^{pm(0)}) \quad (2.66b)$$

$$\mathbf{q}^{pm(1)} = \eta_r (\mathbf{v}^{pm(1)} - \dot{\mathbf{u}}^{pm(1)}) \quad (2.66c)$$

In the same way, the alternative form (2.22) of the fluid mass balance in the powers -2 , -1 , 0 and 1 of ε reads respectively:

$$0 = \operatorname{div}_y \left(\eta_r \mathbf{v}^{pm(-1)} \right) \quad (2.67a)$$

$$-\dot{\eta}_u^{(-1)} = \operatorname{div}_y \left(\eta_r \mathbf{v}^{pm(0)} \right) + \operatorname{div}_x \left(\eta_r \mathbf{v}^{pm(-1)} \right) \quad (2.67b)$$

$$-\dot{\eta}_u^{(0)} = \operatorname{div}_y \left(\eta_r \mathbf{v}^{pm(1)} \right) + \operatorname{div}_x \left(\eta_r \mathbf{v}^{pm(0)} \right) \quad (2.67c)$$

$$-\dot{\eta}_u^{(1)} = \operatorname{div}_x \left(\eta_r \mathbf{v}^{pm(1)} \right) \quad (2.67d)$$

2.3.3.4 Darcy's law

The Darcy's law (2.35) in the powers -1 , 0 and 1 of ε respectively reads:

$$\mathbf{q}^{pm(-1)} = -\mathbf{k}_@ \nabla_y p^{pm(0)} \quad (2.68a)$$

$$\mathbf{q}^{pm(0)} = -\mathbf{k}_@ \left(\nabla_x p^{pm(0)} + \nabla_y p^{pm(1)} \right) \quad (2.68b)$$

$$\mathbf{q}^{pm(1)} = -\mathbf{k}_@ \nabla_x p^{pm(1)} \quad (2.68c)$$

2.3.3.5 Conditions at the cavity boundary

Stress continuity. The (2.43) in the powers -1 , 0 and 1 of ε reads respectively:

$$\boldsymbol{\sigma}^{pm(-1)} @ \mathbf{n} = 0, \quad \boldsymbol{\sigma}^{pm(0)} @ \mathbf{n} = -p^{cf(0)} \mathbf{n}, \quad \boldsymbol{\sigma}^{pm(1)} @ \mathbf{n} = -p^{cf(1)} \mathbf{n} \quad (2.69)$$

Fluid pressure continuity. The (2.44) in the powers 0 and 1 of ε reads respectively:

$$p^{pm(0)} = p^{cf(0)}, \quad p^{pm(1)} = p^{cf(1)} \quad (2.70)$$

which, by taking into account the (2.64), become:

$$p^{pm(0)} = p^{cf(0)}(\mathbf{x}, t), \quad p^{pm(1)} = -\nabla_x (p^{cf(0)}) \cdot \mathbf{y} + \tilde{p}^{cf(1)} \quad (2.71)$$

Fluid mass balance. The (2.45) in the powers -1 , 0 and 1 of ε reads respectively:

$$\mathbf{q}^{pm(-1)} \cdot \mathbf{n} = 0 \quad (2.72a)$$

$$\mathbf{q}^{pm(0)} \cdot \mathbf{n} = (\mathbf{v}^{cf(0)} - \dot{\mathbf{u}}^{pm(0)}) \cdot \mathbf{n} \quad (2.72b)$$

$$\mathbf{q}^{pm(1)} \cdot \mathbf{n} = (\mathbf{v}^{cf(1)} - \dot{\mathbf{u}}^{pm(1)}) \cdot \mathbf{n} \quad (2.72c)$$

while, its integrated form (2.46) on the resized interface Γ between the porous solid and the cavity yields:

$$\int_{\Gamma} \mathbf{q}^{pm(-1)} \cdot \mathbf{n} \, ds = 0 \quad (2.73a)$$

$$\int_{\Gamma} \mathbf{q}^{pm(0)} \cdot \mathbf{n} \, ds = - \int_{\Gamma} \dot{\mathbf{u}}^{pm(0)} \cdot \mathbf{n} \, ds \quad (2.73b)$$

$$\int_{\Gamma} \mathbf{q}^{pm(1)} \cdot \mathbf{n} \, ds = \int_{Y^{cf}} \operatorname{div}_x(\mathbf{v}^{cf(0)}) \, dv - \int_{\Gamma} \dot{\mathbf{u}}^{pm(1)} \cdot \mathbf{n} \, ds \quad (2.73c)$$

where Y^{cf} is the cavity domain included in the resized periodic cell Y (fig. 2.7).

2.3.4 Unit cell problems

By means of a proper selection of the like powers of ε equalities of the different governing equations presented in the previous section, from the (2.56) to (2.73), a set of successive boundary-value problems defined on the unit cell $Y = Y^{pm} \cup Y^{cf}$ (fig. 2.7) are built and investigated below. Their analytical solving provides the expected informations about the macroscopic nature of the fields $\mathbf{u}^{pm(0)}$ and $p^{pm(0)}$, while analytical solutions are obtained for the fields $\mathbf{u}^{pm(1)}$ and $p^{pm(1)}$.

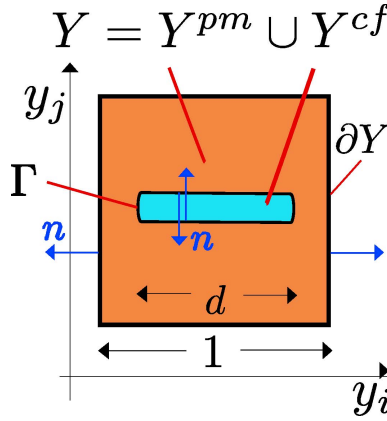


Figure 2.7: Notation in the periodic unit cell Y . Orientation of the unit normal vector \mathbf{n} : outward with respect to Y^{pm}

2.3.4.1 BVP for $\mathbf{u}^{pm(0)}$

At the lowest power of ε , the linear momentum balance (2.62a), the constitutive equation (2.56a) in Y^{pm} and the stress continuity condition (2.69a) on Γ set up a pure mechanical boundary-value problem for $\mathbf{u}^{pm(0)}$:

$$\begin{cases} \text{in } Y^{pm}, & \operatorname{div}_y \boldsymbol{\sigma}^{pm(-1)} = 0 \\ \text{in } Y^{pm}, & \boldsymbol{\sigma}^{pm(-1)} = \mathbf{c} @ \mathbf{e}_y(\mathbf{u}^{pm(0)}) \\ \text{on } \Gamma, & \boldsymbol{\sigma}^{pm(-1)} @ \mathbf{n} = \mathbf{0} \end{cases} \quad (2.74)$$

It worths pointing out that the functions $\boldsymbol{\sigma}^{pm(-1)}$ and $\mathbf{u}^{pm(0)}$ are \mathbf{y} -periodic. In order to investigate this problem, the space \mathcal{Z} of vectors \mathbf{z} is introduced:

$$\mathcal{Z} := \left\{ \mathbf{z}(\mathbf{x}, \mathbf{y}) \mid (\mathbf{x}, \mathbf{y}) \in Y^{pm}, \mathbf{y}\text{-periodic} \right\} \quad (2.75)$$

The virtual power formulation of the problem (2.74) reads:

$$\forall \mathbf{z} \in \mathcal{Z}, \quad \int_{Y^{pm}} \left(\mathbf{c} @ \mathbf{e}_y(\mathbf{u}^{pm(0)}) \right) : \mathbf{e}_y(\mathbf{z}) \, dv = 0 \quad (2.76)$$

and it is apparent that the solution does not depend on the fast space variable \mathbf{y} :

$$\text{in } Y^{pm}, \quad \mathbf{u}^{pm(0)} = \mathbf{u}^{pm(0)}(\mathbf{x}) \quad (2.77)$$

Then, as expected, $\mathbf{u}^{pm(0)}$ is the macroscopic contribution to the displacement field and, by taking into account (2.74b, 2.59a, 2.60a), it follows respectively that:

$$\boldsymbol{\sigma}^{pm(-1)} = 0 \quad \phi_u^{(-1)} = 0 \quad \eta_u^{(-1)} = 0 \quad (2.78)$$

Consequently, the form of the corresponding asymptotic expansions (2.51a, 2.53b, 2.55b, 2.53c) will be updated in the section 2.3.5.

2.3.4.2

At the lowest power of ε , the fluid mass balance (2.65a) and the Darcy's law (2.68a) in Y^{pm} , the linear momentum balance (2.63a) in Y^{cf} , and the fluid pressure continuity (2.71a) on Γ set up a pure hydraulic boundary-value problem for $p^{pm(0)}$:

$$\begin{cases} \text{in } Y^{pm}, & 0 = \text{div}_y \mathbf{q}^{pm(-1)} \\ \text{in } Y^{pm}, & \mathbf{q}^{pm(-1)} = -\mathbf{k}_@ \nabla_y p^{pm(0)} \\ \text{in } Y^{cf}, & 0 = \nabla_y p^{cf(0)} \\ \text{on } \Gamma, & p^{pm(0)} = p^{cf(0)} \end{cases} \quad (2.79)$$

where, as already written in the (2.66a), $\mathbf{q}^{pm(-1)} = \phi_r \mathbf{v}^{pm(-1)}$.

It is worth reminding that both the functions $\mathbf{q}^{pm(-1)}$ and $p^{pm(0)}$ are \mathbf{y} -periodic.

In order to investigate this problem, the space \mathcal{H} of scalars functions h is introduced:

$$\mathcal{H} := \left\{ h(\mathbf{x}, \mathbf{y}) \mid (\mathbf{x}, \mathbf{y}) \in Y^{pm}, \mathbf{y}\text{-periodic} \right\} \quad (2.80)$$

The virtual power formulation of the problem (2.79) reads:

$$\forall h \in \mathcal{H}, \quad \int_{Y^{pm}} \left(\mathbf{k}_@ \nabla_y p^{pm(0)} \right) \cdot \nabla_y h \, dv = 0 \quad (2.81)$$

Then, it is clear that the solution does not depend on the fast space variable \mathbf{y} :

$$p^{pm(0)} = p^{pm(0)}(\mathbf{x}) \quad \text{in } Y^{pm}. \quad (2.82)$$

So, as expected, $p^{pm(0)}$ is the macroscopic contribution to the pore fluid pressure field and, by taking into account (2.79b, 2.66a), it follows that:

$$\mathbf{q}^{pm(-1)} = 0 \quad \implies \quad \mathbf{v}^{pm(-1)} = 0 \quad (2.83)$$

Moreover, given the relations (2.82, 2.79c, 2.79d), it is clear that the fluid pressure at order zero in the powers of ε is homogeneous over all the unit cell:

$$p^{(0)} = p^{(0)}(\mathbf{x}) \quad \text{in } Y = Y^{pm} \cup Y^{cf}. \quad (2.84)$$

Then, the double notation $p^{pm(0)}$ and $p^{cf(0)}$ could be already put aside, but it is kept until the end of the chapter 3 with the aim of making the procedure more clear. Consequently, the form of the corresponding asymptotic expansions (2.51b, 2.53d, 2.55a) will be updated in the section 2.3.5.

2.3.4.3 BVP for $\mathbf{u}^{pm(1)}$

At a higher power of ε , the linear momentum balance (2.62ab), the constitutive equation (2.56b) in Y^{pm} and the stress continuity (2.69b) on Γ set up a pure mechanical boundary-value problem for $\mathbf{u}^{pm(1)}$, being given both $\mathbf{u}^{pm(0)}$ and $p^{pm(0)}$:

$$\begin{cases} \text{in } Y^{pm}, & \operatorname{div}_y (\boldsymbol{\sigma}^{pm(0)} + p^{pm(0)} \mathbf{I}) = 0 \\ \text{in } Y^{pm}, & \boldsymbol{\sigma}^{pm(0)} + p^{pm(0)} \mathbf{I} = \mathbf{c}_@ (\mathbf{e}_x(\mathbf{u}^{pm(0)}) + \mathbf{e}_y(\mathbf{u}^{pm(1)})) + p^{pm(0)} (\mathbf{I} - \mathbf{b}) \\ \text{on } \Gamma, & \boldsymbol{\sigma}^{pm(0)} @ \mathbf{n} = -p^{pm(0)} \mathbf{n} \end{cases} \quad (2.85)$$

where the first two equations are written taking into account that $p^{pm(0)}$ is a macroscopic term.

It is worth reminding that also the functions $\boldsymbol{\sigma}^{pm(0)}$ and $\mathbf{u}^{pm(1)}$ are \mathbf{y} -periodic.

This problem is investigated by means of the vector space \mathcal{Z} , previously defined by the (2.75), and its virtual power formulation reads: $\forall \mathbf{z} \in \mathcal{Z}$,

$$\int_{Y^{pm}} \mathbf{c}_@ \mathbf{e}_y(\mathbf{u}^{pm(1)}) : \mathbf{e}_y(\mathbf{z}) \, dv = - \int_{Y^{pm}} \left(\mathbf{c}_@ \mathbf{e}_x(\mathbf{u}^{pm(0)}) + p^{pm(0)} (\mathbf{I} - \mathbf{b}) \right) : \mathbf{e}_y(\mathbf{z}) \, dv \quad (2.86)$$

let us define the macroscopic and symmetric second order tensor, $\mathbf{T}(\mathbf{x})$, as:

$$\mathbf{T}(\mathbf{x}) := \mathbf{c}_@ \mathbf{e}_x(\mathbf{u}^{pm(0)})(\mathbf{x}) + (\mathbf{I} - \mathbf{b}) p^{pm(0)}(\mathbf{x}) \quad (2.87)$$

It can be decomposed on any orthonormal basis as:

$$\mathbf{T} = T_{ij} (\mathbf{e}_i \otimes \mathbf{e}_j) \quad (2.88)$$

Therefore, the weak formulation (2.86) is rewritten as: $\forall \mathbf{z} \in \mathcal{Z}$,

$$\int_{Y^{pm}} \mathbf{c}_@ \mathbf{e}_y(\mathbf{u}^{pm(1)}) : \mathbf{e}_y(\mathbf{z}) \, dv = - T_{ij} \int_{Y^{pm}} (\mathbf{e}_i \otimes \mathbf{e}_j) : \mathbf{e}_y(\mathbf{z}) \, dv \quad (2.89)$$

Let the vector $\boldsymbol{\xi}^{ij}(\mathbf{y})$ verify:

$$\forall \mathbf{z} \in \mathcal{Z}, \quad \int_{Y^{pm}} \mathbf{c}_@ \mathbf{e}_y(\boldsymbol{\xi}^{ij}) : \mathbf{e}_y(\mathbf{z}) \, dv = - \int_{Y^{pm}} (\mathbf{e}_i \otimes \mathbf{e}_j) : \mathbf{e}_y(\mathbf{z}) \, dv \quad (2.90)$$

Let the superscript symm denote the symmetric part of a second order tensor and let us take into account that $\mathbf{e}_y(\mathbf{z})$ is symmetric by definition. So, it follows that:

$$(\mathbf{e}_i \otimes \mathbf{e}_j) : \mathbf{e}_y(\mathbf{z}) = (\mathbf{e}_i \otimes \mathbf{e}_j)^{\text{symm}} : \mathbf{e}_y(\mathbf{z}) \implies \boldsymbol{\xi}^{ij} = \boldsymbol{\xi}^{ji} \quad (2.91)$$

And given the linearity of the problem, by comparing the (2.89) and the (2.90) it is easily deduced that the solution of the boundary-value problem (2.85) reads:

$$\mathbf{u}^{pm(1)}(\mathbf{x}, \mathbf{y}) = T_{ij}(\mathbf{x}) \boldsymbol{\xi}^{ij}(\mathbf{y}) \quad \text{with} \quad T_{ij} = \mathbf{T} : (\mathbf{e}_i \otimes \mathbf{e}_j) \quad (2.92)$$

where it is already clear that the dependency on the two space variables, \mathbf{x} and \mathbf{y} , is separated.

let us define a linear application from $\mathcal{L}(\mathbf{V})$ to \mathbf{V} as¹:

$$\boldsymbol{\Xi}(\mathbf{y}) := \boldsymbol{\xi}^{ij}(\mathbf{y}) \otimes (\mathbf{e}_i \otimes \mathbf{e}_j) \quad (2.93)$$

actually, it transforms a second order tensor, $\mathbf{S} \in \mathcal{L}(\mathbf{V})$, into a vector such that:

$$\forall \mathbf{S} \in \mathcal{L}(\mathbf{V}), \quad \boldsymbol{\Xi} @ \mathbf{S} = \boldsymbol{\xi}^{ij} \otimes (\mathbf{e}_i \otimes \mathbf{e}_j) : \mathbf{S} = S_{ij} \boldsymbol{\xi}^{ij} \quad (2.94)$$

Therefore, the (2.92) is rewritten as:

$$\mathbf{u}^{pm(1)}(\mathbf{x}, \mathbf{y}) = \boldsymbol{\Xi}(\mathbf{y}) @ \mathbf{T}(\mathbf{x}) \quad (2.95)$$

which given the (2.87) becomes:

$$\mathbf{u}^{pm(1)}(\mathbf{x}, \mathbf{y}) = \boldsymbol{\Xi}(\mathbf{y}) @ \left(\mathbf{c} @ \mathbf{e}_x(\mathbf{u}^{pm(0)}(\mathbf{x})) \right) + \boldsymbol{\Xi}(\mathbf{y}) @ (\mathbf{I} - \mathbf{b}) p^{pm(0)}(\mathbf{x}) \quad (2.96)$$

or, by using the properties of the composition of tensors:

$$\mathbf{u}^{pm(1)}(\mathbf{x}, \mathbf{y}) = \left(\boldsymbol{\Xi}(\mathbf{y}) \circ \mathbf{c} \right) @ \mathbf{e}_x(\mathbf{u}^{pm(0)}(\mathbf{x})) + \boldsymbol{\Xi}(\mathbf{y}) @ (\mathbf{I} - \mathbf{b}) p^{pm(0)}(\mathbf{x}) \quad (2.97)$$

Moreover, given the definition of $\boldsymbol{\Xi}$, (2.93), it also reads:

$$\mathbf{u}^{pm(1)}(\mathbf{x}, \mathbf{y}) = \boldsymbol{\xi}^{lm}(\mathbf{y}) \mathbf{e}_{xlm}(\mathbf{u}^{pm(0)}(\mathbf{x})) + \boldsymbol{\pi}(\mathbf{y}) p^{pm(0)}(\mathbf{x}) \quad (2.98)$$

where the vector $\boldsymbol{\pi}$ is defined as:

$$\boldsymbol{\pi}(\mathbf{y}) = \boldsymbol{\Xi}(\mathbf{y}) @ (\mathbf{I} - \mathbf{b}) = \boldsymbol{\xi}^{ij}(\mathbf{y}) (\delta_{ij} - b_{ij}). \quad (2.99)$$

In the end, it is clear that $\mathbf{u}^{pm(1)}$ depends linearly on the macroscopic strain tensor $\mathbf{e}_x(\mathbf{u}^{pm(0)})$ and on the macroscopic pressure field $p^{pm(0)}$; while, the dependency on the small length scale is concentrated in the coefficients $\boldsymbol{\xi}^{ij}$.

¹The result of the dyadic product between a second order tensor and a vector is a third order tensor.

2.3.4.4 BVP for $p^{pm(1)}$, $\mathbf{v}^{pm(0)}$ and $\mathbf{v}^{cf(0)}$

At a higher power of ε , the fluid mass balance (2.65b), the Darcy's law (2.68a) in Y^{pm} , the linear momentum balance (2.63b) within the constitutive hypothesis, the incompressibility condition (2.58b) of the cavity fluid in Y^{cf} , the fluid mass balance (2.72b) through the interface and the fluid pressure continuity (2.71b) on Γ set up a pure hydraulic boundary-value problem for $p^{pm(1)}$, $\mathbf{v}^{pm(0)}$ and $\mathbf{v}^{cf(0)}$, being given both $\mathbf{u}^{pm(0)}$ and $p^{pm(0)}$:

$$\begin{cases} \text{in } Y^{pm}, & \operatorname{div}_y \mathbf{q}^{pm(0)} = 0 \\ \text{in } Y^{pm}, & \mathbf{q}^{pm(0)} = -\mathbf{k}_@ \left(\nabla_x p^{pm(0)} + \nabla_y p^{pm(1)} \right) \\ \text{in } Y^{cf}, & 0 = \nabla_y p^{cf(1)} + \nabla_x p^{cf(0)} \\ \text{in } Y^{cf}, & 0 = \operatorname{div}_y (\mathbf{v}^{cf(0)}) \\ \text{on } \Gamma, & \mathbf{q}^{pm(0)} \cdot \mathbf{n} = \left(\mathbf{v}^{cf(0)} - \dot{\mathbf{u}}^{pm(0)} \right) \cdot \mathbf{n} \\ \text{on } \Gamma, & p^{pm(1)} = p^{cf(1)} \end{cases} \quad (2.100)$$

where, as already written in the (2.66b), $\mathbf{q}^{pm(0)} = \phi_r(\mathbf{v}^{pm(0)} - \dot{\mathbf{u}}^{pm(0)})$, and the (2.100d) is written taking into account that $\mathbf{u}^{pm(0)}$ is a macroscopic term.

This problem can be split in two sub-problems to be solved successively: a first one composed by the (2.100a, 2.100b, 2.100c, 2.100f), the solution of which are $p^{pm(1)}$ and $\mathbf{v}^{pm(0)}$; then, a second one composed by the (2.100d, 2.100e) for $\mathbf{v}^{cf(0)}$.

It is worth remarking that, as already written in the (2.64b) and as clear from the (2.100c), $p^{cf(1)}$ is defined up to an additive constant. Then, given the (2.100f), it is possible to look for a particular solution of the first sub-problem of the (2.100) which reads:

$$\begin{cases} \text{in } Y^{pm}, & \operatorname{div}_y \mathbf{q}^{pm(0)} = 0 \\ \text{in } Y^{pm}, & \mathbf{q}^{pm(0)} = -\mathbf{k}_@ \left(\nabla_x p^{pm(0)} + \nabla_y p^{pm(1)} \right) \\ \text{on } \Gamma, & p^{pm(1)} = -(\nabla_x p^{pm(0)}) \cdot \mathbf{y} \end{cases} \quad (2.101)$$

Being $p^{pm(1)}$ determined up to an additive constant, then $\mathbf{v}^{pm(0)}$ is uniquely determined by the (2.101b).

Let us define the space \mathcal{W} of scalar functions w as:

$$\mathcal{W} := \left\{ w(\mathbf{x}, \mathbf{y}) \mid (\mathbf{x}, \mathbf{y}) \in Y^{pm}, \mathbf{y}\text{-periodic}, \nabla_y w = \mathbf{0} \text{ on } \Gamma \right\} \quad (2.102)$$

Then the virtual power formulation of the problem (2.101) reads:

$$\forall w \in \mathcal{W}, \quad \int_{Y^{pm}} \left(\mathbf{k}_@ (\nabla_x p^{pm(0)} + \nabla_y p^{pm(1)}) \right) \cdot \nabla_y w \, dv = 0 \quad (2.103)$$

Let $\zeta^i(\mathbf{y})$ be the solution of the following problem:

$$\begin{cases} \text{in } Y^{cf}, & \zeta^i(\mathbf{y}) = -\mathbf{e}_i \cdot \mathbf{y} \\ \text{on } \Gamma, \forall w \in \mathcal{W}, & \int_{Y^{pm}} \left(\mathbf{k}_@(\mathbf{e}_i + \nabla_y \zeta^i(\mathbf{y})) \right) \cdot \nabla_y w \, dv = 0 \end{cases} \quad (2.104)$$

Given the linearity of the problem, it is easily deduced that:

$$p^{pm(1)}(\mathbf{x}, \mathbf{y}) = \zeta^i(\mathbf{y}) \sum_i \nabla_x p^{pm(0)}(\mathbf{x}) \cdot \mathbf{e}_i \quad (2.105)$$

And by defining the vector $\mathbf{Z}(\mathbf{y})$ as:

$$\mathbf{Z}(\mathbf{y}) = \sum_i \zeta^i(\mathbf{y}) \mathbf{e}_i \quad (2.106)$$

then, the (2.105) is rewritten as:

$$p^{pm(1)}(\mathbf{x}, \mathbf{y}) = \nabla_x p^{pm(0)}(\mathbf{x}) \cdot \mathbf{Z}(\mathbf{y}) \quad (2.107)$$

It is worth remarking that $p^{pm(1)}$ depends linearly from the gradient of the macroscopic pressure $\nabla_x p^{pm(0)}$; while, the dependency on the small length scale is concentrated in the coefficients $\zeta^i(\mathbf{y})$.

Therefore, being given $p^{pm(1)}$ and $\mathbf{v}^{pm(0)}$, the second sub-problem of the (2.100) in $\mathbf{v}^{cf(0)}$ reads:

$$\begin{cases} \text{in } Y^{cf}, & \text{div}_y (\mathbf{v}^{cf(0)} - \dot{\mathbf{u}}^{pm(0)}) = 0 \\ \text{on } \Gamma, & \mathbf{q}^{pm(0)} \cdot \mathbf{n} = (\mathbf{v}^{cf(0)} - \dot{\mathbf{u}}^{pm(0)}) \cdot \mathbf{n} \end{cases} \quad (2.108)$$

and, as already known, by means of these equations $\mathbf{v}^{cf(0)}$ is not determinable. Notwithstanding that, it is shown in the calculus below that they enable to determine the integral $\int_{Y^{cf}} (\mathbf{v}^{cf(0)} - \dot{\mathbf{u}}^{pm(0)}) \, dv$ which is helpful to write the macroscopic equations.

A useful calculus. In this section, it is presented the calculus for determination of the integral $\int_{Y^{cf}} (\mathbf{v}^{cf(0)} - \dot{\mathbf{u}}^{pm(0)}) \, dv$ which is useful in the analytical developments leading to the homogenized Darcy's law (section 2.4.5). Let us define the space \mathcal{Q} of scalars functions q as:

$$\mathcal{Q} := \left\{ q(\mathbf{x}, \mathbf{y}) \mid (\mathbf{x}, \mathbf{y}) \in Y = Y^{pm} \cup Y^{cf} \right\} \quad (2.109)$$

Then, the virtual power formulation of the (2.101a) reads:

$$\forall q \in \mathcal{Q}, \quad - \int_{Y^{pm}} \mathbf{q}^{pm(0)} \cdot \nabla_y q \, dv + \int_{\partial Y} \mathbf{q}^{pm(0)} \cdot \mathbf{n} \, q \, ds + \int_{\Gamma} (\mathbf{v}^{cf(0)} - \dot{\mathbf{u}}^{pm(0)}) \cdot \mathbf{n} \, q \, ds = 0 \quad (2.110)$$

where the fluid mass balance (2.108b) through Γ is taken into account. And the virtual power formulation of the (2.108a) reads: $\forall q \in \mathcal{Q}$,

$$\int_{Y^{cf}} (\mathbf{v}^{cf(0)} - \dot{\mathbf{u}}^{pm(0)}) \cdot \nabla_y q \, dv + \int_{\Gamma} q (\mathbf{v}^{cf(0)} - \dot{\mathbf{u}}^{pm(0)}) \cdot \mathbf{n} \, ds = 0 \quad (2.111)$$

where the signs are the consequence of the orientation of the unit normal vector \mathbf{n} : inward with respect to Y^{cf} (fig. 2.7). The combination of the (2.110) and of the (2.111) yields the weak formulation of the (2.101a, 2.108a, 2.108b): $\forall q \in \mathcal{Q}$,

$$- \int_{Y^{pm}} \mathbf{q}^{pm(0)} \cdot \nabla_y q \, dv - \int_{Y^{cf}} (\mathbf{v}^{cf(0)} - \dot{\mathbf{u}}^{pm(0)}) \cdot \nabla_y q \, dv + \int_{\partial Y} \mathbf{q}^{pm(0)} \cdot \mathbf{n} \, q \, ds = 0 \quad (2.112)$$

Now, let us introduce a second and enriched space $\tilde{\mathcal{Q}}$ of scalars functions \tilde{q} as:

$$\tilde{\mathcal{Q}} := \left\{ \tilde{q}(\mathbf{x}, \mathbf{y}) \mid (\mathbf{x}, \mathbf{y}) \in Y = Y^{pm} \cup Y^{cf}, \tilde{q} = \mathbf{a}(\mathbf{x}) \cdot \mathbf{y} \right\} \quad (2.113)$$

The weak formulation (2.112) can be rewritten by using \tilde{q} as test function instead of q and it reads: $\forall \mathbf{a}(\mathbf{x})$,

$$\mathbf{a} \cdot \left(- \int_{Y^{pm}} \mathbf{q}^{pm(0)} \, dv - \int_{Y^{cf}} (\mathbf{v}^{cf(0)} - \dot{\mathbf{u}}^{pm(0)}) \, dv + \int_{\partial Y} (\mathbf{q}^{pm(0)} \cdot \mathbf{n}) \, \mathbf{y} \, ds \right) = 0 \quad (2.114)$$

or, as $\mathbf{a}(\mathbf{x})$ is any vector:

$$\int_{Y^{cf}} (\mathbf{v}^{cf(0)} - \dot{\mathbf{u}}^{pm(0)}) \, dv = - \int_{Y^{pm}} \mathbf{q}^{pm(0)} \, dv + \int_{\partial Y} (\mathbf{q}^{pm(0)} \cdot \mathbf{n}) \, \mathbf{y} \, ds \quad (2.115)$$

which proves that, just like $\mathbf{v}^{pm(0)}$, also the investigated integral is uniquely determined. With the aim of determining it, it is useful going back to the weak formulation (2.112) and rewriting it by means of a \mathbf{y} -periodic test function $q = \zeta^i$. So, given the (2.104a), it reads:

$$- \int_{Y^{pm}} \mathbf{q}^{pm(0)} \cdot \nabla_y \zeta^i \, dv + \int_{Y^{cf}} (\mathbf{v}^{cf(0)} - \dot{\mathbf{u}}^{pm(0)}) \cdot \mathbf{e}_i \, dv = 0 \quad (2.116)$$

which entails:

$$- \sum_i \left[\int_{Y^{pm}} \mathbf{q}^{pm(0)} \cdot \nabla_y \zeta^i \, dv \right] \mathbf{e}_i + \sum_i \left[\int_{Y^{cf}} (\mathbf{v}^{cf(0)} - \dot{\mathbf{u}}^{pm(0)}) \cdot \mathbf{e}_i \, dv \right] \mathbf{e}_i = 0 \quad (2.117)$$

that is:

$$\int_{Y^{cf}} (\mathbf{v}^{cf(0)} - \dot{\mathbf{u}}^{pm(0)}) \, dv = \int_{Y^{pm}} \left(\sum_i \mathbf{e}_i \otimes \nabla_y \zeta^i \right) @ \mathbf{q}^{pm(0)} \, dv \quad (2.118)$$

Given the definition (2.106) of the vector $\mathbf{Z}(\mathbf{y})$, it follows that:

$$\nabla_y \mathbf{Z}(\mathbf{y}) = \sum_i \mathbf{e}_i \otimes \nabla_y \zeta^i(\mathbf{y}) \quad (2.119)$$

Finally, the (2.118) is rewritten as follows and provides a useful expression of the integral at the left member:

$$\int_{Y^{cf}} (\mathbf{v}^{cf(0)} - \dot{\mathbf{u}}^{pm(0)}) dv = \int_{Y^{pm}} \nabla_y \mathbf{Z} @ \mathbf{q}^{pm(0)} dv \quad (2.120)$$

2.3.5 Synopsis of asymptotic expansions

From the previous sections, $\mathbf{u}^{pm(0)}$ and $p^{pm(0)}$ are known to be the macroscopic contribution, respectively, to the displacement and pore fluid pressure field, (2.77) and (2.82):

$$\mathbf{u}^{pm(0)} = \mathbf{u}^{pm(0)}(\mathbf{x}, t) \quad p^{pm(0)} = p^{pm(0)}(\mathbf{x}, t)$$

While the terms representative of the oscillations due to the meso-structure, $\mathbf{u}^{pm(1)}$ and $p^{pm(1)}$, are linearly dependent on the macroscopic terms and the dependency on the small length scale \mathbf{x}/ε is respectively concentrated in the coefficients $\boldsymbol{\xi}^{lm}$ and ζ^i , as written in the (2.98) and in the (2.105):

$$\mathbf{u}^{pm(1)}\left(\mathbf{x}, \frac{\mathbf{x}}{\varepsilon}\right) = \boldsymbol{\xi}^{lm}(\mathbf{x}/\varepsilon) e_{xlm}(\mathbf{u}^{pm(0)}(\mathbf{x})) + \boldsymbol{\pi}(\mathbf{x}/\varepsilon) p^{pm(0)}(\mathbf{x})$$

and

$$p^{pm(1)}\left(\mathbf{x}, \frac{\mathbf{x}}{\varepsilon}\right) = \zeta^i(\mathbf{x}/\varepsilon) \sum_i \nabla_x p^{pm(0)}(\mathbf{x}) \cdot \mathbf{e}_i$$

Then the form of the asymptotic expansions of all the variables, from (2.51a) to (2.55b), are updated as follows:

$$\mathbf{u}^{pm(\varepsilon)}(\mathbf{x}) = \mathbf{u}^{pm(0)}(\mathbf{x}) + \varepsilon \mathbf{u}^{pm(1)}\left(\mathbf{x}, \frac{\mathbf{x}}{\varepsilon}\right) + \dots \quad (2.121a)$$

$$p^{pm(\varepsilon)}(\mathbf{x}) = p^{pm(0)}(\mathbf{x}) + \varepsilon p^{pm(1)}\left(\mathbf{x}, \frac{\mathbf{x}}{\varepsilon}\right) + \dots \quad (2.121b)$$

$$\mathbf{v}^{cf(\varepsilon)}(\mathbf{x}) = \mathbf{v}^{cf(0)}(\mathbf{x}, \mathbf{x}/\varepsilon) + \varepsilon \mathbf{v}^{cf(1)}\left(\mathbf{x}, \frac{\mathbf{x}}{\varepsilon}\right) + \dots \quad (2.121c)$$

and

$$\boldsymbol{\sigma}^{cf(\varepsilon)}(\mathbf{x}) = \boldsymbol{\sigma}^{cf(0)}(\mathbf{x}) + \varepsilon \boldsymbol{\sigma}^{cf(1)}\left(\mathbf{x}, \frac{\mathbf{x}}{\varepsilon}\right) + \dots \quad (2.122a)$$

$$\boldsymbol{\sigma}^{pm(\varepsilon)}(\mathbf{x}) = \boldsymbol{\sigma}^{pm(0)}\left(\mathbf{x}, \frac{\mathbf{x}}{\varepsilon}\right) + \varepsilon \boldsymbol{\sigma}^{pm(1)}\left(\mathbf{x}, \frac{\mathbf{x}}{\varepsilon}\right) + \dots \quad (2.122b)$$

$$\mathbf{v}^{pm(\varepsilon)}(\mathbf{x}) = \mathbf{v}^{pm(0)}\left(\mathbf{x}, \frac{\mathbf{x}}{\varepsilon}\right) + \varepsilon \mathbf{v}^{pm(1)}\left(\mathbf{x}, \frac{\mathbf{x}}{\varepsilon}\right) + \dots \quad (2.122c)$$

$$\phi_u^{(\varepsilon)}(\mathbf{x}) = \phi_u^{(0)}\left(\mathbf{x}, \frac{\mathbf{x}}{\varepsilon}\right) + \varepsilon \phi_u^{(1)}\left(\mathbf{x}, \frac{\mathbf{x}}{\varepsilon}\right) + \dots \quad (2.122d)$$

and

$$\mathbf{q}^{pm(\varepsilon)}(\mathbf{x}) = \mathbf{q}^{pm(0)}\left(\mathbf{x}, \frac{\mathbf{x}}{\varepsilon}\right) + \varepsilon \mathbf{q}^{pm(1)}\left(\mathbf{x}, \frac{\mathbf{x}}{\varepsilon}\right) + \dots \quad (2.123a)$$

$$\eta_u^{(\varepsilon)}(\mathbf{x}) = \eta_u^{(0)}\left(\mathbf{x}, \frac{\mathbf{x}}{\varepsilon}\right) + \varepsilon \eta_u^{(1)}\left(\mathbf{x}, \frac{\mathbf{x}}{\varepsilon}\right) + \dots \quad (2.123b)$$

2.4 Macroscopic description

2.4.1 Linear momentum balance

Let us define the homogenized stress Σ over the unit cell Y as:

$$|Y| \Sigma := \int_Y \boldsymbol{\sigma}^{(0)} dv \quad (2.124)$$

where $|Y|$ is the volume of the cell Y and $\boldsymbol{\sigma}^{(0)}$ is such that:

$$\boldsymbol{\sigma}^{(0)} = \begin{cases} \boldsymbol{\sigma}^{pm(0)} & \text{in } Y^{pm} \\ \boldsymbol{\sigma}^{cf(0)} & \text{in } Y^{cf} \end{cases} \quad (2.125)$$

Then, the definition above also reads:

$$|Y| \Sigma = \int_{Y^{pm}} \boldsymbol{\sigma}^{pm(0)} dv + \int_{Y^{cf}} \boldsymbol{\sigma}^{cf(0)} dv \quad (2.126)$$

Now, the linear momentum balance (2.62ac) is integrated over the unit cell:

$$\int_Y (\operatorname{div}_x \boldsymbol{\sigma}^{(0)} + \operatorname{div}_y \boldsymbol{\sigma}^{(1)}) dv = 0 \quad (2.127)$$

or equivalently:

$$\int_Y \operatorname{div}_x \boldsymbol{\sigma}^{(0)} dv + \int_{Y^{pm}} \operatorname{div}_y \boldsymbol{\sigma}^{pm(1)} dv + \int_{Y^{cf}} \operatorname{div}_y \boldsymbol{\sigma}^{cf(1)} dv = 0 \quad (2.128)$$

By taking into account both the \mathbf{y} -periodicity and stress continuity on the interface for $\boldsymbol{\sigma}^{(1)}$, then the previous relation reads:

$$\int_Y \operatorname{div}_x \boldsymbol{\sigma}^{(0)} dv = 0 \quad (2.129)$$

It is worth remarking that the unit cell Y does not depend on the macroscopic space variable \mathbf{x} : in fact, it is assumed that the distribution of the cavities is periodic in the body Ω . Therefore, the divergence operator with respect to \mathbf{x} can be pushed out from the integral on Y and (2.129) becomes:

$$\operatorname{div}_x \Sigma = 0 \quad (2.130)$$

2.4.2 Constitutive law

The constitutive relation (2.56b) of the porous matrix and the constitutive hypothesis (2.57a) for the cavity fluid are substituted in the definition (2.126) of the homogenized stress, it yields:

$$|Y| \Sigma = \int_{Y^{pm}} \mathbf{c} @ \left(\mathbf{e}_x(\mathbf{u}^{pm(0)}) + \mathbf{e}_y(\mathbf{u}^{pm(1)}) \right) dv - p^{pm(0)} (\mathbf{b} |Y^{pm}| + \mathbf{I} |Y^{cf}|) \quad (2.131)$$

According to the (2.97), $\mathbf{u}^{pm(1)}$ is a linear function of the macroscopic strain, $\mathbf{e}_x(\mathbf{u}^{pm(0)})$, and of the macroscopic fluid pressure, $p^{pm(0)}$, then the previous equation is rewritten as:

$$\boldsymbol{\Sigma} = \mathbf{C} @ \mathbf{e}_x(\mathbf{u}^{pm(0)}) - \mathbf{B} p^{pm(0)} \quad (2.132)$$

where \mathbf{C} is the homogenized elastic tensor and \mathbf{B} is the homogenized Biot's tensor.

2.4.2.1 Homogenized coefficients.

By substituting (2.97) in (2.131), the formulae of the homogenized coefficients read:

$$|Y| \mathbf{C}(\mathbf{y}) := \mathbf{c} |Y^{pm}| + \int_{Y^{pm}} \mathbf{c} @ \mathbf{e}_y(\boldsymbol{\xi}^{kl}) dv \quad (2.133a)$$

$$|Y| \mathbf{B}(\mathbf{y}) := \mathbf{b} |Y^{pm}| + \mathbf{I} |Y^{cf}| - \int_{Y^{pm}} \mathbf{c} @ \mathbf{e}_y(\boldsymbol{\pi}) dv \quad (2.133b)$$

or, by using the index notation:

$$|Y| C_{ijkl} := c_{ijkl} |Y^{pm}| + \int_{Y^{pm}} c_{ijmn} e_{y_{mn}}(\boldsymbol{\xi}^{kl}) dv \quad (2.134a)$$

$$|Y| B_{ij} := b_{ij} |Y^{pm}| + \delta_{ij} |Y^{cf}| - \int_{Y^{pm}} c_{ijkh} e_{y_{kh}}(\boldsymbol{\pi}) dv \quad (2.134b)$$

2.4.3 Variation of macro-porosities

The macroscopic porosity H , already introduced in (1.34), is here re-defined with reference to the unit cell Y as:

$$H := \frac{|Y^{cf}| + \eta_r |Y^{pm}|}{|Y|} \quad (2.135)$$

It is worth remarking that, being explicitly in the small transformation framework, there is no need to distinguish between H and H_r : in fact, at the order zero in terms of displacements, they are equal. In the same way, in the following, all the volume subdomains involved are implicitly the ones of the reference configuration.

The relation (1.53) describing the variation of the macroscopic porosity H_u , is here rewritten in terms of the asymptotic expansions: actually, the terms $\text{div}_x \mathbf{u}$ and η_u are replaced by their expansion at order zero:

$$\begin{aligned} H_u = \frac{1}{|Y|} & \left(\int_{Y^{pm}} \eta_u^{(0)} dv + (\eta_r - 1) \int_{Y^{pm}} \left(\text{div}_x \mathbf{u}^{pm(0)} + \text{div}_y \mathbf{u}^{pm(1)} \right) dv \right) \\ & + \frac{1}{|Y|} (1 - H) \int_Y \left(\text{div}_x \mathbf{u}^{pm(0)} + \text{div}_y \mathbf{u}^{pm(1)} \right) dv \end{aligned} \quad (2.136)$$

By taking into account the independence of $\text{div}_x \mathbf{u}^{pm(0)}$ on \mathbf{y} , the \mathbf{y} -periodicity of $\mathbf{u}^{pm(1)}$ and the following relation deduced by using the definition (2.135):

$$(\eta_r - 1) |Y^{pm}| + (1 - H) |Y| = 0 \quad (2.137)$$

finally, the (2.136) becomes:

$$H_u = \frac{1}{|Y|} \left(\int_{Y^{pm}} \eta_u^{(0)} dv + (\eta_r - 1) \int_{Y^{pm}} \operatorname{div}_y \mathbf{u}^{pm(1)} dv \right) \quad (2.138)$$

It is worth remarking that in those calculations, the field $\mathbf{u}^{pm(1)}$ is extended in Y^{cf} by continuity.

2.4.3.1 Homogenized coefficients.

The constitutive relation (2.60b) of the Eulerian microscopic porosity is substituted in (2.138) and it yields:

$$H_u = \frac{1}{|Y|} \int_{Y^{pm}} \left((\mathbf{b} - \eta_r \mathbf{I}) : (\mathbf{e}_y(\mathbf{u}^{pm(1)}) + \mathbf{e}_x(\mathbf{u}^{pm(0)})) + s p^{pm(0)} + (\eta_r - 1) \operatorname{div}_y \mathbf{u}^{pm(1)} \right) dv \quad (2.139)$$

which also reads:

$$H_u = \frac{1}{|Y|} \int_{Y^{pm}} \left((\mathbf{b} - \mathbf{I}) : (\mathbf{e}_y(\mathbf{u}^{pm(1)}) + \mathbf{e}_x(\mathbf{u}^{pm(0)})) + s p^{pm(0)} + (1 - \eta_r) \operatorname{div}_x \mathbf{u}^{pm(0)} \right) dv \quad (2.140)$$

or:

$$\begin{aligned} H_u = & \frac{1}{|Y|} \int_{Y^{pm}} \left((\mathbf{b} - \mathbf{I}) : (\mathbf{e}_y(\mathbf{u}^{pm(1)}) + \mathbf{e}_x(\mathbf{u}^{pm(0)})) + s p^{pm(0)} \right) dv \\ & + \frac{1}{|Y|} (|Y^{pm}| + |Y^{cf}| - |Y^{cf}| - \eta_r |Y^{pm}|) \operatorname{div}_x \mathbf{u}^{pm(0)} \end{aligned} \quad (2.141)$$

By using the definition (2.135) of the Eulerian macroscopic porosity H , it also reads:

$$H_u = \frac{1}{|Y|} \int_{Y^{pm}} \left((\mathbf{b} - \mathbf{I}) : (\mathbf{e}_y(\mathbf{u}^{pm(1)}) + \mathbf{e}_x(\mathbf{u}^{pm(0)})) + s p^{pm(0)} \right) dv + (1 - H) \operatorname{div}_x \mathbf{u}^{pm(0)} \quad (2.142)$$

or, by means of (1.60b), in terms of the Lagrangian macroscopic porosity Φ_u :

$$\Phi_u = \frac{1}{|Y|} \int_{Y^{pm}} \left((\mathbf{b} - \mathbf{I}) : (\mathbf{e}_y(\mathbf{u}^{pm(1)}) + \mathbf{e}_x(\mathbf{u}^{pm(0)})) + s p^{pm(0)} \right) dv + \operatorname{div}_x \mathbf{u}^{pm(0)} \quad (2.143)$$

Now, by taking into account (2.97), that is, $\mathbf{u}^{pm(1)}$ depends linearly on the macroscopic strain $\mathbf{e}_x(\mathbf{u}^{pm(0)})$ and on the macroscopic fluid pressure $p^{pm(0)}$ it is possible to define the homogenized Biot's tensor $\tilde{\mathbf{B}}$ and the homogenized Biot's modulus S by:

$$\begin{aligned} & \tilde{\mathbf{B}} : \mathbf{e}_x(\mathbf{u}^{pm(0)}) + S p^{pm(0)} \\ &= \frac{1}{|Y|} \int_{Y^{pm}} \left((\mathbf{b} - \mathbf{I}) : (\mathbf{e}_y(\mathbf{u}^{pm(1)}) + \mathbf{e}_x(\mathbf{u}^{pm(0)})) + s p^{pm(0)} \right) dv + \operatorname{div}_x \mathbf{u}^{pm(0)} \end{aligned} \quad (2.144)$$

By substituting (2.97) in (2.144), the formulae of the homogenized coefficients follow:

$$|Y| \tilde{\mathbf{B}} := |Y^{pm}| \mathbf{b} + \mathbf{I} |Y^{cf}| + \int_{Y^{pm}} (\mathbf{b} - \mathbf{I}) \circ \mathbf{e}_y(\boldsymbol{\xi}^{ij}) dv \quad (2.145a)$$

$$|Y| S := |Y^{pm}| s + \int_{Y^{pm}} (\mathbf{b} - \mathbf{I}) : \mathbf{e}_y(\boldsymbol{\pi}) dv \quad (2.145b)$$

By using the index notation, they reads:

$$|Y| \tilde{B}_{ij} := |Y^{pm}| b_{ij} + \delta_{ij} |Y^{cf}| + \int_{Y^{pm}} (b_{kl} - \delta_{kl}) e_{ykl}(\boldsymbol{\xi}^{ij}) dv \quad (2.146a)$$

$$|Y| S := |Y^{pm}| s + \int_{Y^{pm}} (b_{kl} - \delta_{kl}) e_{ykl}(\boldsymbol{\pi}) dv \quad (2.146b)$$

2.4.3.2 Constitutive relations.

Then, the relation which describes the variation of the Eulerian macroscopic porosity H_u as a function of the macroscopic strain $\mathbf{e}_x(\mathbf{u}^{pm(0)})$ and of the macroscopic pressure $p^{pm(0)}$ reads:

$$H_u = (\tilde{\mathbf{B}} - H\mathbf{I}) : \mathbf{e}_x(\mathbf{u}^{pm(0)}) + S p^{pm(0)} \quad (2.147)$$

or equivalently, by using (1.60b), in terms of Lagrangian macroscopic porosity Φ_u as:

$$\Phi_u = \tilde{\mathbf{B}} : \mathbf{e}_x(\mathbf{u}^{pm(0)}) + S p^{pm(0)} \quad (2.148)$$

2.4.3.3 A proof

In the mesoscopic description, in reason of the thermodynamics, the Biot's coefficient \mathbf{b} appears in both the constitutive relation (2.27) of the porous matrix and in the relation (2.33) of the Lagrangian microporosity ϕ_u . Given that the homogenization does not affect the thermodynamics and even at the macroscopic scale this equality must hold up. Then, the macroscopic coefficients \mathbf{B} and $\tilde{\mathbf{B}}$, defined in (2.133b, 2.145a), must be equal. The proof is provided in this section.

The weak formulation (2.86) of the unit cell problem for $\mathbf{u}^{pm(1)}$ can be written for two particular test functions $\mathbf{z} \in \mathcal{Z}$ which are derived from the solution (2.98) of the same problem. As first, the (2.86) is rewritten for the combination:

$$\mathbf{e}_x(\mathbf{u}^{pm(0)}(\mathbf{x})) = \mathbf{I}, \quad p^{pm(0)} = 0 \quad (2.149)$$

which implies that $\mathbf{u}^{pm(1)} = \boldsymbol{\xi}^{ij}$, and by imposing $\mathbf{z} = \boldsymbol{\pi}$:

$$\int_{Y^{pm}} \mathbf{c} @ \mathbf{e}_y(\boldsymbol{\xi}^{ij}) : \mathbf{e}_y(\boldsymbol{\pi}) \, dv = - \int_{Y^{pm}} \mathbf{c} @ \mathbf{e}_y(\boldsymbol{\pi}) : \mathbf{I} \, dv \quad (2.150)$$

Now, the (2.86) is rewritten for the combination $\mathbf{e}_x(\mathbf{u}^{pm(0)}(\mathbf{x})) = \mathbf{0}$ and $p^{(0)} = 1$ which implies that $\mathbf{u}^{pm(1)} = \boldsymbol{\pi}$, and by imposing $\mathbf{z} = \boldsymbol{\xi}^{ij}$:

$$\int_{Y^{pm}} \mathbf{c} @ \mathbf{e}_y(\boldsymbol{\pi}) : \mathbf{e}_y(\boldsymbol{\xi}^{ij}) \, dv = \int_{Y^{pm}} (\mathbf{b} - \mathbf{I}) : \mathbf{e}_y(\boldsymbol{\xi}^{ij}) \, dv \quad (2.151)$$

Given the symmetry of the tensors involved and the properties of the transpose matrix, the comparison between (2.150) and (2.151) yields:

$$\int_{Y^{pm}} (\mathbf{b} - \mathbf{I}) : \mathbf{e}_y(\boldsymbol{\xi}^{ij}) \, dv + \int_{Y^{pm}} \mathbf{c} @ \mathbf{e}_y(\boldsymbol{\pi}) : \mathbf{I} \, dv = 0 \quad (2.152)$$

By using the definitions (2.133b, 2.145a) of the homogenized coefficients \mathbf{B} and $(\tilde{\mathbf{B}})$, it follows that:

$$|Y|(\tilde{\mathbf{B}} - \mathbf{B}) = \int_{Y^{pm}} \left(\mathbf{b} + (\mathbf{b} - \mathbf{I}) \circ \mathbf{e}_y(\boldsymbol{\xi}^{ij}) \right) dv + \int_{Y^{pm}} \mathbf{c} @ \mathbf{e}_y(\boldsymbol{\pi}) dv \quad (2.153)$$

which, given the (2.152), yields the expected result:

$$\tilde{\mathbf{B}} = \mathbf{B} \quad (2.154)$$

2.4.4 Fluid mass balance

The expansion (2.67c) of the fluid balance in terms of the absolute fluid velocity, \mathbf{v}^{pm} , and of the variation of the Eulerian microscopic porosity, η_u , is integrated over the porous part Y^{pm} of the unit cell:

$$0 = \int_{Y^{pm}} \left(\dot{\eta}_u^{(0)} + \operatorname{div}_y \left(\eta_r \mathbf{v}^{pm(1)} \right) + \operatorname{div}_x \left(\eta_r \mathbf{v}^{pm(0)} \right) \right) dv \quad (2.155)$$

which, by taking into account the \mathbf{y} -periodicity of $\mathbf{v}^{pm(1)}$ and $\mathbf{u}^{pm(1)}$, becomes:

$$0 = \int_{Y^{pm}} \left(\dot{\eta}_u^{(0)} + \operatorname{div}_x \left(\eta_r \mathbf{v}^{pm(0)} \right) \right) dv + \int_{\Gamma} \eta_r \left(\mathbf{v}^{pm(1)} - \dot{\mathbf{u}}^{pm(1)} \right) \cdot \mathbf{n} \, ds + \int_{\Gamma} \eta_r \dot{\mathbf{u}}^{pm(1)} \cdot \mathbf{n} \, ds \quad (2.156)$$

Now, the fluid mass balance (2.72c) through the interface is introduced and, by means of the divergence theorem, the previous equation is rewritten as:

$$0 = \int_{Y^{pm}} \left(\dot{\eta}_u^{(0)} + \operatorname{div}_x \left(\eta_r \mathbf{v}^{pm(0)} \right) \right) dv - \int_{Y^{cf}} \operatorname{div}_y \mathbf{v}^{cf(1)} \, dv + \int_{\Gamma} (\eta_r - 1) \dot{\mathbf{u}}^{pm(1)} \cdot \mathbf{n} \, ds \quad (2.157)$$

which, by using the incompressibility condition (2.58b) of the cavity fluid and (2.138), reads also:

$$0 = |Y| \dot{H}_u + \int_{Y^{pm}} \operatorname{div}_x \left(\eta_r \mathbf{v}^{pm(0)} \right) dv + \int_{Y^{cf}} \operatorname{div}_x \mathbf{v}^{cf(0)} dv \quad (2.158)$$

So, by taking into account that the unit cell Y does not depend on the macroscopic space variable \mathbf{x} , the (2.158) reads:

$$0 = \operatorname{div}_x \left(\mathbf{V} H \right) + \dot{H}_u \quad (2.159)$$

where \mathbf{V} denotes the macroscopic absolute fluid velocity which is defined as:

$$\mathbf{V} := \frac{1}{|Y| H} \int_Y \tilde{\mathbf{v}}^{(0)} dv = \frac{1}{|Y| H} \left(\int_{Y^{pm}} \eta_r \mathbf{v}^{pm(0)} dv + \int_{Y^{cf}} \mathbf{v}^{cf(0)} dv \right) \quad (2.160)$$

where the absolute velocity field $\tilde{\mathbf{v}}^{(0)}$ is defined as:

$$\tilde{\mathbf{v}}^{(0)} = \begin{cases} \eta_r \mathbf{v}^{pm(0)} & \text{in } Y^{pm} \\ \mathbf{v}^{cf(0)} & \text{in } Y^{cf} \end{cases} \quad (2.161)$$

As an alternative, by using the (1.60b), the (2.158) can be rewritten as:

$$0 = \operatorname{div}_x \mathbf{Q} + \dot{\Phi}_u \quad (2.162)$$

where \mathbf{Q} denotes the macroscopic relative flow vector of fluid volume which is defined as:

$$\mathbf{Q} := H \left(\mathbf{V} - \dot{\mathbf{u}}^{pm(0)} \right) \quad (2.163)$$

or, given (2.160), as:

$$\mathbf{Q} := \frac{1}{|Y|} \int_Y \tilde{\mathbf{q}}^{pm(0)} dv = \frac{1}{|Y|} \left(\int_{Y^{pm}} \mathbf{q}^{pm(0)} dv + \int_{Y^{cf}} \left(\mathbf{v}^{cf(0)} - \dot{\mathbf{u}}^{pm(0)} \right) dv \right) \quad (2.164)$$

with the relative fluid vector $\tilde{\mathbf{q}}^{pm(0)}$ defined as:

$$\tilde{\mathbf{q}}^{pm(0)} = \begin{cases} \mathbf{q}^{pm(0)} & \text{in } Y^{pm} \\ \mathbf{v}^{cf(0)} - \dot{\mathbf{u}}^{pm(0)} & \text{in } Y^{cf} \end{cases} \quad (2.165)$$

In the end, as it was at the mesoscopic scale, (2.22, 2.20), even at the macroscopic one, (2.159, 2.162), the fluid mass balance is written in two equivalent formulations: the one in terms of absolute velocity and Eulerian porosity, the other one in terms of relative flow and Lagrangian porosity.

2.4.5 Darcy's law

Given the definition (2.160) of the macroscopic absolute fluid velocity \mathbf{V} and (2.163) of the macroscopic relative flow vector $\mathbf{Q} := H(\mathbf{V} - \dot{\mathbf{u}}^{pm(0)})$, it follows that:

$$\mathbf{Q} = \frac{1}{|Y|} \left(\int_{Y^{pm}} \eta_r \mathbf{v}^{pm(0)} dv + \int_{Y^{cf}} \mathbf{v}^{cf(0)} dv \right) - \left(\frac{|Y^{cf}| + \eta_r |Y^{pm}|}{|Y|} \right) \dot{\mathbf{u}}^{pm(0)} \quad (2.166)$$

where the definition (2.135) of the macroporosity H is applied. By taking into account that $\dot{\mathbf{u}}^{pm(0)}$ does not depend on \mathbf{y} , the (2.166) is rewritten as:

$$|Y| \mathbf{Q} = \int_{Y^{pm}} \mathbf{q}^{pm(0)} dv + \int_{Y^{cf}} (\mathbf{v}^{cf(0)} - \dot{\mathbf{u}}^{pm(0)}) dv \quad (2.167)$$

and, given the (2.120), it becomes:

$$|Y| \mathbf{Q} = \int_{Y^{pm}} (\mathbf{I} + \nabla_y \mathbf{Z}) @ \mathbf{q}^{pm(0)} dv \quad (2.168)$$

Now, the mesoscopic relative flow vector $\mathbf{q}^{pm(0)}$ is rewritten by means of the Darcy's law and it yields:

$$|Y| \mathbf{Q} = - \int_{Y^{pm}} (\mathbf{I} + \nabla_y \mathbf{Z}) \circ \mathbf{k} @ (\nabla_x p^{pm(0)} + \nabla_y p^{pm(1)}) dv \quad (2.169)$$

Given the (2.107), that is to say that $p^{pm(1)}$ depends linearly on the gradient of the macroscopic pressure, $\nabla_x p^{pm(0)}$, its differential with respect to the space variable \mathbf{y} reads:

$$dp^{pm(1)} = \nabla_x p^{pm(0)} \cdot (\nabla_y \mathbf{Z} @ d\mathbf{y}) = (\nabla_y \mathbf{Z}^t @ \nabla_x p^{pm(0)}) \cdot d\mathbf{y} \quad (2.170)$$

which clearly implies that:

$$\nabla_y p^{pm(1)} = \nabla_y \mathbf{Z}^t @ \nabla_x p^{pm(0)} \quad (2.171)$$

In the end, by substituting the (2.171) in the (2.169), the macroscopic Darcy's law reads:

$$\mathbf{Q} = -\mathbf{K} @ \nabla_x p^{pm(0)} \quad (2.172)$$

where \mathbf{K} is the homogenized permeability and it is defined as:

$$|Y| \mathbf{K} := - \int_{Y^{pm}} (\mathbf{I} + \nabla_y \mathbf{Z}) \circ \mathbf{k} \circ (\mathbf{I} + \nabla_y \mathbf{Z}^t) dv \quad (2.173)$$

or, by using (2.119), as follows:

$$|Y| \mathbf{K} := - \int_{Y^{pm}} \left(\mathbf{I} + \sum_i \mathbf{e}_i \otimes \nabla_y \zeta^i \right) \circ \mathbf{k} \circ \left(\mathbf{I} + \sum_i \nabla_y \zeta^i \otimes \mathbf{e}_i \right) dv \quad (2.174)$$

2.4.6 Synopsis of macroscopic description

The macroscopic equations describing the hydro-mechanical behaviour of the equivalent continuum to the porous solid with fluid-filled cavities are listed below.

The equilibrium equation and the constitutive law,

$$\operatorname{div}_x \boldsymbol{\Sigma} = 0, \quad \boldsymbol{\Sigma} = \mathbf{C} @ \mathbf{e}_x(\mathbf{u}^{pm(0)}) - \mathbf{B} p^{pm(0)} \quad (2.175)$$

where \mathbf{C} is the homogenized elastic tensor and \mathbf{B} is the homogenized Biot's tensor:

$$|Y| \mathbf{C} := \mathbf{c} |Y^{pm}| + \int_{Y^{pm}} \mathbf{c} @ \mathbf{e}_y(\boldsymbol{\xi}^{kl}) dv \quad (2.176a)$$

$$|Y| \mathbf{B} := \mathbf{b} |Y^{pm}| + \mathbf{I} |Y^{cf}| - \int_{Y^{pm}} \mathbf{c} @ \mathbf{e}_y(\boldsymbol{\pi}) dv \quad (2.176b)$$

The fluid mass balance

$$0 = \operatorname{div}_x \mathbf{Q} + \dot{\Phi}_u \quad (2.177)$$

with

$$\mathbf{Q} := H (\mathbf{V} - \dot{\mathbf{u}}^{pm(0)}), \quad H := \frac{|Y^{cf}| + \eta_r |Y^{pm}|}{|Y|} \quad (2.178)$$

The constitutive relation for the variation of the macroscopic Lagrangian porosity:

$$\Phi_u = \tilde{\mathbf{B}} : \mathbf{e}_x(\mathbf{u}^{pm(0)}) + S p^{pm(0)} \quad (2.179)$$

where the homogenized Biot's tensor $\tilde{\mathbf{B}}$ and the homogenized Biot's modulus S are defined by:

$$|Y| \tilde{\mathbf{B}} := \mathbf{b} |Y^{pm}| + \mathbf{I} |Y^{cf}| + \int_{Y^{pm}} (\mathbf{b} - \mathbf{I}) \circ \mathbf{e}_y(\boldsymbol{\xi}^{ij}) dv \quad (2.180a)$$

$$|Y| S := s |Y^{pm}| + \int_{Y^{pm}} (\mathbf{b} - \mathbf{I}) : \mathbf{e}_y(\boldsymbol{\pi}) dv \quad (2.180b)$$

where it has been proved that $\tilde{\mathbf{B}} = \mathbf{B}$. The Darcy's law:

$$\mathbf{Q} = -\mathbf{K} @ \nabla_x p^{pm(0)} \quad (2.181)$$

where $\mathbf{K}(\mathbf{x}, \mathbf{y})$ is the homogenized permeability and it is defined as:

$$|Y| \mathbf{K} := - \int_{Y^{pm}} \left(\mathbf{I} + \nabla_y \mathbf{Z} \right) \circ \mathbf{k} \circ \left(\mathbf{I} + \nabla_y \mathbf{Z}^t \right) dv \quad (2.182)$$

2.5 Numerical solution of unit cell problems

In this section the numerical evaluation of the homogenized coefficients is presented.

Given the definitions (2.176, 2.180b) of the homogenized elasticity tensor \mathbf{C} , the Biot's coupling tensor \mathbf{B} and Biot's modulus S , it is apparent that the characteristic functions $\boldsymbol{\xi}^{lm}(\mathbf{y})$ and $\boldsymbol{\pi}(\mathbf{y})$ must be computed in order to evaluate the homogenized coefficients. That is, the corresponding unit cell problems have to be solved numerically and, once it is done, the numerical evaluation of the homogenized coefficients reduces to the evaluation of the integrals appearing in their definitions.

Moreover, even if the problems are quasi-static, this procedure is repeated for several values of the cavity length.

Remark 2.5.1. *It is worth remarking a limit of the model: given the hypothesis of mesoscopic fluid-filled cavities not connected in a network, that is, every single cavity exchanges fluid only with the surrounding porous saturated solid, then the cavity length does not influence the homogenized permeability \mathbf{K} .*

The relation (2.98) defines $\mathbf{u}^{pm(1)}$ as follows:

$$e_{y_{kh}}(\mathbf{u}^{pm(1)}) = e_{y_{kh}}(\boldsymbol{\xi}^{lm})e_{x_{lm}}(\mathbf{u}^{pm(0)}) - e_{y_{kh}}(\boldsymbol{\pi})p^{pm(0)} \quad (2.183)$$

and, by substitution in the constitutive relation (2.56b) of the porous medium, the pure mechanical boundary value problem (2.85) of higher order reads

$$0 = \frac{\partial}{\partial y_j} \left[c_{ijkh} \left(e_{x_{lm}}(\mathbf{u}^{pm(0)}) (\delta_{kl}\delta_{hm} + e_{y_{kh}}(\boldsymbol{\xi}^{lm})) - e_{y_{kh}}(\boldsymbol{\pi})p^{pm(0)} \right) - b_{ij}p^{pm(0)} \right] \quad (2.184a)$$

$$-p^{pm(0)}n_i = \left[c_{ijkh} \left(e_{x_{lm}}(\mathbf{u}^{pm(0)}) (\delta_{kl}\delta_{hm} + e_{y_{kh}}(\boldsymbol{\xi}^{lm})) - e_{y_{kh}}(\boldsymbol{\pi})p^{pm(0)} \right) - b_{ij}p^{pm(0)} \right] n_j \quad (2.184b)$$

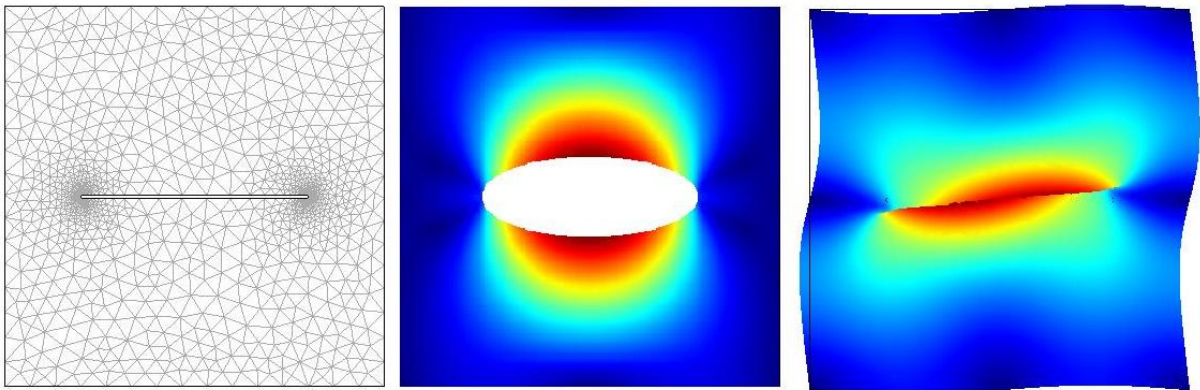


Figure 2.8: Numerical solution of unit cell problems: unstructured mesh (left), plots of the deformed configuration and of the norm of $\boldsymbol{\xi}^{22}$ (center) and $\boldsymbol{\xi}^{12}$ (right).

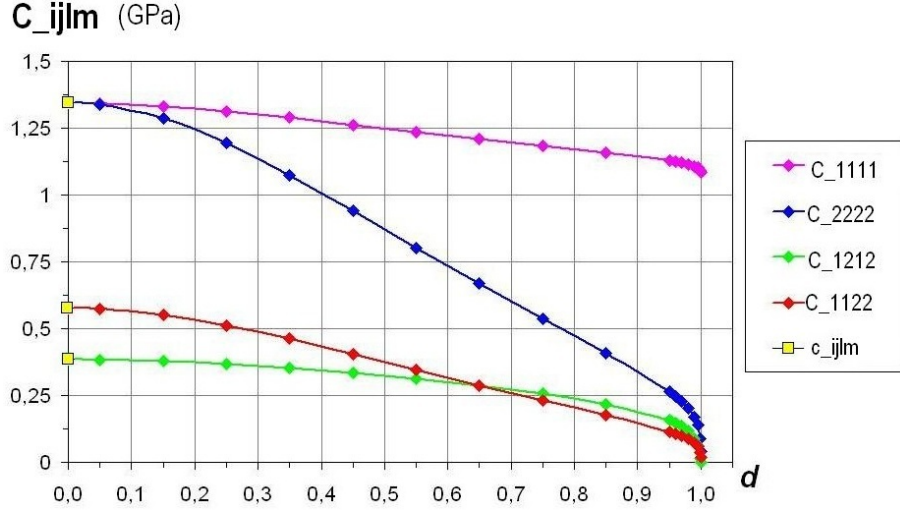


Figure 2.9: Terms of the homogenized elasticity tensor appearing in constitutive equation (2.175) as a function of cavity length.

From a numerical point of view the (2.184) represents 3+1 boundary value problems: in fact, for

$$\begin{cases} p^{pm(0)} = 0 \\ e_{x_{lm}} = \delta_{kl}\delta_{hm} = 1 \quad \text{with} \quad lm = 11, 22, 12, 21 \end{cases} \quad (2.185)$$

we have that $\mathbf{u}^{pm(1)} = \boldsymbol{\xi}^{lm}$ and we get the following 4 boundary value problems in the unknown $\boldsymbol{\xi}^{lm}(\mathbf{y})$ with $lm=11, 22, 12$ and 22 .

$$\begin{cases} 0 = \frac{\partial}{\partial y_j} (c_{ijlm} + c_{ijkh}e_{y_{kh}}(\boldsymbol{\xi}^{lm})) & \text{in } Y^{pm} \\ 0 = (c_{ijlm} + c_{ijkh}e_{y_{kh}}(\boldsymbol{\xi}^{lm}))n_j & \text{on } \Gamma \\ \text{Periodicity on } \partial Y \end{cases} \quad (2.186)$$

While for

$$\begin{cases} p^{pm(0)} = -1 \\ e_{x_{lm}} = 0 \end{cases} \quad (2.187)$$

then $\mathbf{u}^{pm(1)} = \boldsymbol{\pi}$ and we get the following boundary value problem in the unknown $\boldsymbol{\pi}(\mathbf{y})$

$$\begin{cases} \frac{\partial}{\partial y_j} (c_{ijkh}e_{y_{kh}}(\boldsymbol{\pi}) + b_{ij}) & \text{in } Y^{pm}, \\ 1n_i = (c_{ijkh}e_{y_{kh}}(\boldsymbol{\pi}) + b_{ij})n_j & \text{on } \Gamma \\ \text{Periodicity on } \partial Y \end{cases} \quad (2.188)$$

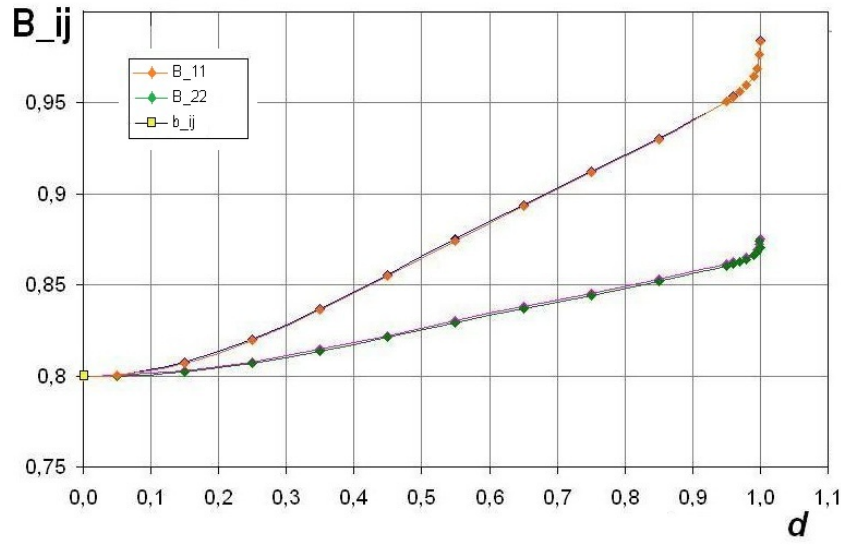


Figure 2.10: Terms of the homogenized Biot's tensors appearing in constitutive equations (2.175, 2.179) as a function of cavity length

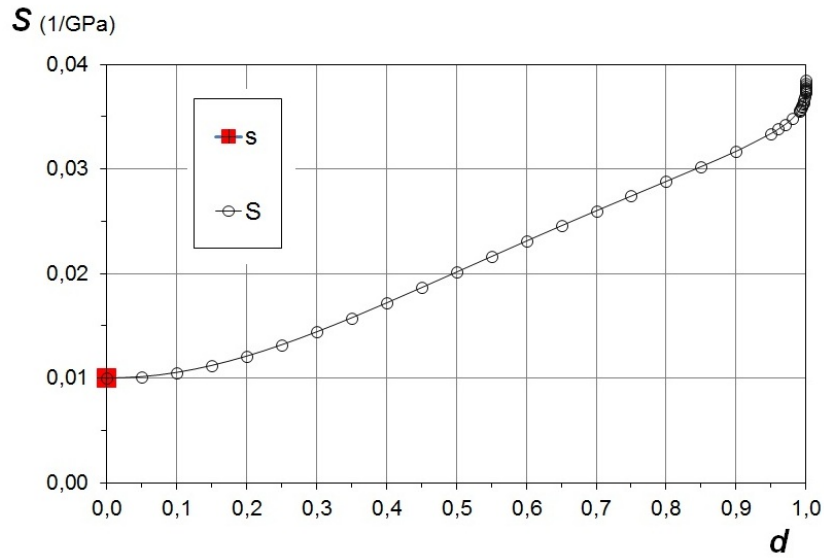


Figure 2.11: Homogenized storage modulus S appearing in constitutive equations (2.179) as a function of cavity length d .

The implementation of this serie of unit cell problems in a Finite Element Code provides the solution of the functions $\xi^{lm}(\mathbf{y})$ (fig. 2.8) and $\pi(\mathbf{y})$. Then, by evaluation of the integrals appearing in the definitions of the homonized coefficients, their numerical values are obtained and they are represented as function of the cavity length in the figures 2.9, 2.10 and 2.11.

The following values of the mesoscopic parameters characterising the porous matrix were used in the calculations:

$$E = 1GPa \quad \nu = 0.3 \quad b = 0.8 \quad s = 1 \cdot 10^{-11} \quad \eta = 0.4 \quad (2.189)$$

while, concerning the geometry of cavity, the thickness is 0.01, that is, 1/100 of the entire unit cell, and the edges are modelled as semicircles.

2.6 Conclusions

In this chapter, we employed the method of homogenization based on asymptotic developments in order to deduce the macroscopic description of a solid with double-scale fluid-filled heterogeneities: the microscopic saturated pores and the mesoscopic crack-like cavities. It worths noting that no phenomenological assumptions have been considered for the macroscopic equations.

By the end of the chapter, the numerical evaluation of homogenized elasticity tensor, Biot's coupling tensor and Biot's modulus (i.e. mechanical and capacity properties) is presented.

The model will be used in the next chapter where the evolution of the fluid-filled cavities will be taken into account. For this, the effective coefficients obtained here will be considered as functions of the length of the cavities playing the role of damage parameter.

Chapter 3

Energy analysis and damage evolution law

3.1 Introduction

In the chapter 2, by means of the method of the asymptotic homogenization, the macroscopic description for the porous solid with fluid-filled cavities is obtained. That is, for the investigated geomaterial characterised by double-scale fluid-filled heterogeneities, a Biot-like model which describes the hydro-mechanical behaviour of the equivalent continuum is deduced.

The objective of this chapter is to enrich the poroelastic model with damage, that is, it is assumed that the mesoscopic fluid-filled cavities may propagate. It means that a link between the meso-structural fracture phenomena and the corresponding macroscopic damage is required. This link is given by homogenization combined with mesoscopic hydro-mechanical energy analysis leading to the damage evolution law.

The following assumptions about the geometry of the propagation are made (fig. 3.1): the trajectory of propagation is smooth and a priori known; only the semi-circular edges of the interface are moving and all their material points have the same velocity \mathbf{v} ; the

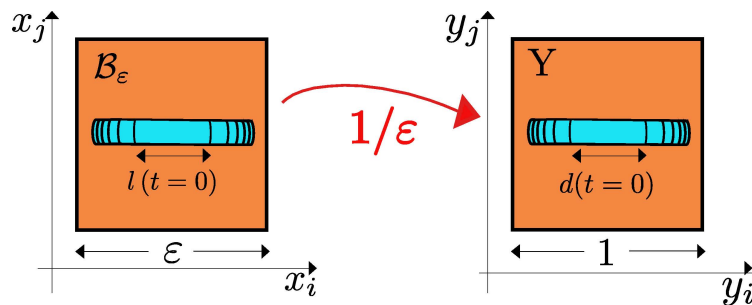


Figure 3.1: Geometrical assumption about the propagation of the mesoscopic fluid-filled cavity. Periodic cell \mathcal{B}_ϵ with cavity length l . Resized unit cell Y with cavity length d

propagation of the cavity fronts is symmetric with respect to a middle point, then the cavity evolution is completely described by the evolution of the cavity length, denoted by l or d depending on the change of variables, which is referred to as damage variable.

In the section 3.2, in order to have a clear physical interpretation of the mesoscopic energetic terms appearing in the following energy analysis, it is proposed a study of the microscopic structure. Actually, the strain energy of the solid phase and the dissipation associated to the flow of the pore fluid are defined and, then, the corresponding mesoscopic terms are deduced by upscaling.

In the section 3.3, the aim is to define the physical energy release rate. Then, following the approach proposed by Gurtin (1979a), a mesoscopic energy analysis is performed in the whole body and the exact fields of the mesoscopic description (section 2.2) are considered. Lastly, in the section 3.4, we extend to the case of evolving fluid-filled cavities the method developed in Dascalu, Bilbie and Agiasofitou (2008) and Dascalu (2009), which combines the mesoscopic cell energy analysis and the asymptotic homogenization method to obtain effective damage evolution laws.

3.2 From micro- to meso-energy terms

In this section, starting from the definition of the volumetric density of the strain energy of the solid phase and of the dissipation associated to the flow of the pore fluid, the corresponding mesoscopic terms are defined by means of asymptotic developments and average values. Lastly, these latter ones are written in terms of poroelastic mesoscopic coefficients.

3.2.1 Strain energy

Let $\psi^{s(e)}$, with e denoting the size of the microscopic periodic cell, be the microscopic volumetric density of strain energy of the solid phase which is defined as follows:

$$\psi^{s(e)} := \frac{1}{2} \boldsymbol{\sigma}^{s(e)} : \mathbf{e}_x(\mathbf{u}^{s(e)}) \quad (3.1)$$

By means of the asymptotic expansions (B.4a, B.4b) of $\mathbf{u}^{s(e)}$ and $p^{pf(e)}$, the development of $\psi^{s(e)}$ reads:

$$\psi^{s(e)} = \psi^{s(0)} + e \psi^{s(1)} + \dots \quad (3.2)$$

with the term of order zero in the energy rate of e which, by means of the corresponding term (B.5e) in the expansion of the constitutive law, reads as follows:

$$\psi^{s(0)} = \frac{1}{2} \boldsymbol{\sigma}^{s(0)} : \left(\mathbf{e}_x(\mathbf{u}^{s(0)}) + \mathbf{e}_y(\mathbf{u}^{s(1)}) \right) \quad (3.3)$$

Taking into account that the fluid is assumed to be incompressible, then the mesoscopic volumetric density of strain energy $\psi^{pm(\varepsilon)}$ of the porous matrix can be defined as the average value of $\psi^{s(0)}$ over the entire microscopic periodic cell Z (fig. 3.2):

$$\psi^{pm(\varepsilon)} := \frac{1}{|Z|} \int_{Z^s} \psi^{s(0)} \, ds \quad (3.4)$$

where ds is the infinitesimal surface element. Given the constitutive law (B.5e) for the solid phase at order zero in the powers of e , its rate $\dot{\psi}^{pm(\varepsilon)}$ reads:

$$\dot{\psi}^{pm(\varepsilon)} = \frac{1}{|Z|} \int_{Z^s} \dot{\psi}^{s(0)} \, ds = \frac{1}{|Z|} \int_{Z^s} \boldsymbol{\sigma}^{s(0)} : \left(\mathbf{e}_x(\dot{\mathbf{u}}^{s(0)}) + \mathbf{e}_y(\dot{\mathbf{u}}^{s(1)}) \right) \, ds \quad (3.5)$$

Given the equilibrium equation (B.5a) in the solid part Z^s of the microscopic periodic cell, it follows that:

$$\boldsymbol{\sigma}^{s(0)} : \mathbf{e}_y(\dot{\mathbf{u}}^{s(1)}) = \boldsymbol{\sigma}^{s(0)} : \nabla_y(\dot{\mathbf{u}}^{s(1)}) = \operatorname{div}_y(\boldsymbol{\sigma}^{s(0)} @ \dot{\mathbf{u}}^{s(1)}) \quad (3.6)$$

Then, by taking into account the term of order zero in the powers of e of the stress continuity condition at the interface Γ^{s-pf} between the pore fluid and the solid phase, and the periodicity on the external boundary ∂Z of the microscopic unit cell Z , the (3.5) becomes:

$$\dot{\psi}^{pm(\varepsilon)} = \frac{1}{|Z|} \left[\mathbf{e}_x(\dot{\mathbf{u}}^{s(0)}) : \int_{Z^s} \boldsymbol{\sigma}^{s(0)} \, ds - p^{pf(0)} \int_{\Gamma^{s-pf}} \dot{\mathbf{u}}^{s(1)} \cdot \mathbf{n} \, d\lambda \right] \quad (3.7)$$

where $d\lambda$ is the infinitesimal line element. Let the mesoscopic stress tensor $\boldsymbol{\sigma}^{pm(\varepsilon)}$ of the porous matrix be defined as the average value of the zero order term in the powers of e of the microscopic stress tensor $\boldsymbol{\sigma}^{(e)}$ over the entire microscopic periodic cell Z :

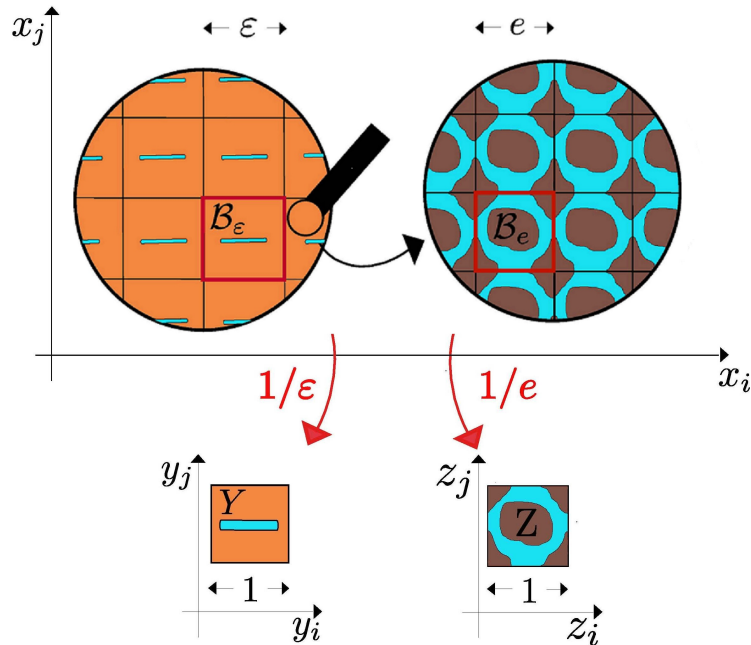


Figure 3.2: Mesoscopic and microscopic periodic structures. \mathcal{B}_ε and \mathcal{B}_e are the periodic cells, their sizes are such that: $\varepsilon \gg e$. Rescaling of \mathcal{B}_ε in $Y = Y^{pm} \cup Y^{cf}$, and of \mathcal{B}_e in $Z = Z^s \cup Z^{pf}$.

$$\boldsymbol{\sigma}^{pm(\varepsilon)} := \frac{1}{|Z|} \int_Z \boldsymbol{\sigma}^{(0)} ds = \frac{1}{|Z|} \left(\int_{Z^s} \boldsymbol{\sigma}^{s(0)} ds - \int_{Z^{pf}} \boldsymbol{\sigma}^{pf(0)} ds \right) \quad (3.8)$$

and, given the relation (B.5g) of order zero in the power of e of the constitutive law for the pore fluid, it reads also:

$$\boldsymbol{\sigma}^{pm(\varepsilon)} = \frac{1}{|Z|} \int_{Z^s} \boldsymbol{\sigma}^{s(0)} ds - \eta_r p^{pf(0)} \mathbf{I} \quad (3.9)$$

where η_r is the Eulerian mesoscopic porosity in the reference configuration (1.22).

By means of the no-slip condition (B.5k) on Γ^{s-pf} and of the incompressibility condition (B.5c) of the pore fluid in Y^{pf} , the following identities follow:

$$\int_{\Gamma^{s-pf}} \dot{\mathbf{u}}^{s(1)} \mathbf{n} d\lambda = \int_{\Gamma^{s-pf}} \mathbf{v}^{pf(1)} \mathbf{n} d\lambda = \operatorname{div}_x \int_{Y^{pf}} \mathbf{v}^{pf(0)} ds = |Y^{pm}| \operatorname{div}_x \mathbf{v}^{pm(\varepsilon)} \quad (3.10)$$

where $\mathbf{v}^{pm(\varepsilon)}$ is the mesoscopic pore fluid velocity and it is defined as the average value of the microscopic pore fluid velocity on the entire periodic cell Z as follows:

$$\mathbf{v}^{pm(\varepsilon)} := \frac{1}{|Z^{pf}|} \int_{Z^{pf}} \mathbf{v}^{pf(0)} ds \quad (3.11)$$

Let $\mathbf{q}^{pm(\varepsilon)}$ be the relative fluid flow vector defined as follows:

$$\mathbf{q}^{pm(\varepsilon)} = \eta_r (\mathbf{v}^{pm(\varepsilon)} - \dot{\mathbf{u}}^{pm(\varepsilon)}) \quad (3.12)$$

Remark 3.2.1. Differently from Auriault (2004) (see appendix B), where the mesoscopic pore fluid velocity $\mathbf{v}_{Aur}^{pm(\varepsilon)}$ is defined as:

$$\mathbf{v}_{Aur}^{pm(\varepsilon)} := \frac{1}{|Z|} \int_{Z^{pf}} \mathbf{v}^{pf(0)} ds \quad (3.13)$$

and implies

$$\mathbf{q}_{Aur}^{pm(\varepsilon)} := \mathbf{v}_{Aur}^{pm(\varepsilon)} - \eta_r \dot{\mathbf{u}}^{pm(\varepsilon)} \quad (3.14)$$

in this thesis the definition (3.11) is adopted and leads to (3.12).

Remark 3.2.2. In analogy with the remark 1.4.3, the microscopic terms of order zero $\mathbf{u}^{s(0)}$ and $p^{pf(0)}$ in the power of e can be set as the mesoscopic displacement $\mathbf{u}^{pm(\varepsilon)}$ and pore fluid pressure $p^{pm(\varepsilon)}$.

Then, by using the (3.8, 3.10), the expression (3.7) of the $\dot{\psi}^{pm(\varepsilon)}$ is rewritten as follows:

$$\dot{\psi}^{pm(\varepsilon)} = \boldsymbol{\sigma}^{pm(\varepsilon)} : \mathbf{e}_x (\dot{\mathbf{u}}^{pm(\varepsilon)}) - p^{pm(\varepsilon)} \operatorname{div}_x \mathbf{q}^{pm(\varepsilon)} \quad (3.15)$$

By taking into account the mesoscopic fluid mass balance (2.20), the mesoscopic Biot's constitutive laws (2.27, 2.33) for the porous matrix and the variation of mesoscopic porosity respectively, the volumetric density of the strain energy rate $\dot{\psi}^{pm(\varepsilon)}$ in the porous matrix reads:

$$\dot{\psi}^{pm(\varepsilon)} = \mathbf{c} @ \mathbf{e}_x(\mathbf{u}^{pm(\varepsilon)}) : \mathbf{e}_x(\dot{\mathbf{u}}^{pm(\varepsilon)}) + s p^{pm(\varepsilon)} \dot{p}^{pm(\varepsilon)} \quad (3.16)$$

and, by integration in time, it follows that:

$$\psi^{pm(\varepsilon)} = \frac{1}{2} \left(\mathbf{c} @ \mathbf{e}_x(\mathbf{u}^{pm(\varepsilon)}) : \mathbf{e}_x(\mathbf{u}^{pm(\varepsilon)}) + s (p^{pm(\varepsilon)})^2 \right) \quad (3.17)$$

Remark 3.2.3. For an incompressible fluid, the (2.25) links the fluid mass content m^{pm} to the variation of the Lagrangian mesoscopic porosity ϕ_u . Then, the relation proposed in Callari (2007) for the volumetric density of strain energy $\psi^{pm(\varepsilon)}$ in terms of m^{pm} is rewritten below in terms of ϕ_u :

$$\psi^{pm(\varepsilon)} = \frac{1}{2} \mathbf{c} @ \mathbf{e}_x(\mathbf{u}^{pm(\varepsilon)}) : \mathbf{e}_x(\mathbf{u}^{pm(\varepsilon)}) + \frac{(\mathbf{b} : \mathbf{e}_x(\mathbf{u}^{pm(\varepsilon)}))^2}{2s} + \frac{\phi_u^{pm(\varepsilon)}}{s} \left(\frac{\phi_u^{pm(\varepsilon)}}{2} - \mathbf{b} : \mathbf{e}_x(\mathbf{u}^{pm(\varepsilon)}) \right) \quad (3.18)$$

And, by means of the constitutive relation (2.33) for $\phi_u^{pm(\varepsilon)}$, it is easily proved¹ that the relations (3.18) and (3.17) are identical.

3.2.2 Dissipation in the pore fluid

As already written in the (2.29), the viscosity of the pore fluid is of order two in the powers of the microscopic scale parameter e . Moreover, it is assumed to be incompressible.

Then, the pore fluid is not capable to store any energy. However, a dissipation of energy is associated to its motion through the pores.

Let $\mathcal{D}^{pf(e)}$ be the volumetric dissipation of the pore fluid at the microscopic scale which is defined as follows:

$$\mathcal{D}^{pf(e)} := -\boldsymbol{\sigma}^{pf(e)} : \mathbf{D}_x(\mathbf{v}^{pf(e)}) \quad (3.19)$$

where $\mathbf{D}_x(\mathbf{v}^{pf(e)})$ denotes the strain rate tensor, that is the symmetric part of the gradient of the velocity field $\mathbf{v}^{pf(e)}$ of the pore fluid.

By means of the asymptotic expansions (B.5f) of $\mathbf{D}_x(\mathbf{v}^{pf(e)})$, the development of $\mathcal{D}^{pf(e)}$ reads:

¹For $\mathbf{b} = b\mathbf{I}$, the following identities hold:

$$\begin{aligned} b(\mathbf{I} \otimes \mathbf{I}) \mathbf{e}_x(\mathbf{u}^{pm(\varepsilon)}) : \mathbf{e}_x(\mathbf{u}^{pm(\varepsilon)}) &= \left(\mathbf{b} : \mathbf{e}_x(\mathbf{u}^{pm(\varepsilon)}) \right)^2 \\ b(\mathbf{I} \otimes \mathbf{I})_{ijkh} e_{xkh}(\mathbf{u}^{pm(\varepsilon)}) e_{xij}(\mathbf{u}^{pm(\varepsilon)}) &= b^2 \delta_{ij} e_{xij}(\mathbf{u}^{pm(\varepsilon)}) \delta_{kh} e_{xkh}(\mathbf{u}) = \left(b \delta_{ij} e_{xij}(\mathbf{u}^{pm(\varepsilon)}) \right)^2 \end{aligned}$$

$$\mathcal{D}^{pf(e)} = \mathcal{D}^{pf(0)} + e \mathcal{D}^{pf(1)} + \dots \quad (3.20)$$

with the term of order zero in the powers of e which reads as follows:

$$\mathcal{D}^{pf(0)} = -\boldsymbol{\sigma}^{pf(1)} : \mathbf{D}_y(\mathbf{v}^{pf(0)}) = -2\mu \mathbf{D}_y(\mathbf{v}^{pf(0)}) : \mathbf{D}_y(\mathbf{v}^{pf(0)}) \quad (3.21)$$

where the corresponding terms in the expansion of the constitutive law (B.5h) and the fluid incompressibility (B.5b) are taken into account.

At the mesoscopic scale, the volumetric density of dissipation $\mathcal{D}^{pm(\varepsilon)}$ in porous matrix is defined as the average value of $\mathcal{D}^{pf(0)}$ over the entire microscopic periodic cell Z :

$$\mathcal{D}^{pm(\varepsilon)} := \frac{1}{|Z|} \int_{Z^{pf}} \mathcal{D}^{pf(0)} \, ds \quad (3.22)$$

With the aim of writing $\mathcal{D}^{pm(\varepsilon)}$ in terms of mesoscopic quantities, the following calculus is developed. The equilibrium equation at order zero (B.5a) is multiplied by the pore fluid velocity at the order zero $\mathbf{v}^{pf(0)}$ and integrated over the pore fluid subdomain Z^{pf} of the microscopic periodic unit cell:

$$\int_{Z^{pf}} \mathbf{v}^{pf(0)} \cdot \left(\operatorname{div}_x \boldsymbol{\sigma}^{pf(0)} + \operatorname{div}_y \boldsymbol{\sigma}^{pf(1)} \right) \, ds = 0 \quad (3.23)$$

By using the constitutive law (B.5g) of the fluid pore at order zero in the power of e and the integration by parts, it follows that:

$$-\nabla_x p^{pf(0)} \cdot \int_{Z^{pf}} \mathbf{v}^{pf(0)} \, ds + \int_{Z^{pf}} \boldsymbol{\sigma}^{pf(1)} : \mathbf{D}_y(\mathbf{v}^{pf(0)}) \, ds + \int_{\Gamma^{s-f}} \boldsymbol{\sigma}^{pf(1)} @ \mathbf{n} \cdot \mathbf{v}^{pf(0)} \, d\lambda = 0 \quad (3.24)$$

Given the no-slip condition (B.5j) on the interface Γ^{s-pf} , then it follows that:

$$\begin{aligned} \int_{\Gamma^{s-pf}} \boldsymbol{\sigma}^{pf(1)} @ \mathbf{n} \cdot \mathbf{v}^{pf(0)} \, d\lambda &= -\dot{\mathbf{u}}^{s(0)} \cdot \int_{Z^{pf}} \operatorname{div}_y(\boldsymbol{\sigma}^{pf(1)}) \, ds \\ &= \dot{\mathbf{u}}^{s(0)} \cdot \int_{Z^{pf}} \operatorname{div}_x(\boldsymbol{\sigma}^{pf(0)}) \, ds = |Z^{pf}| \dot{\mathbf{u}}^{s(0)} \cdot \nabla_x p^{pf(0)} \end{aligned} \quad (3.25)$$

Then, by using the definition (3.22) of \mathcal{D}^{pf} and given the remark 3.2.2, the energy rate balance (3.24) is rewritten as:

$$\mathcal{D}^{pm(\varepsilon)} = -\mathbf{q}^{pm(\varepsilon)} \cdot \nabla_x p^{pm(\varepsilon)} = \mathbf{k} @ \nabla_x p^{pm(\varepsilon)} \cdot \nabla_x p^{pm(\varepsilon)} \quad (3.26)$$

where it has been used also the mesoscopic Darcy's law (2.35).

3.3 Global energy analysis at the mesoscale

Following Gurtin (1979a), a mesoscopic energy analysis is performed in the whole body Ω (fig. 3.3) before applying the homogenization method, that is, the exact fields of the mesoscopic description (section 2.2) are taken into account. Then, the physical definition of the fracture energy release rate is obtained.

In the physical space, the mesoscopic structure is locally periodic, in the sense that the length of the cavities may vary smoothly with respect to the spatial variable, being ε the size of the period, l the cavity length and $d\Lambda$ the infinitesimal line element.

As already written in the section 2.2, at the mesoscopic scale of observation, the whole body Ω appears as a porous solid which contains a distribution of fluid-filled cavities. So, it can be described as the union of two disjoint subdomains: the porous matrix subdomain Ω^{pm} and the set of fluid-filled cavities Ω^{cf} ; that is, $\Omega = \Omega^{pm} \cup \Omega^{cf}$ and $\emptyset = \Omega^{pm} \cap \Omega^{cf}$ (fig. 2.2).

The fluid-filled cavity volume subdomain is defined as $\Omega^{cf} = \bigcup_{\alpha=1}^A c_\alpha$ where c_α is the α -th cavity out of A cavities. The boundary $\partial\Omega^{pm}$ of the porous matrix is composed by an external part $\partial\Omega$ and an internal one $\partial\Omega^{cf} = \bigcup_{\alpha=1}^A \partial c_\alpha$, such that $\partial\Omega^{pm} = \partial\Omega \cup \partial\Omega^{cf}$.

A synopsis of the mesoscopic equations governing the hydro-mechanical behaviour of the porous solid with fluid-filled cavities is already provided in the section 2.2.6. However, in order to perform the global energy analysis, the condition on the external boundary $\partial\Omega$ have to be added and they are introduced below²:

$$\boldsymbol{\sigma}^{pm(\varepsilon)} \cdot \mathbf{n} = \mathbf{F} \quad \text{on } \partial\Omega \quad (3.27a)$$

$$\mathbf{q}^{pm(\varepsilon)} \cdot \mathbf{n} = W \quad \text{on } \partial\Omega \quad (3.27b)$$

²It is worth pointing out that in the section 2.2.6 the exact mesoscopic fields are not denoted by the superscript (ε) simply because the idea of a series of periodic mesoscopic structures of period $\varepsilon \rightarrow 0$ was not yet introduced.

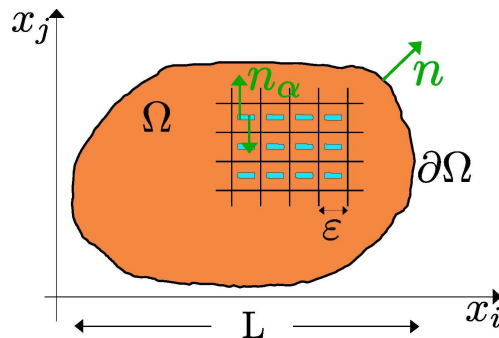


Figure 3.3: The body Ω with its mesoscopic and locally periodic structure. The unit vector \mathbf{n} is the outward normal of the porous matrix Ω^{pm} and it is denoted as \mathbf{n}_α on the boundary of the α th cavity.

where \mathbf{n} is the outward normal to Ω^{pm} (fig. 3.3).

3.3.1 Weak formulation of linear momentum balance

The virtual power formulation of the equilibrium equation (2.47a) in the whole body Ω reads: $\forall \mathbf{w}$,

$$0 = - \int_{\Omega} \boldsymbol{\sigma}^{(\varepsilon)} : \mathbf{e}_x(\mathbf{w}) \, dS + \int_{\partial\Omega} (\boldsymbol{\sigma}^{(\varepsilon)} \otimes \mathbf{n}) \cdot \mathbf{w} \, d\Lambda \quad (3.28)$$

where dS and $d\Lambda$ are the infinitesimal surface and line element respectively. By taking into account the constitutive relations (2.47e) and (2.47f) and the stress boundary condition (3.27a) on $\partial\Omega$, it becomes: $\forall \mathbf{w}$,

$$0 = - \int_{\Omega^{pm}} (\mathbf{c} \otimes \mathbf{e}_x(\mathbf{u}^{pm(\varepsilon)}) - \mathbf{b} p^{pm(\varepsilon)}) : \mathbf{e}_x(\mathbf{w}) \, dS - \sum_{\alpha=1}^A p_{\alpha}^{cf(\varepsilon)} \int_{\partial c_{\alpha}} \mathbf{w} \cdot \mathbf{n}_{\alpha} \, d\Lambda + \int_{\partial\Omega} \mathbf{F} \cdot \mathbf{w} \, d\Lambda \quad (3.29)$$

with \mathbf{n}_{α} being the inward unit normal vector to the cavity c_{α} (fig. 3.3) and the fluid pressure $p_{\alpha}^{cf(\varepsilon)}$ being homogeneous in every single cavity.

3.3.2 Weak formulation of fluid mass balance

The virtual power formulation of the fluid volume balance (2.47c) in the porous matrix Ω^{pm} reads: $\forall h$,

$$0 = \int_{\Omega^{pm}} (\dot{\phi}_u^{(\varepsilon)} h - \mathbf{q}^{pm(\varepsilon)} \cdot \nabla_x h) \, dS + \int_{\partial\Omega^{pm}} h \mathbf{q}^{pm(\varepsilon)} \cdot \mathbf{n} \, d\Lambda \quad (3.30)$$

Given the boundary condition (3.27b), the fluid volume conservation across the cavity interface (2.47j), the cavity fluid incompressibility (2.47b) and by imposing to the test function h to be homogeneous in every single cavity c_{α} , just like the cavity fluid pressure, it becomes: $\forall h$ s.t. $h = h_{\alpha}$ in c_{α} ,

$$0 = \int_{\Omega^{pm}} (\dot{\phi}_u^{(\varepsilon)} h - \mathbf{q}^{pm(\varepsilon)} \cdot \nabla_x h) \, dS + \int_{\partial\Omega} h W \, d\Lambda - \sum_{\alpha=1}^A h_{\alpha} \int_{\partial c_{\alpha}} \dot{\mathbf{u}}^{pm(\varepsilon)} \cdot \mathbf{n}_{\alpha} \, d\Lambda \quad (3.31)$$

By inserting also the constitutive law (2.47g), it follows that: $\forall h$ s.t. $h = h_{\alpha}$ in c_{α} ,

$$\begin{aligned} 0 = & \int_{\Omega^{pm}} \left((\mathbf{b} : \mathbf{e}_x(\dot{\mathbf{u}}^{pm(\varepsilon)}) + s \dot{p}^{pm(\varepsilon)}) h - \mathbf{q}^{pm(\varepsilon)} \cdot \nabla_x h \right) \, dS \\ & + \int_{\partial\Omega} h W \, d\Lambda - \sum_{\alpha=1}^A h_{\alpha} \int_{\partial c_{\alpha}} \dot{\mathbf{u}}^{pm(\varepsilon)} \cdot \mathbf{n}_{\alpha} \, d\Lambda \end{aligned} \quad (3.32)$$

3.3.3 Weak formulation of cavity fluid incompressibility

The virtual power formulation of the cavity fluid incompressibility (2.47b) reads: $\forall h$,

$$0 = \int_{\Omega^{cf}} \left(\operatorname{div}_{\mathbf{x}}(h \mathbf{v}^{cf(\varepsilon)}) - \mathbf{v}^{cf(\varepsilon)} \cdot \nabla_x h \right) dS \quad (3.33)$$

or: $\forall h$ s.t. $h = h_\alpha$ in c_α ,

$$0 = \sum_{\alpha=1}^A h_\alpha \int_{\partial c_\alpha} \mathbf{v}^{cf(\varepsilon)} \cdot \mathbf{n}_\alpha d\Lambda + \sum_{\alpha=1}^A \int_{c_\alpha} \mathbf{v}^{cf(\varepsilon)} \cdot \nabla_x h_\alpha dS \quad (3.34)$$

where, because of $\nabla_x h_\alpha = 0$, the second term vanishes. In the end, by also making use of the interface condition (2.47j), the (3.34) becomes:

$$0 = \sum_{\alpha=1}^A h_\alpha \int_{\partial c_\alpha} (\mathbf{q}^{pm(\varepsilon)} + \dot{\mathbf{u}}^{pm(\varepsilon)}) \cdot \mathbf{n}_\alpha d\Lambda \quad (3.35)$$

3.3.4 Energy rate balance

3.3.4.1 Stationary cavities

The weak formulation of the full mesoscopic problem (2.47, 3.27) is obtained by combining the relations (3.29) and (3.32) as follows:

$$\begin{aligned} 0 = & \int_{\partial\Omega} (\mathbf{F} \cdot \mathbf{w} - h W) d\Lambda + \sum_{\alpha=1}^A \left(h_\alpha \int_{\partial c_\alpha} \dot{\mathbf{u}}^{pm(\varepsilon)} \cdot \mathbf{n}_\alpha d\Lambda - p_\alpha^{cf(\varepsilon)} \int_{\partial c_\alpha} \mathbf{w} \cdot \mathbf{n}_\alpha d\Lambda \right) \\ & - \int_{\Omega^{pm}} \left((\mathbf{c} @ \mathbf{e}_x(\mathbf{u}^{pm(\varepsilon)}) - \mathbf{b} p^{pm(\varepsilon)}) : \mathbf{e}_x(\mathbf{w}) + (\mathbf{b} : \mathbf{e}_x(\dot{\mathbf{u}}^{pm(\varepsilon)}) + s \dot{p}^{pm(\varepsilon)}) h - \mathbf{q}^{pm(\varepsilon)} \cdot \nabla_x h \right) dS \end{aligned} \quad (3.36)$$

In order to get the real power involved in the deformation of the medium, let us set $\mathbf{w} = \dot{\mathbf{u}}^{pm(\varepsilon)}$, $h = p^{pm(\varepsilon)}$ and $h_\alpha = p_\alpha^{cf(\varepsilon)}$. Moreover, the fluid pressure continuity (2.47h) on the cavity boundary is taken into account and so the previous relation can be rewritten as:

$$\begin{aligned} & - \int_{\Omega^{pm}} \mathbf{q}^{pm(\varepsilon)} \cdot \nabla_x p^{pm(\varepsilon)} dS = \int_{\partial\Omega} (\mathbf{F} \cdot \dot{\mathbf{u}} - p^{pm(\varepsilon)} W) d\Lambda \\ & - \int_{\Omega^{pm}} \left(\mathbf{c} @ \mathbf{e}_x(\mathbf{u}^{pm(\varepsilon)}) : \mathbf{e}_x(\dot{\mathbf{u}}^{pm(\varepsilon)}) + s p^{pm(\varepsilon)} \dot{p}^{pm(\varepsilon)} \right) dS \end{aligned} \quad (3.37)$$

which, given the definitions (3.17, 3.26) of the mesoscopic volumetric density of the strain energy $\psi^{pm(\varepsilon)}$ respectively, and of the dissipation $\mathcal{D}^{pm(\varepsilon)}$ associated to the pore fluid motion at the mesoscopic scale, becomes:

$$\int_{\Omega^{pm}} \mathcal{D}^{pm(\varepsilon)} dS = \int_{\partial\Omega} (\mathbf{F} \cdot \dot{\mathbf{u}}^{pm(\varepsilon)} - p^{pm(\varepsilon)} W) d\Lambda - \int_{\Omega^{pm}} \frac{\partial \psi^{pm(\varepsilon)}}{\partial t} dS \quad (3.38)$$

The physical meaning of which is clear: the power supplied through the boundary $\partial\Omega$ is both stored in the poroelastic matrix Ω^{pm} and dissipated because of the fluid flow through the porous matrix.

Remark 3.3.1. In the (3.38), the integral defined on $\partial\Omega$ can be rewritten by means of the divergence theorem and of the boundary conditions (3.27a, 3.27b) as:

$$\begin{aligned} \int_{\partial\Omega} (\mathbf{F} \cdot \dot{\mathbf{u}}^{pm(\varepsilon)} - p^{pm(\varepsilon)} W) d\Lambda &= \int_{\partial\Omega} (\boldsymbol{\sigma}^{pm} \otimes \mathbf{n} \cdot \dot{\mathbf{u}}^{pm(\varepsilon)} - p^{pm(\varepsilon)} \mathbf{q}^{pm} \cdot \mathbf{n}) d\Lambda \\ &= \int_{\Omega^{pm}} \operatorname{div}_{\mathbf{x}} \left(\boldsymbol{\sigma}^{pm(\varepsilon)} \otimes \dot{\mathbf{u}} - p^{pm(\varepsilon)} \mathbf{q}^{pm(\varepsilon)} \right) dS - p^{pm(\varepsilon)} \int_{\partial\Omega^{cf}} (\mathbf{q}^{pm(\varepsilon)} + \dot{\mathbf{u}}^{pm(\varepsilon)}) \cdot \mathbf{n} d\Lambda \end{aligned} \quad (3.39)$$

where the second term of the last expression is a zero as already shown in the (3.35). Then, by also taking into account the linear momentum balance in Ω^{pm} and the symmetry of the second order tensor $\boldsymbol{\sigma}^{pm(\varepsilon)}$, it follows that:

$$\int_{\partial\Omega} (\mathbf{F} \cdot \dot{\mathbf{u}}^{pm(\varepsilon)} - p^{pm(\varepsilon)} W) d\Lambda = \int_{\Omega^{pm}} \left(\boldsymbol{\sigma}^{pm(\varepsilon)} : \mathbf{e}_x(\dot{\mathbf{u}}^{pm(\varepsilon)}) - \operatorname{div}_{\mathbf{x}}(p^{pm(\varepsilon)} \mathbf{q}^{pm(\varepsilon)}) \right) dS \quad (3.40)$$

Taking into account the remark above, the energy balance (3.38) reads also:

$$\int_{\Omega^{pm}} \mathcal{D}^{pm(\varepsilon)} dS = \int_{\Omega^{pm}} \left(\boldsymbol{\sigma}^{pm(\varepsilon)} : \mathbf{e}_x(\dot{\mathbf{u}}^{pm(\varepsilon)}) - \operatorname{div}_{\mathbf{x}}(p^{pm(\varepsilon)} \mathbf{q}^{pm(\varepsilon)}) - \dot{\psi}^{pm(\varepsilon)} \right) dS \quad (3.41)$$

or

$$0 = \int_{\Omega^{pm}} \left(\boldsymbol{\sigma}^{pm(\varepsilon)} : \mathbf{e}_x(\dot{\mathbf{u}}^{pm(\varepsilon)}) + p^{pm(\varepsilon)} \dot{\phi}_u^{(\varepsilon)} - \dot{\psi}^{pm(\varepsilon)} \right) dS \quad (3.42)$$

Remark 3.3.2. By writing the weak formulations in a subdomain of Ω and not on the entire domain, as done in this section, given the arbitrariness of Ω^{pm} , both the (3.41, 3.42) can be written in a local form as:

$$\mathcal{D}^{pm(\varepsilon)} = \boldsymbol{\sigma}^{pm(\varepsilon)} : \mathbf{e}_x(\dot{\mathbf{u}}^{pm(\varepsilon)}) - \operatorname{div}_{\mathbf{x}}(p^{pm(\varepsilon)} \mathbf{q}^{pm(\varepsilon)}) - \dot{\psi}^{pm(\varepsilon)} \quad (3.43)$$

or equivalently:

$$0 = \boldsymbol{\sigma}^{pm(\varepsilon)} : \mathbf{e}_x(\dot{\mathbf{u}}^{pm(\varepsilon)}) + p^{pm(\varepsilon)} \dot{\phi}_u^{(\varepsilon)} - \dot{\psi}^{pm(\varepsilon)} \quad (3.44)$$

3.3.4.2 Evolving cavities and fracture energy release rate

Now the possible propagation of the mesoscopic fluid-filled cavities is taken into account and the porous subdomain Ω^{pm} becomes dependent on time through the length l_α of the α th cavity : $\Omega^{pm} = \Omega^{pm}[l_\alpha(t)]$. So, by means of an adaptation of the Reynolds transport theorem (see appendix D) and of the conditions (2.47i, 2.47f) at the cavity boundary, the energy rate balance (3.38) is rewritten as:

$$\begin{aligned} & \int_{\Omega^{pm}} \mathcal{D}^{pm(\varepsilon)} dS + \sum_{\alpha=1}^A \int_{\partial c_\alpha^{fr}} -\psi^{pm(\varepsilon)} \mathbf{v}_\alpha \cdot \mathbf{n}_\alpha d\Lambda \\ &= \int_{\partial\Omega} (\mathbf{F} \cdot \dot{\mathbf{u}}^{pm(\varepsilon)} - p^{pm(\varepsilon)} W) d\Lambda - \frac{d}{dt} \int_{\Omega^{pm}} \psi^{pm(\varepsilon)} dS \end{aligned} \quad (3.45)$$

where ∂c_α^{fr} is the union of the left and right front of the α th cavity which move with a propagation speed vector $\mathbf{v}_\alpha = (\dot{l}_\alpha/2)\mathbf{m}_\alpha$, \dot{l}_α is the cavity length rate and \mathbf{n}_α is the inward normal to the cavity c_α (fig. 3.3.4.2). And its physical meaning is clear: the power supplied through the boundary $\partial\Omega$ is partially stored in the poroelastic matrix Ω^{pm} and partially dissipated because of both the fluid flow and the cavity propagation. In the same way, the (3.42) becomes:

$$\begin{aligned} & \int_{\Omega^{pm}} \mathcal{D}^{pm(\varepsilon)} dS + \sum_{\alpha=1}^A \int_{\partial c_\alpha^{fr}} -\psi^{pm(\varepsilon)} \mathbf{v}_\alpha \cdot \mathbf{n}_\alpha d\Lambda \\ &= \int_{\Omega^{pm}} \left(\boldsymbol{\sigma}^{pm(\varepsilon)} : \mathbf{e}_x(\dot{\mathbf{u}}^{pm(\varepsilon)}) - \text{div}_{\mathbf{x}}(p^{pm(\varepsilon)} \mathbf{q}^{pm(\varepsilon)}) \right) dS - \frac{d}{dt} \int_{\Omega^{pm}} \psi^{pm(\varepsilon)} dS \end{aligned} \quad (3.46)$$

From the energy rate balances (3.45) or (3.46), the fracture energy release rate per unit length $\mathcal{G}_\alpha^{(\varepsilon)}$ of the α th cavity (fig. 3.3.4.2) is defined as the integral on the cavity fronts ∂c_α^{fr} divided by \dot{l}_α and it reads:

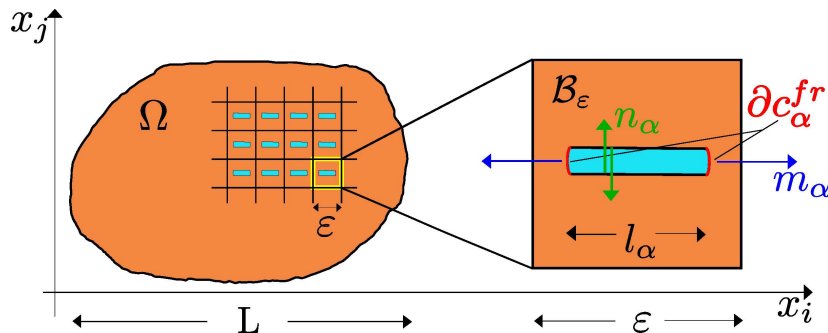


Figure 3.4: Nomenclature in the α th periodic cell: ∂c_α^{fr} is the set of the two cavity fronts; \mathbf{n}_α is the inward normal unit vector to the cavity boundary; \mathbf{m}_α is the unit vector in the direction of the propagation.

$$\mathcal{G}_\alpha^{(\varepsilon)} := \frac{1}{\dot{l}_\alpha} \int_{\partial c_\alpha^{fr}} -\psi^{pm(\varepsilon)} \mathbf{v}_\alpha \cdot \mathbf{n} \, d\Lambda = \int_{\partial c_\alpha^{fr}} -\frac{1}{2} \psi^{pm(\varepsilon)} \mathbf{m}_\alpha \cdot \mathbf{n}_\alpha \, d\Lambda \quad (3.47)$$

It is worth remarking that the fracture energy release rate depends on the cavity length l_α through both the strain energy density $\psi^{pm(\varepsilon)}$ and the cavity fronts ∂c_α^{fr} .

3.3.5 Modeling of cavity propagation

Let us assume a Griffith-type energy criterion, that is, the propagation occurs when the fracture energy release rate $\mathcal{G}_\alpha^{(\varepsilon)}$ reaches a critical energy threshold \mathcal{G}_f , also called critical fracture energy rate of the material. The cavity propagation is completely described by the following laws:

$$\mathcal{G}_\alpha^{(\varepsilon)} - \mathcal{G}_f \leq 0 \quad (3.48a)$$

$$\dot{l}_\alpha \geq 0 \quad (3.48b)$$

$$\dot{l}_\alpha (\mathcal{G}_\alpha^{(\varepsilon)} - \mathcal{G}_f) = 0 \quad (3.48c)$$

The (3.48a) says that the fracture energy release rate cannot become bigger than the critical fracture energy rate. The (3.48b) asserts the damage irreversibility. While the (3.48c) expresses an energy rate balance when the cavity is propagating ($\dot{l}_\alpha \neq 0$): the energy that the body is ready to spend per unit cavity length advance is equal with the critical energy necessary to break the bonds in the specific material.

It is worth remarking that the relations (3.48) have the form of the Kuhn-Tucker conditions (Koiter 1960; Maier 1970) for the Plasticity Theory (Hill 1950; Lubliner 1990; Simo and Hughes 1998).

3.3.6 Fracture criteria

In the case of brittle fracture, the critical fracture energy \mathcal{G}_f is a material constant \mathcal{G}_c :

$$\mathcal{G}_f = \mathcal{G}_c \quad (3.49)$$

On the contrary, in the case of quasi-brittle fracture, \mathcal{G}_f is a constitutive function which depends on the crack length l_α and, eventually, also on its rate \dot{l}_α , that is:

$$\mathcal{G}_f = \mathcal{G}_f(l_\alpha, \dot{l}_\alpha) \quad (3.50)$$

In the case of no-time dependence, an example of constitutive function for quasi-brittle materials is proposed by Bazant and Planas (1997) who considered an equivalent elastic medium in which the presence of the process zone near the crack tip is replaced by a special propagation law which reads:

$$\mathcal{G}_f = \frac{\mathcal{G}_c (l_\alpha - l_{\alpha 0})}{c_f} \quad (3.51)$$

where $l_{\alpha 0}$ is the initial crack length and c_f is the material length governing the fracture process zone size.

3.4 Cell energy analysis at the mesoscale

In this section, it is performed a mesoscopic cell energy analysis coupled with homogenization which leads to the damage evolution law. It is worth remarking that the involved fields are terms of the asymptotic developments which are cut to the first order in the powers of ε (par. 2.3.2), that is, this energy analysis is performed in an approximated framework.

3.4.1 From meso- to macro-energy terms

3.4.1.1 Strain energy

At the mesoscopic scale, let us expand asymptotically the volumetric density of strain energy $\psi^{pm(\varepsilon)}$ as follows:

$$\psi^{pm(\varepsilon)} = \psi^{pm(0)} + \varepsilon \psi^{pm(1)} + \dots \quad (3.52)$$

From the (3.17) about $\psi^{pm(\varepsilon)}$, it follows that:

$$\psi^{pm(0)} = \frac{1}{2} \left(\mathbf{c} @ \left(\mathbf{e}_x(\mathbf{u}^{pm(0)}) + \mathbf{e}_y(\mathbf{u}^{pm(1)}) \right) : \left(\mathbf{e}_x(\mathbf{u}^{pm(0)}) + \mathbf{e}_y(\mathbf{u}^{pm(1)}) \right) + s (p^{pm(0)})^2 \right) \quad (3.53)$$

In analogy with the procedure presented in the section 3.2.1, being assumed that the fluid is incompressible, the volumetric density of macroscopic strain energy Ψ can be defined as the average value of $\psi^{pm(0)}$ over the entire mesoscopic periodic cell Y (fig. 3.2):

$$\Psi := \frac{1}{|Y|} \int_{Y^{pm}} \psi^{pm(0)} \, ds \quad (3.54)$$

that, given the expression (3.53) of $\psi^{pm(0)}$, reads also:

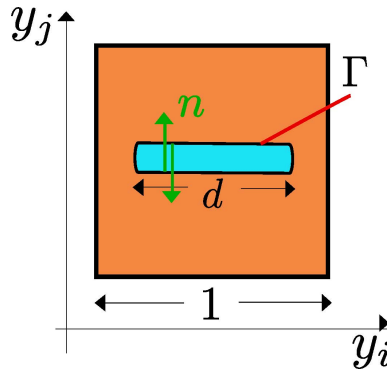


Figure 3.5: Nomenclature in the α th periodic cell and in the corresponding unit cell.

$$\Psi = \frac{1}{|Y|} \int_{Y^{pm}} \frac{1}{2} \left[\mathbf{c}_@ \left(\mathbf{e}_x(\mathbf{u}^{pm(0)}) + \mathbf{e}_y(\mathbf{u}^{pm(1)}) \right) : \left(\mathbf{e}_x(\mathbf{u}^{pm(0)}) + \mathbf{e}_y(\mathbf{u}^{pm(1)}) \right) + s (p^{pm(0)})^2 \right] ds \quad (3.55)$$

By taking into account the constitutive law (2.85b) for the porous matrix at order zero in the powers of ε , and the weak formulation (2.86) of the equilibrium equation (2.85a) with $\mathbf{z} = \mathbf{u}^{pm(1)}$, it follows that:

$$\Psi = \frac{1}{|Y|} \int_{Y^{pm}} \frac{1}{2} \left[(\boldsymbol{\sigma}^{pm(0)} + p^{(0)} \mathbf{b}) : \mathbf{e}_x(\mathbf{u}^{pm(0)}) + p^{pm(0)} (\mathbf{b} - \mathbf{I}) : \mathbf{e}_y(\mathbf{u}^{pm(1)}) + s (p^{pm(0)})^2 \right] ds \quad (3.56)$$

or

$$\begin{aligned} \Psi = \frac{1}{|Y|} \int_{Y^{pm}} \frac{1}{2} & \left[\boldsymbol{\sigma}^{pm(0)} : \mathbf{e}_x(\mathbf{u}^{pm(0)}) + p^{(0)} \mathbf{I} : \mathbf{e}_x(\mathbf{u}^{pm(0)}) \right. \\ & \left. + p^{pm(0)} (\mathbf{b} - \mathbf{I}) : \left(\mathbf{e}_x(\mathbf{u}^{pm(0)}) + \mathbf{e}_y(\mathbf{u}^{pm(1)}) \right) + s (p^{pm(0)})^2 \right] ds \end{aligned} \quad (3.57)$$

which, given the definition (2.126) of the macroscopic stress tensor $\boldsymbol{\Sigma}$, entails:

$$\begin{aligned} \Psi = \frac{1}{2} & \left[\boldsymbol{\Sigma} : \mathbf{e}_x(\mathbf{u}^{pm(0)}) + p^{pm(0)} \mathbf{I} : \mathbf{e}_x(\mathbf{u}^{pm(0)}) \right. \\ & \left. + \frac{1}{|Y|} p^{pm(0)} \int_{Y^{pm}} \left((\mathbf{b} - \mathbf{I}) : \left(\mathbf{e}_x(\mathbf{u}^{pm(0)}) + \mathbf{e}_y(\mathbf{u}^{pm(1)}) \right) + s p^{pm(0)} \right) ds \right] \end{aligned} \quad (3.58)$$

where the relation (2.143) about the variation of macroscopic Lagrangian porosity Φ_u is recognized. Then, by substitution in (3.58), it yields:

$$\Psi = \frac{1}{2} \left(\boldsymbol{\Sigma} : \mathbf{e}_x(\mathbf{u}^{pm(0)}) + \Phi_u p^{pm(0)} \right) \quad (3.59)$$

or, by means of the macroscopic constitutive relations (2.175b, 2.179), also as a function of the homogenized coefficients \mathbf{C} and S :

$$\Psi = \frac{1}{2} \left(\mathbf{C}_@ \mathbf{e}_x(\mathbf{u}^{pm(0)}) : \mathbf{e}_x(\mathbf{u}^{pm(0)}) + S (p^{pm(0)})^2 \right) \quad (3.60)$$

3.4.1.2 Dissipation in the fluid

At the mesoscopic scale, let us expand asymptotically the dissipation $\mathcal{D}^{pm(\varepsilon)}$ in the pore fluid as follows:

$$\mathcal{D}^{pm(\varepsilon)} = \mathcal{D}^{pm(0)} + \varepsilon \mathcal{D}^{pm(1)} + \dots \quad (3.61)$$

From the relation (3.26) about $\mathcal{D}^{pm(\varepsilon)}$, it follows that:

$$\mathcal{D}^{pm(0)} = -\mathbf{q}^{pm(0)} \cdot (\nabla_x p^{pm(0)} + \nabla_y p^{pm(1)}) = \mathbf{k}_@(\nabla_x p^{pm(0)} + \nabla_y p^{pm(1)}) \cdot (\nabla_x p^{pm(0)} + \nabla_y p^{pm(1)}) \quad (3.62)$$

At the macroscopic scale, let us define the dissipation \mathcal{D} in the fluid as the average of $\mathcal{D}^{pm(0)}$ over the entire mesoscopic periodic cell Y :

$$\mathcal{D} := \frac{1}{|Y|} \int_{Y^{pm}} \mathcal{D}^{pm(0)} \, ds \quad (3.63)$$

The virtual power formulation of the fluid volume balance (2.101a) within $h = p^{pm(1)}$ reads:

$$0 = - \int_{Y^{pm}} \mathbf{q}^{pm(0)} \cdot \nabla_y p^{pm(1)} \, ds + \int_{\Gamma} p^{cf(1)} (\mathbf{v}^{cf(0)} - \dot{\mathbf{u}}^{pm(0)}) \cdot \mathbf{n} \, d\lambda \quad (3.64)$$

where the fluid pressure continuity (2.70b) and the fluid mass balance (2.72b) at the cavity boundary have been taken into account. Given the (2.58a), it is known that $\mathbf{v}^{cf(0)}$ does not depend on the mesoscopic structure and it follows that:

$$0 = \int_{Y^{pm}} \mathbf{q}^{pm(0)} \cdot \nabla_y p^{pm(1)} \, ds + \int_{Y^{cf}} \nabla_y p^{cf(1)} \cdot (\mathbf{v}^{cf(0)} - \dot{\mathbf{u}}^{pm(0)}) \, ds \quad (3.65)$$

The fluid pressure at the order zero in the powers of ε is homogeneous in the whole mesoscopic unit cell Y , that is, $p^{pm(0)} = p^{cf(0)}$. Then, by taking into account the linear momentum balance (2.63b) in the cavity, the (3.65) becomes:

$$\int_{Y^{pm}} \mathbf{q}^{pm(0)} \cdot (\nabla_x p^{pm(0)} + \nabla_y p^{pm(1)}) \, ds = \nabla_x p^{pm(0)} \cdot \left[\int_{Y^{pm}} \mathbf{q}^{pm(0)} \, ds + \int_{Y^{cf}} (\mathbf{v}^{cf(0)} - \dot{\mathbf{u}}^{pm(0)}) \, ds \right] \quad (3.66)$$

where, among square brackets, it is easily recognized the definition (2.164) of the macroscopic relative flow vector of fluid volume \mathbf{Q} . While, the left member is the dissipation in the fluid phase \mathcal{D} at the macroscopic scale as defined in the (3.63) and multiplied by the measure of the unit cell $|Y|$. Then the rewriting of the (3.66) provides an expression of \mathcal{D} in terms of only macroscopic quantities:

$$\mathcal{D} = -\mathbf{Q} \cdot \nabla_x p^{pm(0)} = \mathbf{K}_@ \nabla_x p^{pm(0)} \cdot \nabla_x p^{pm(0)} \quad (3.67)$$

where \mathbf{K} is the homogenized permeability tensor.

3.4.2 Energy rate balance

As already done in the section 3.3.4 for the entire body and with the exact fields, the energy rate balance is here built for the resized periodic cell y and by taking into account the asymptotic developments of the involved fields. With this aim, the linear momentum balance in Y , the fluid volume balance in Y^{pm} and the cavity fluid incompressibility are

taken into account.

By setting $\mathbf{z} = \dot{\mathbf{u}}^{pm(1)}$, the weak formulation (2.86) of the balance equation (2.85a) reads:

$$0 = \int_{Y^{pm}} (\boldsymbol{\sigma}^{pm(0)} + p^{pm(0)} \mathbf{I}) : \mathbf{e}_y(\dot{\mathbf{u}}^{pm(1)}) \, ds \quad (3.68)$$

It is useful to rewrite it as follows:

$$0 = \int_{Y^{pm}} \left((\boldsymbol{\sigma}^{pm(0)} + p^{pm(0)} \mathbf{I}) : \left(\mathbf{e}_y(\dot{\mathbf{u}}^{pm(1)}) + (1-1) \mathbf{e}_x(\dot{\mathbf{u}}^{pm(0)}) \right) + (1-1) s p^{pm(0)} \dot{p}^{pm(0)} \right) \, ds \quad (3.69)$$

Moreover, with the same logic already applied in the writing of the energy balance for the global problem, the virtual power formulation (3.64) of the fluid mass balance is added to the (3.69) and it yields:

$$\begin{aligned} 0 = & - \int_{Y^{pm}} \mathbf{q}^{pm(0)} \cdot (\nabla_x p^{pm(0)} + \nabla_y p^{pm(1)}) \, ds \\ & + \nabla_x p^{pm(0)} \cdot \left[\int_{Y^{pm}} \mathbf{q}^{pm(0)} \, ds + \int_{Y^{cf}} (\mathbf{v}^{cf(0)} - \dot{\mathbf{u}}^{pm(0)}) \, ds \right] \\ & + \int_{Y^{pm}} \left((\boldsymbol{\sigma}^{pm(0)} + p^{pm(0)} \mathbf{I}) : \left(\mathbf{e}_y(\dot{\mathbf{u}}^{pm(1)}) + (1-1) \mathbf{e}_x(\dot{\mathbf{u}}^{pm(0)}) \right) + (1-1) s p^{pm(0)} \dot{p}^{pm(0)} \right) \, ds \end{aligned} \quad (3.70)$$

3.4.2.1 Stationary cavity

By using the constitutive law (2.85b) for the stress tensor at order zero and by regrouping properly the terms, the (3.70) becomes:

$$\begin{aligned} - \int_{Y^{pm}} \mathbf{q}^{pm(0)} \cdot (\nabla_x p^{pm(0)} + \nabla_y p^{pm(1)}) \, ds = & \left[\int_{Y^{pm}} \boldsymbol{\sigma}^{pm(0)} \, ds - |Y^{cf}| p^{pm(0)} \mathbf{I} \right] : \mathbf{e}_x(\dot{\mathbf{u}}^{pm(0)}) \\ & - \nabla_x p^{pm(0)} \cdot \left[\int_{Y^{pm}} \mathbf{q}^{pm(0)} \, ds + \int_{Y^{cf}} (\mathbf{v}^{cf(0)} - \dot{\mathbf{u}}^{pm(0)}) \, ds \right] \\ & + p^{pm(0)} \left[|Y| \operatorname{div}_x(\dot{\mathbf{u}}^{pm(0)}) + \int_{Y^{pm}} \frac{\partial f^{poro(0)}}{\partial t} \, ds \right] - \int_{Y^{pm}} \frac{\partial \psi^{pm(0)}}{\partial t} \, ds \end{aligned} \quad (3.71)$$

where $f^{poro(0)}$ is defined as:

$$f^{poro(0)} = (\mathbf{b} - \mathbf{I}) : (\mathbf{e}_y(\mathbf{u}^{pm(1)}) + \mathbf{e}_x(\mathbf{u}^{pm(0)})) + s p^{pm(0)} \quad (3.72)$$

or equivalently, given the expansion (2.59b) of the variation of the Lagrangian mesoscopic porosity ϕ_u , as:

$$f^{poro(0)} = \phi_u^{(0)} - (\operatorname{div}_x(\mathbf{u}^{pm(0)}) + \operatorname{div}_y(\mathbf{u}^{pm(1)})) \quad (3.73)$$

Then, by using the time derivative of the (2.143), the definition (2.126) of the homogenized stress Σ , the definition (3.55) of the macroscopic strain energy Ψ and the definition (3.67) of the dissipation in the fluid \mathcal{D} , the (3.71) is rewritten as:

$$\mathcal{D} = \Sigma : \mathbf{e}_x(\dot{\mathbf{u}}^{pm(0)}) - \operatorname{div}_x(p^{pm(0)}\mathbf{Q}) - \dot{\Psi} \quad (3.74)$$

or equivalently as:

$$0 = \Sigma : \mathbf{e}_x(\dot{\mathbf{u}}^{pm(0)}) + p^{pm(0)}\dot{\Phi}_u - \dot{\Psi} \quad (3.75)$$

3.4.2.2 Evolving cavity

It is taken into account that the cavities may propagate. Then, the porous domain Y^{pm} depends on the time through the damage variable d , $Y^{pm} = Y^{pm}[d(t)]$. So, by means of an adaptation of the Reynolds transport theorem (D.1), the following relations hold:

$$\int_{Y^{pm}} \frac{\partial f^{poro(0)}}{\partial t} ds = \frac{d}{dt} \int_{Y^{pm}} f^{poro(0)} ds - \int_{\Gamma_{fr}} f^{poro(0)} \mathbf{v} \cdot \mathbf{n} d\lambda \quad (3.76)$$

$$\int_{Y^{pm}} \frac{\partial \psi^{pm(0)}}{\partial t} ds = \frac{d}{dt} \int_{Y^{pm}} \psi^{pm(0)} ds - \int_{\Gamma_{fr}} \psi^{pm(0)} \mathbf{v} \cdot \mathbf{n} d\lambda \quad (3.77)$$

where $\mathbf{v} = (\dot{d}/2)\mathbf{m}$ is the propagation speed of all the material points belonging to the crack fronts Γ_{fr} , \mathbf{n} is the outward normal to the boundary ∂Y^{pm} . The (3.76, 3.77) are inserted in the (3.71) which becomes:

$$\begin{aligned} & \int_{\Gamma_{fr}} \left(-\psi^{pm(0)} + p^{pm(0)} f^{poro(0)} \right) \mathbf{v} \cdot \mathbf{n} d\lambda - \int_{Y^{pm}} \mathbf{q}^{pm(0)} \cdot (\nabla_x p^{pm(0)} + \nabla_y p^{pm(1)}) ds \\ &= -\nabla_x p^{pm(0)} \cdot \left[\int_{Y^{pm}} \mathbf{q}^{pm(0)} ds + \int_{Y^{cf}} (\mathbf{v}^{cf(0)} - \dot{\mathbf{u}}^{pm(0)}) ds \right] \\ & \quad + p^{pm(0)} \frac{d}{dt} \left[|Y| \operatorname{div}_x(\mathbf{u}^{pm(0)}) + \int_{Y^{pm}} f^{poro(0)} ds \right] \\ & \quad + \left(\int_{Y^{pm}} \boldsymbol{\sigma}^{pm(0)} ds - |Y^{cf}| p^{pm(0)} \mathbf{I} \right) : \mathbf{e}_x(\dot{\mathbf{u}}^{pm(0)}) - \frac{d}{dt} \int_{Y^{pm}} \psi^{pm(0)} ds \end{aligned} \quad (3.78)$$

As already done in the no-propagation case, by using the time derivative of the (2.143), the definition (2.126) of the homogenized stress Σ , the definition (3.55) of the macroscopic strain energy Ψ and the definition (3.67) of the dissipation in the fluid \mathcal{D} , the (3.78) is rewritten as:

$$\frac{d}{2} \int_{\Gamma_{fr}} \left(-\psi^{pm(0)} + p^{pm(0)} f^{poro(0)} \right) \mathbf{m} \cdot \mathbf{n} d\lambda + \mathcal{D} = \Sigma : \mathbf{e}_x(\dot{\mathbf{u}}^{pm(0)}) - \operatorname{div}_x(p^{pm(0)}\mathbf{Q}) - \dot{\Psi} \quad (3.79)$$

or equivalently:

$$\frac{\dot{d}}{2} \int_{\Gamma_{fr}} \left(-\psi^{pm(0)} + p^{pm(0)} f^{poro(0)} \right) \mathbf{m} \cdot \mathbf{n} \, d\lambda = \boldsymbol{\Sigma} : \mathbf{e}_x(\dot{\mathbf{u}}^{pm(0)}) + p^{pm(0)} \dot{\Phi}_u - \dot{\Psi} \quad (3.80)$$

3.4.2.3 Damage energy release rate

By taking into account the macroscopic constitutive relations (2.175b, 2.179) and by remarking that the homogenized coefficients depend on time, it follows that:

$$\begin{aligned} \boldsymbol{\Sigma} : \mathbf{e}_x(\dot{\mathbf{u}}^{pm(0)}) + \dot{\Phi}_u p^{pm(0)} &= \left(\mathbf{C}_{@} \mathbf{e}_x(\mathbf{u}^{pm(0)}) - \mathbf{B} p^{pm(0)} \right) : \mathbf{e}_x(\dot{\mathbf{u}}^{pm(0)}) \\ &+ \left(\dot{\mathbf{B}} : \mathbf{e}_x(\mathbf{u}^{pm(0)}) + \dot{S} p^{pm(0)} + \mathbf{B} : \mathbf{e}_x(\dot{\mathbf{u}}^{pm(0)}) + S \dot{p}^{pm(0)} \right) p^{pm(0)} \end{aligned} \quad (3.81)$$

or, by means of the relation (3.60) which gives the macroscopic strain energy Ψ as a function of the homogenized parameters \mathbf{C} and S , equivalently:

$$\begin{aligned} &\boldsymbol{\Sigma} : \mathbf{e}_x(\dot{\mathbf{u}}^{pm(0)}) + \dot{\Phi}_u p^{pm(0)} - \dot{\Psi} \\ &= -\frac{1}{2} \dot{\mathbf{C}}_{@} \mathbf{e}_x(\mathbf{u}^{pm(0)}) : \mathbf{e}_x(\mathbf{u}^{pm(0)}) + \dot{\mathbf{B}} p^{pm(0)} : \mathbf{e}_x(\mathbf{u}^{pm(0)}) + \frac{1}{2} \dot{S} (p^{pm(0)})^2 \end{aligned} \quad (3.82)$$

Moreover, the homogenized coefficients are time dependent through the characteristic functions, that is, through the damage variable $d = d(\mathbf{x})$:

$$\dot{\mathbf{C}} = \frac{d\mathbf{C}}{dt} = \frac{d\mathbf{C}}{dd} \dot{d}, \quad \dot{\mathbf{B}} = \frac{d\mathbf{B}}{dt} = \frac{d\mathbf{B}}{dd} \dot{d}, \quad \dot{S} = \frac{dS}{dt} = \frac{dS}{dd} \dot{d}. \quad (3.83)$$

By using the relations (3.82, 3.83), the energy rate balance (3.80) becomes: $\forall \dot{d}$,

$$\dot{d} \left[\int_{\Gamma_{fr}} \frac{1}{2} \left(-\psi^{pm(0)} + p^{pm(0)} f^{poro(0)} \right) \mathbf{m} \cdot \mathbf{n} \, d\lambda - Y_d(d) \right] = 0 \quad (3.84)$$

where $Y_d(d)$ is the simplified notation of $Y_d = Y_d(d, \mathbf{e}_x(\mathbf{u}^{pm(0)}), p^{pm(0)})$ and denotes the damage energy release rate which is defined as follows:

$$\begin{aligned} Y_d &= Y_d(d, \mathbf{e}_x(\mathbf{u}^{pm(0)}), p^{pm(0)}) \\ &:= -\frac{1}{2} \frac{d\mathbf{C}}{dd} @ \mathbf{e}_x(\mathbf{u}^{pm(0)}) : \mathbf{e}_x(\mathbf{u}^{pm(0)}) + \frac{d\mathbf{B}}{dd} p^{pm(0)} : \mathbf{e}_x(\mathbf{u}^{pm(0)}) + \frac{1}{2} \frac{dS}{dd} (p^{pm(0)})^2 \end{aligned} \quad (3.85)$$

Given the arbitrariness of \dot{d} , the local form of the (3.84) reads:

$$Y_d(d) = \int_{\Gamma_{fr}} \frac{1}{2} \left(-\psi^{pm(0)} + p^{pm(0)} f^{poro(0)} \right) \mathbf{m} \cdot \mathbf{n} \, d\lambda \quad (3.86)$$

3.4.2.4 Approximation due to small thickness of the cavity

It is worth remarking that the objective of this work is to model fluid-filled cracks or cavities of small thickness. When such a cavity approaches a line crack, the fields near the tip converge to the crack fields, with the corresponding singularities.

Let us focus the attention on the integral of the energy rate balance (3.86). By means of the definitions (3.53) of $\psi^{pm(0)}$ and (3.72) of $f^{poro(0)}$, it follows that:

$$\begin{aligned} & \int_{\Gamma_{fr}} \left(-\psi^{pm(0)} + p^{pm(0)} f^{poro(0)} \right) \mathbf{m} \cdot \mathbf{n} \, d\lambda = \\ & - \int_{\Gamma_{fr}} \frac{1}{2} \left(\mathbf{c} @ \left(\mathbf{e}_x(\mathbf{u}^{pm(0)}) + \mathbf{e}_y(\mathbf{u}^{pm(1)}) \right) : \left(\mathbf{e}_x(\mathbf{u}^{pm(0)}) + \mathbf{e}_y(\mathbf{u}^{pm(1)}) \right) + s (p^{pm(0)})^2 \right) \mathbf{m} \cdot \mathbf{n} \, d\lambda \\ & + p^{pm(0)} \int_{\Gamma_{fr}} \left((\mathbf{b} - \mathbf{I}) : (\mathbf{e}_y(\mathbf{u}^{pm(1)}) + \mathbf{e}_x(\mathbf{u}^{pm(0)})) + s p^{pm(0)} \right) \mathbf{m} \cdot \mathbf{n} \, d\lambda \end{aligned} \quad (3.87)$$

By comparing the two integrals of the right member, it is clear that the first one has as a limit a $1/r$ singularity, while the second one tends to a $1/\sqrt{r}$ singularity. This is clearly due to the second order term in $\mathbf{e}_y(\mathbf{u}^{pm(1)})$ appearing in $\psi^{pm(0)}$.

Then, the second integral of the (3.87) vanishes in the limit at the crack tip and it can be neglected with respect to the first one for small thickness of the cavity close to the line crack. In what follows, only the first term will be considered:

$$\int_{\Gamma_{fr}} \left(-\psi^{pm(0)} + p^{pm(0)} f^{poro(0)} \right) \mathbf{m} \cdot \mathbf{n} \, d\lambda = - \int_{\Gamma_{fr}} \psi^{pm(0)} \mathbf{m} \cdot \mathbf{n} \, d\lambda + \dots \quad (3.88)$$

Then, the energy rate balance (3.86) becomes

$$Y_d(d) = \int_{\Gamma_{fr}} -\frac{1}{2} \psi^{pm(0)} \mathbf{m} \cdot \mathbf{n} \, d\lambda \quad (3.89)$$

3.4.2.5 Asymptotic expansion of the fracture energy release rate

The fracture energy release rate $\mathcal{G}_\alpha^{(\varepsilon)}$, previously defined in (3.47), can be asymptotically developed in the powers of ε by using the asymptotic expansion (3.52) of the strain energy ψ^{pm} , by taking into account that the cavity fronts ∂c_α^{fr} depends on ε and the following relations between the correspondent quantities in the periodic cell and in the resized one (fig. 3.6):

$$l_\alpha = \varepsilon d, \quad d\Lambda = \varepsilon d\lambda \quad (3.90)$$

Then, the change of variables $\mathbf{x} \leftrightarrow \mathbf{y} = \mathbf{x}/\varepsilon$ between the space variables provides the aimed asymptotic development which starts with a term of order one in the powers of ε and reads:

$$\mathcal{G}_\alpha^{(\varepsilon)} = \varepsilon \mathcal{G}_\alpha^{(1)} + \varepsilon^2 \mathcal{G}_\alpha^{(2)} + \dots \quad (3.91)$$

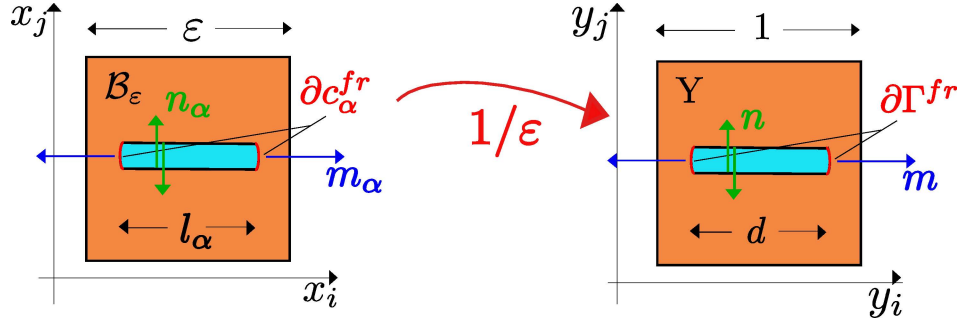


Figure 3.6: Nomenclature in the α th periodic cell and in the corresponding unit cell.

with

$$\mathcal{G}_\alpha^{(1)} := \int_{\partial\Gamma_\alpha^{fr}} -\frac{1}{2}\psi^{pm(0)} \mathbf{m} \cdot \mathbf{n} \, d\lambda \quad (3.92)$$

It is worth remarking that the unit vectors \mathbf{m} and \mathbf{n} are not affected by the change of variables (fig. 3.6).

Then, the energy rate balance (3.89) for a propagating cavity gets the following final form:

$$Y_d(d) = \mathcal{G}_\alpha^{(1)} \quad (3.93)$$

with the damage energy release rate $Y_d(d)$ already defined in the (3.85).

Remark 3.4.1. *We note that, for the case without fluid, when the last two terms of the damage energy release rate Y_d are missing, the obtained energy rate balance reduces to the one proposed by Dascalu, Bilbie and Agiasofitou (2008) and Dascalu (2009).*

Remark 3.4.2. *The energy rate balance (3.93) here proposed has the same form of the one proposed by Dormieux, Kondo and Ulm (2006a) for the case of a non porous solid with fluid-filled cracks. It is important to note that in our approach the energy rate balance is completely obtained by homogenization, that is, by upscaling the energy analysis performed at the mesoscopic scale; while in their work it is proposed by thermodynamic arguments directly applied to the macroscopic scale.*

3.4.3 Modeling of cavity propagation

In the section 3.3.5, with reference to a real mesoscopic structure fully described by a periodic cell of finite size ε , it is presented the modeling of the propagation of a cavity of length l_α . Now, it is considered a (virtual) limit process for ε going to zero and it is

rewritten by means of the relation (3.90), $l_\alpha = \varepsilon d(\mathbf{x})$, and of the asymptotic development (3.91) of $\mathcal{G}_\alpha^{(\varepsilon)}$ cut at the first term:

$$\mathcal{G}_\alpha^{(\varepsilon)} = \varepsilon \mathcal{G}_\alpha^{(1)} + \dots \quad (3.94)$$

Then, it is necessary and logic to consider that, in the same mesoscopic structure, the critical fracture energy rate \mathcal{G}_f depends on ε also and it can be approximated by the following asymptotic development:

$$\mathcal{G}_f = \varepsilon \mathcal{G}_f^{(1)} + \dots \quad (3.95)$$

and it is consistent with the assumptions made in (Dascalu 2009). Then, by substituting the (3.95) in the (3.48), the cavity propagation is completely described by the following laws:

$$\mathcal{G}_\alpha^{(1)} - \mathcal{G}_f^{(1)} \leq 0 \quad (3.96a)$$

$$\dot{d} \geq 0 \quad (3.96b)$$

$$\dot{d}(\mathcal{G}_\alpha^{(1)} - \mathcal{G}_f^{(1)}) = 0 \quad (3.96c)$$

As already remarked for the (3.48) in the section 3.3.5, the (3.96a) says that the fracture energy release rate cannot become bigger than the critical fracture energy rate; the (3.96b) asserts the damage irreversibility; while the (3.96c) expresses an energy rate balance when the cavity is propagating ($\dot{d} \neq 0$): the energy that the body is ready to spend per unit cavity length advance is equal with the critical energy necessary to break the bonds in the specific material. As expected, the relations (3.96) have the form of the Kuhn-Tucker conditions.

3.5 Damage laws

The combination of the energy rate balance (3.93) and of the description of the cavity propagation (3.96) provides the following damage laws:

$$Y_d(d) - \frac{\mathcal{G}_f}{\varepsilon} \leq 0 \quad (3.97a)$$

$$\dot{d} \geq 0 \quad (3.97b)$$

$$\dot{d}\left(Y_d(d) - \frac{\mathcal{G}_f}{\varepsilon}\right) = 0 \quad (3.97c)$$

The (3.97a) says that damage energy release rate $Y_d(d)$ cannot become bigger than the critical fracture energy rate $\mathcal{G}_f^{(1)}$; the (3.97b) asserts the damage irreversibility; while the (3.97c) expresses the damage evolution law: when the cavity is evolving, ($\dot{d} \neq 0$), the damage energy release rate $Y_d(d)$ is equal with the critical energy $\mathcal{G}_f^{(1)}$ necessary to break the bonds in the specific material. As expected, the relations (3.97) have the form of the Kuhn-Tucker conditions.

Lastly, it is worth remarking that, given the use of the asymptotic development (3.95), these damage laws have the mesostructural length ε as a variable, such that, they are also able to reproduce the well known size effect of fracture at the mesoscopic scale. This is the main difference with respect to the damage models obtained by a phenomenological approach which do not have this property.

3.6 Conclusions

In this chapter, we deduced an evolution law for damage for evolving fluid-filled cavities in a porous material.

The damage law was completely obtained from the mesoscopic equations by using homogenization based on asymptotic developments and energy analysis.

These developments extend the previous results concerning the case of evolving micro-cracks without fluid and lead to a form of the damage law similar to other models of fluid coupling damage obtained by phenomenological arguments.

Numerical investigations of the predictions of the damage law and, specifically, the fluid pressure influence on damage evolution will be given in the next chapter.

Chapter 4

Numerical study of macroscopic local behaviour

In the previous chapters a poroelastic damage model has been developed by means of homogenization and energy analysis. In this chapter the objective is to investigate the influence of the macroscopic fluid pressure and of the macroscopic deformation on damage evolution. Then, some representative predictions of this model obtained by means of numerical integration are presented.

Hereafter, in order to simplify the notation, the macroscopic deformation tensor $\mathbf{e}_x(\mathbf{u}^{(0)})$ and the macroscopic pressure $p^{pm(0)}$ are denoted by \mathbf{E}_x and P respectively.

4.1 Employed poroelastic damage model

The model is fully described by the following set of equations, composed by the macroscopic balances of linear momentum (4.1a) and fluid mass (4.1b), the damage evolution law (4.1c) and the damage irreversibility condition (4.1d):

$$\mathbf{0} = \operatorname{div}_x \boldsymbol{\Sigma} \quad (4.1a)$$

$$0 = \operatorname{div}_x \mathbf{Q} + \dot{\Phi}_u \quad (4.1b)$$

$$0 = \dot{d} \left[Y_d - \frac{\mathcal{G}_f}{\varepsilon} \right] \quad (4.1c)$$

$$\dot{d} \geq 0 \quad (4.1d)$$

the macroscopic Biot's constitutive relations:

$$\boldsymbol{\Sigma} = \mathbf{C} @ \mathbf{E}_x - \mathbf{B} P \quad (4.2a)$$

$$\Phi_u = \mathbf{B} : \mathbf{E}_x + S P \quad (4.2b)$$

the damage energy release rate Y_d is already defined in (3.85) and rewritten as follows:

$$-Y_d = \frac{1}{2} \frac{d\mathbf{C}}{dd} @ \mathbf{E}_x : \mathbf{E}_x - \frac{d\mathbf{B}}{dd} P : \mathbf{E}_x - \frac{1}{2} \frac{dS}{dd} P^2 \quad (4.3)$$

4.2 Homogenized parameters and their derivatives

The dependence of the homogenized coefficients \mathbf{C}, \mathbf{B} and S on the damage variable d was presented in the chapter 2.5 (figures 2.9, 2.10, 2.11). Now, given the expression (4.3) for the damage energy release rate Y_d and with the aim of solving the damage equation (4.1c), it is clear that the derivatives of the homogenized coefficients with respect to the damage variable must be calculated.

In particular, the numerical values of both the homogenized coefficients and of their derivatives are required $\forall d \in [d^0, 1]$. On the contrary, as described in the section 2.5, the homogenized coefficients have been computed for about thirty values of d . Hence, the numerical continuous functions $\mathbf{C}(d), \mathbf{B}(d)$ and $S(d)$ are obtained by interpolation of these sampling values.

4.3 Incremental resolution algorithm

An integration algorithm for the investigation of the local hydro-mechanical behaviour and of the damage evolution predicted by the set of the governing equations (4.1, 4.2, 4.3) is described in the following. In conditions of increasing damage, that is, $\dot{d} > 0$, the term in parenthesis appearing in the damage evolution law (4.1c) vanishes. So, for given macroscopic fluid pressure P and deformation \mathbf{E}_x , the resolution of the damage equation consists in the resolution of an algebraic equation in the variable d .¹

Then, it is possible to formulate an algorithm where the macroscopic balances (4.1a, 4.1b) and the damage evolution law (4.1c) are not solved simultaneously.

In the considered incremental approach, the solution d^{n+1} satisfying (4.1c) for $\dot{d} > 0$ is determined by means of a bisection root-finding method where the irreversibility condition (4.1d) is imposed by searching a solution d^{n+1} larger than the solution d^n at the previous step. If such a solution is not found, then the damage is not evolving ($\dot{d} = 0$).

Hence, the algorithm reads:

1. Data initialization:

- $n = 0$;
- $d = d^0 = 0.05$;
- Evaluation for $d = d_0$ of the homogenized coefficients:

$$\mathbf{C}^0 := \mathbf{C}(d^0), \quad \mathbf{B}^0, \quad S^0; \quad (4.4)$$

and of their derivatives:

$$\left(\frac{d\mathbf{C}}{dd} \right)^0, \quad \left(\frac{d\mathbf{B}}{dd} \right)^0, \quad \left(\frac{dS}{dd} \right)^0 \quad (4.5)$$

¹It is worth remarking that in the case of a time dependent constitutive function $\mathcal{G}_f = \mathcal{G}_f(\dot{l}_\alpha)$, the damage equation is not algebraic anymore, but differential as shown by Dascalu (2009) in the context of homogenization for damage.

2. Computation of $d^{n+1} \in [d^n, 1]$ by solving the damage equation (4.1c) by means of the bisection method.
3. Evaluation for $d = d^{n+1}$ of the homogenized coefficients:

$$\mathbf{C}^{n+1}, \quad \mathbf{B}^{n+1}, \quad S^{n+1}; \quad (4.6)$$

and of their derivatives:

$$\left(\frac{d\mathbf{C}}{dd} \right)^{n+1}, \quad \left(\frac{d\mathbf{B}}{dd} \right)^{n+1}, \quad \left(\frac{dS}{dd} \right)^{n+1}. \quad (4.7)$$

4. Computation for $d = d^{n+1}$ of the stress:

$$\boldsymbol{\Sigma}^{n+1} = \mathbf{C}^{n+1} @ \mathbf{E}_x^{n+1} - \mathbf{B}^{n+1} P^{n+1} \quad (4.8)$$

and of the induced variation of the porosity:

$$\Phi_u^{n+1} = \mathbf{B}^{n+1} : \mathbf{E}_x^{n+1} + S^{n+1} P^{n+1} \quad (4.9)$$

5. If $n < n_{max}$, then $n = n + 1$ and go back to item 3. Otherwise go to item 7.
6. End.

4.4 Numerical examples

In order to investigate the influence of the macroscopic fluid pressure P and of the macroscopic deformation \mathbf{E}_x on the damage evolution, two different tests are performed, assuming a fully drained response for both of them.

Both quasi-brittle and brittle damage are considered with a Griffith-type energy criterion, that is, the propagation occurs when the physical energy release rate $\mathcal{G}^{(1)}$ (3.92) reaches the critical energy threshold $\mathcal{G}_f^{(1)}$:

$$\mathcal{G}^{(1)} = \mathcal{G}_f^{(1)} \quad (4.10)$$

For the case of quasi-brittle damage, the equivalent fracture criterion proposed by Bazant and Planas (1997) is adopted. It was already introduced in (3.51) for the physical space and $\mathcal{G}_f^{(1)}$ is rewritten as follows for the resized unit cell Y :

$$\mathcal{G}_f^{(1)}(d) = \frac{\mathcal{G}_c (d - d_0) \varepsilon}{c_f} \quad (4.11)$$

where d_0 is the initial cavity length, c_f is the material length governing the fracture process zone size, ε is the size of the mesoscopic periodic cell and \mathcal{G}_c is a material constant. In such a case, the critical energy fracture $\mathcal{G}_f^{(1)}$ is a constitutive function, that is, it evolves

with damage and, in reason of that, the damage evolution is expected to be smooth. For the case of brittle damage, it is assumed that \mathcal{G}_f is a material constant:

$$\mathcal{G}_f^{(1)} = \mathcal{G}_c \quad (4.12)$$

and the damage evolution is expected to happen abruptly, evolving directly from the initial value $d_0 = 0.05$ to the final one $d = 1$.

With the exception of the plots corresponding to the variation of the parameter, the reported in the figures from 4.2 to 4.4 are obtained from calculations performed by setting $c_f = 8 \cdot 10^{-4}$ and $\mathcal{G}_c = 50 \text{ J/m}^2$.

In both the tests described below, the expectations concerning the smooth damage evolution for the the quasi-brittle case and the abrupt one for the brittle case are matched.

The first test (“test 1” in the captions of the figures) consists in imposing a strain tensor which has only the component E_{x22} not vanishing and an increasing fluid pressure P . This is repeated for different values of imposed constant strain E_{x22} (fig. 4.1).

In the quasi-brittle case (fig. 4.2), E_{x22} ranges in $0.0 \div 7.0 \cdot 10^{-3}$. It is apparent that, for increasing strain E_{x22} , the cavity propagation is faster, in the sense that, the unit cell is completely damaged $d = 1$ for lower values of the imposed pressure P . At the same time, a threshold for the strain is detected: already for zero pressure $P = 0$, that is, at the first loading step, the cavity length jumps from the initial value $d_0 = 0.05$ to a larger one if $E_{x22} \geq 0.6 \cdot 10^{-3}$.

The test is repeated for the case of brittle damage (fig. 4.3) and above all it worths noting that E_{x22} ranges in $0.0 \div 3.0 \cdot 10^{-4}$, that is, one order of magnitude lower with respect to the quasi-brittle case (fig. 4.2). Notwithstanding that, it is observed that tendency is similar: for increasing imposed strain, the cavity propagation is triggered at decreasing values of pore pressure.

Moreover, in the figure 4.4, for the brittle case it is observed that, for an increasing material constant G_c , the cavity propagation is slower and it was expected because G_c is a strength of the material.

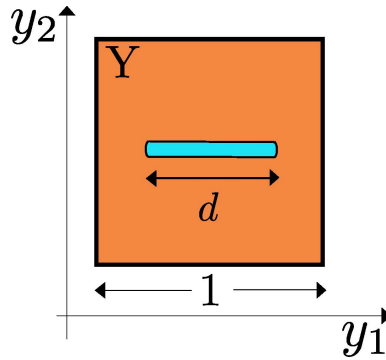


Figure 4.1: Orientation of the axes 1 and 2 in the periodic unit cell Y .

In the second test (“test 2” in the captions of the figures), an increasing E_{x22} is imposed with all the other components of the macroscopic strain tensor vanishing and for different values of imposed constant fluid pressure P .

In the quasi-brittle case (fig. 4.5), P ranges in $0.0 \div 7.5$ MPa and it is apparent that for increasing pressure P , the cavity propagation is faster. The numerical investigation also provides a threshold of $P \approx 533 \text{ kPa}$: that is, if the fluid pressure is higher than this value, then the cavities propagate $d \geq d_0 = 0.05$ even for zero strain $E_{x22} = 0$.

As expected, by performing a cross check for the two threshold, each one detected in one of the two test, a perfect correspondence is found: that is, the threshold for the strain coming from the first test is exactly confirmed from the results of the second test, and viceversa. Moreover, in the same simulation, the variation of the Lagrangian porosity is computed (4.9) and it is clear that Φ_u increases with damage.

The test is repeated for the case of brittle damage (fig. 4.6) and above all it worths noting that E_{x22} ranges in $0.0 \div 0.5$ MPa, that is, one order of magnitude lower with respect to the quasi-brittle case (fig. 4.5). Notwithstanding that, it is observed that tendency is similar: for increasing imposed pressure, the cavity propagation is triggered at decreasing values of strain.

Moreover, for the quasi-brittle case, a parametric analysis is performed to investigate the influence of the parameters characterising the constitutive function $G_f^{(1)}(d)$ (4.11): the material constant G_c and the material length governing the fracture process zone size c_f . In figure 4.7, it is shown that, for increasing G_c in the range $10 \div 400 \text{ J/m}^2$, the cavity propagation is slower, as expected. In the figure 4.8, for an increasing fracture process zone around the tip such that c_f ranges in $0.2 \div 1.0 \cdot 10^{-3} \text{ m}$, it is observed that the cavity propagation is faster.

During the calculations it is observed that a smaller time step amplitude Δt allows to find roots which are closer to $d = 1$ but this is extremely expensive in terms of the computation time. That’s the reason why Δt is set to be varying along the loading path from $\Delta t = 0.1$ in the beginning to $\Delta t = 0.001$ in the end.

In summary, the obtained results show that damage significantly increases for imposed increasing values of macroscopic fluid pressure. This response is qualitatively consistent with experimental results of drained tests (e.g. see references cited by Bart, Shao and Lydzba (2000)) However, we plan to perform further investigations for a fully satisfying model calibration, considering the BVPs of more realistic test setting and the effects of hydromechanical coupling.

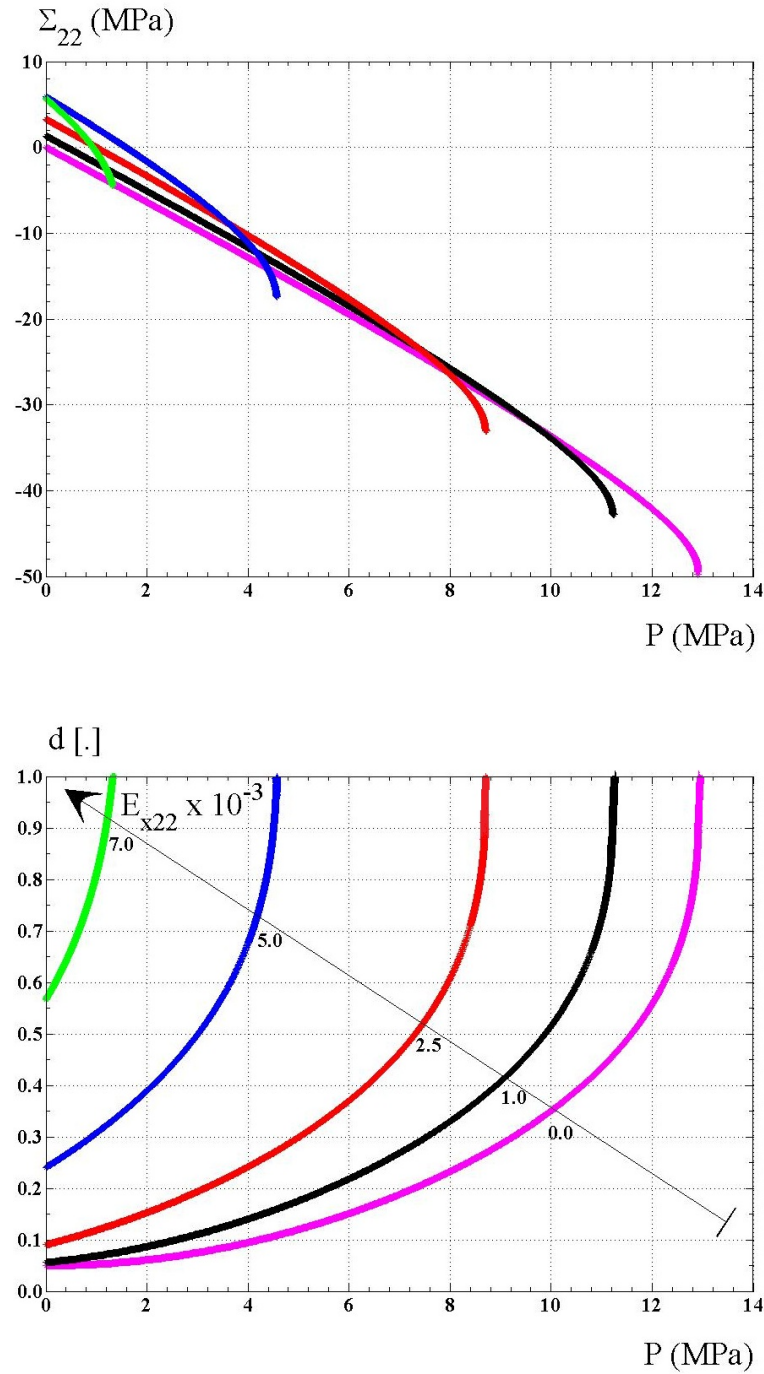


Figure 4.2: Quasi-brittle damage (Test 1): stress Σ_{22} (top) and damage variable d (bottom) versus the imposed macroscopic pressure P and for different values of imposed constant strain: $E_{x22} = 0.0000$ (magenta), $E_{x22} = 0.0010$ (black), $E_{x22} = 0.0025$ (red), $E_{x22} = 0.0050$ (blue) and $E_{x22} = 0.0075$ (green).

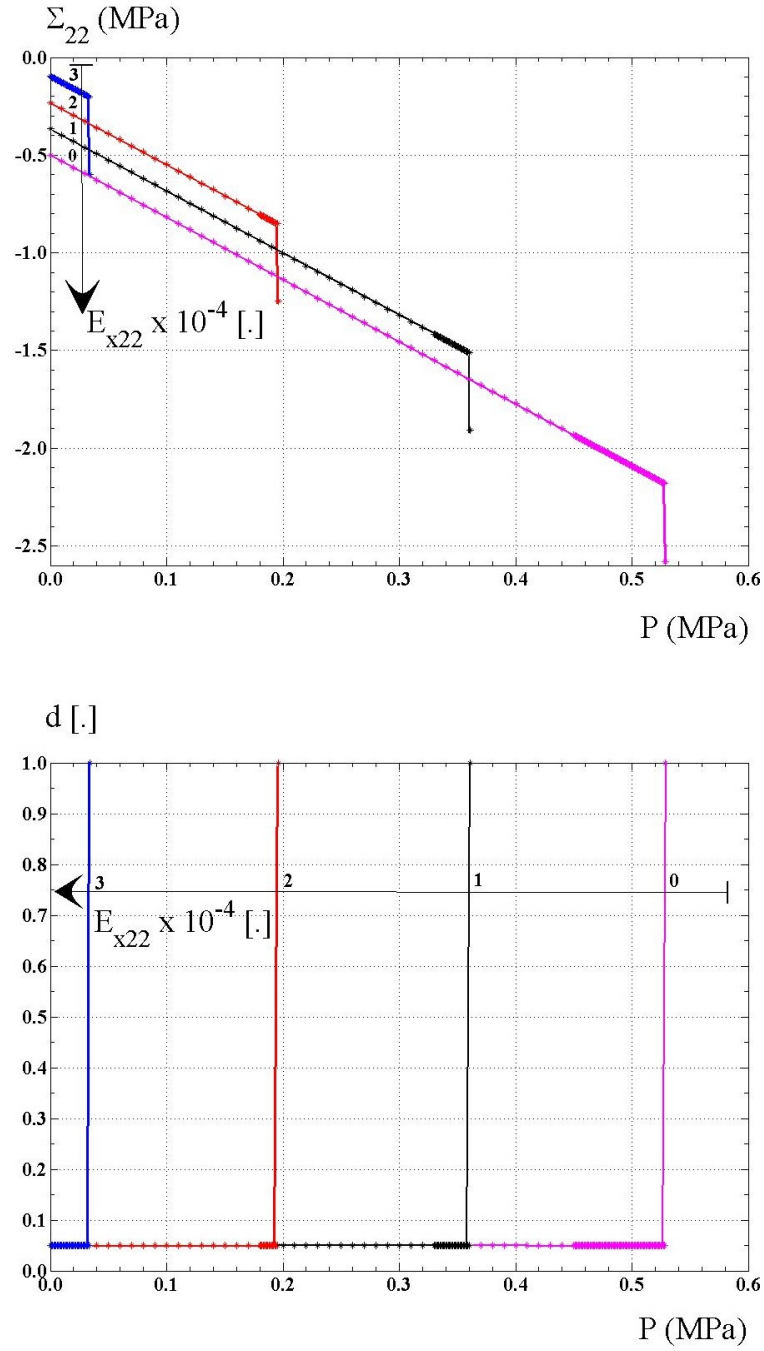


Figure 4.3: Brittle damage (Test 1): stress Σ_{22} (top) and damage variable d (bottom) as functions of imposed macroscopic pressure P and for different values of imposed constant strain: $E_{x22} = 0.0000$ (magenta), $E_{x22} = 0.0001$ (black), $E_{x22} = 0.0002$ (red), $E_{x22} = 0.0003$ (blue).

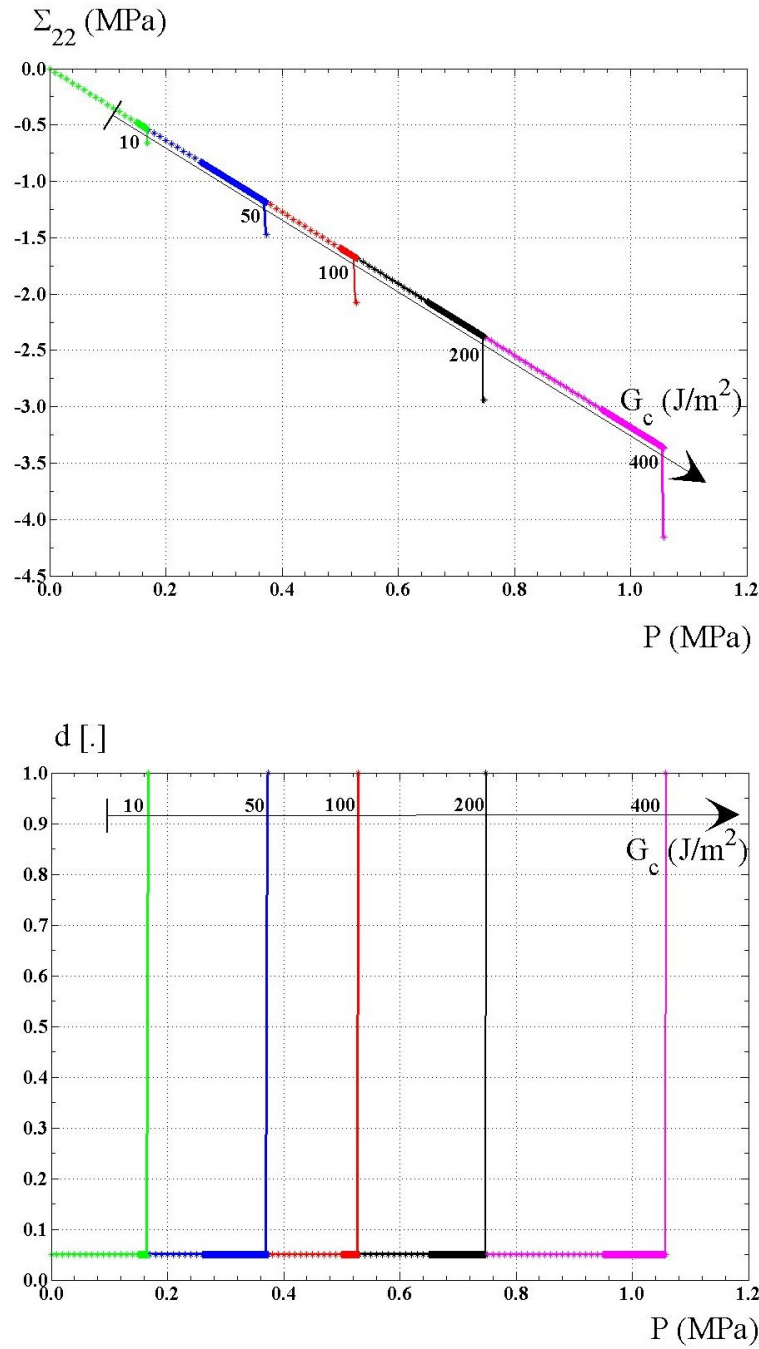


Figure 4.4: Brittle damage (Test 1): stress Σ_{22} (top) and damage variable d (bottom) as functions of imposed macroscopic pressure P and for different values of constant fracture energy: $G_c = 400 \text{ J/m}^2$ (magenta), $G_c = 200 \text{ J/m}^2$ (black), $G_c = 100 \text{ J/m}^2$ (red), $G_c = 50 \text{ J/m}^2$ (blue) and $G_c = 10 \text{ J/m}^2$ (green).

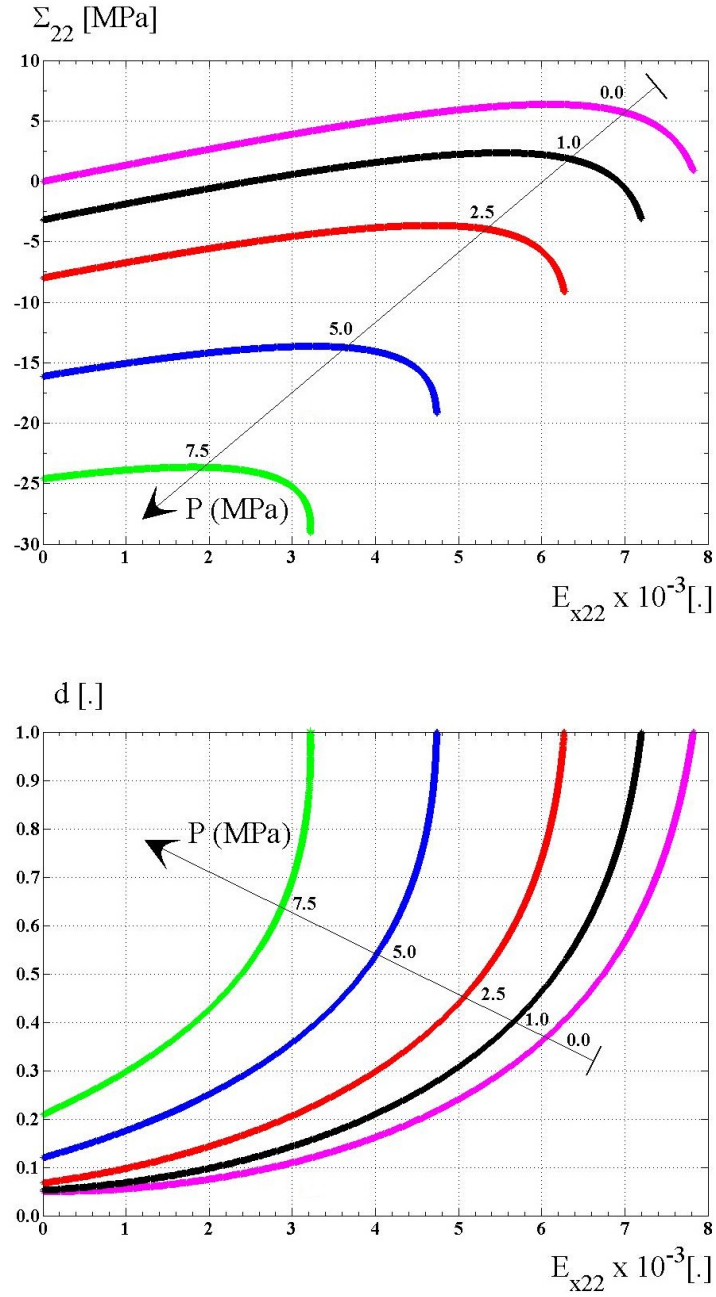


Figure 4.5: Quasi-brittle damage (Test 2): stress Σ_{22} (top) and damage variable d (bottom) as functions of imposed macroscopic strain E_{x22} and for different values of constant pressure: $P = 0.0$ MPa (magenta), $P = 1$ MPa (black), $P = 2.5$ MPa (red), $P = 5$ MPa (blue) and $P = 7.5$ MPa (green).

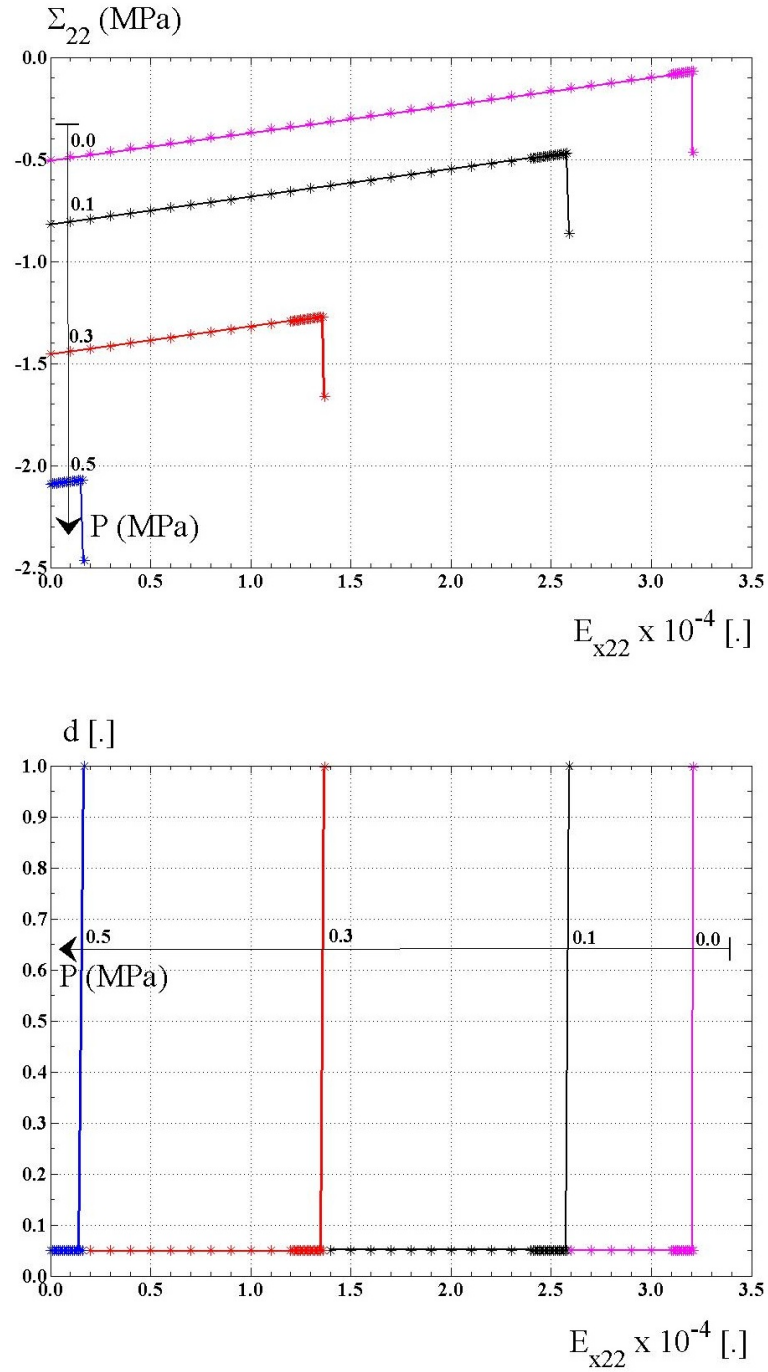


Figure 4.6: Brittle damage (Test 2): stress Σ_{22} (top) and damage variable d (bottom) as functions of imposed macroscopic strain E_{x22} and for different values of constant pressure: $P = 0.0$ MPa (magenta), $P = 0.1$ MPa (black), $P = 0.3$ MPa (red) and $P = 0.5$ MPa (blue).

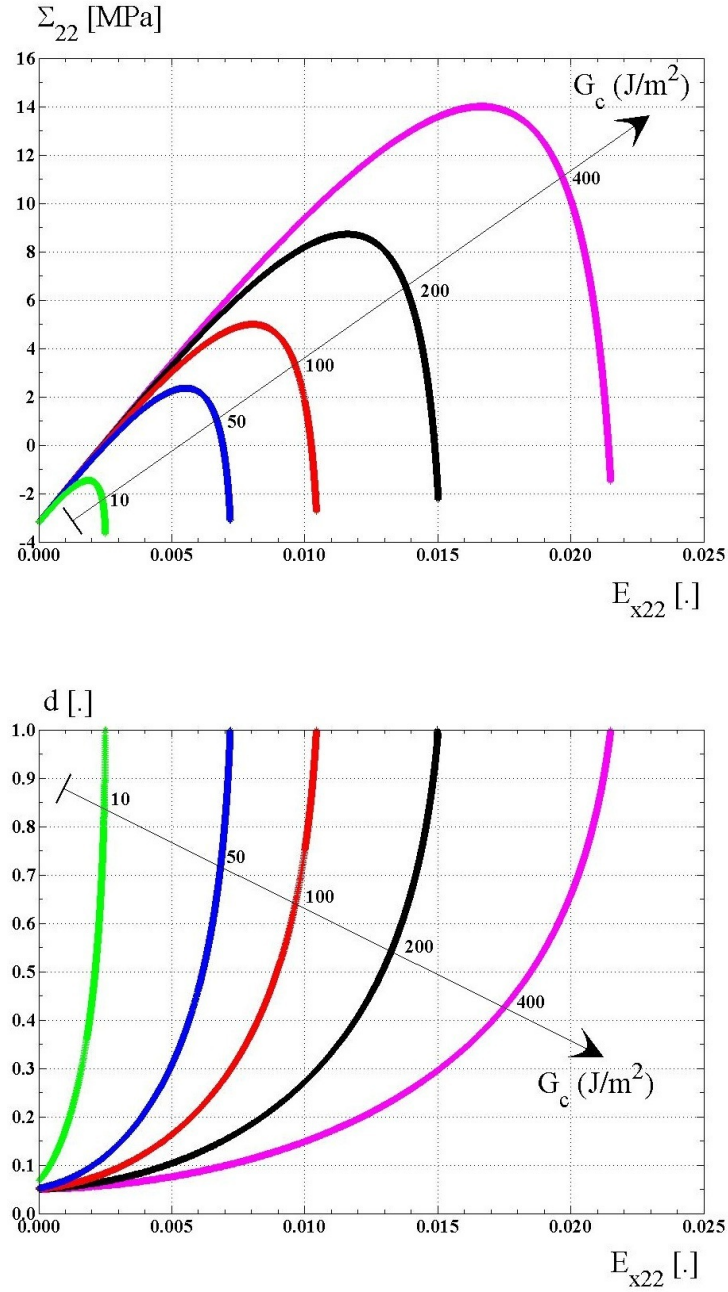


Figure 4.7: Quasi-brittle damage (Test 2): stress Σ_{22} (top) and damage variable d (bottom) as functions of imposed macroscopic strain E_{x22} and for different values of constant fracture energy: $G_c = 400 J/m^2$ (magenta), $G_c = 200 J/m^2$ (black), $G_c = 100 J/m^2$ (red), $G_c = 50 J/m^2$ (blue) and $G_c = 10 J/m^2$ (green).

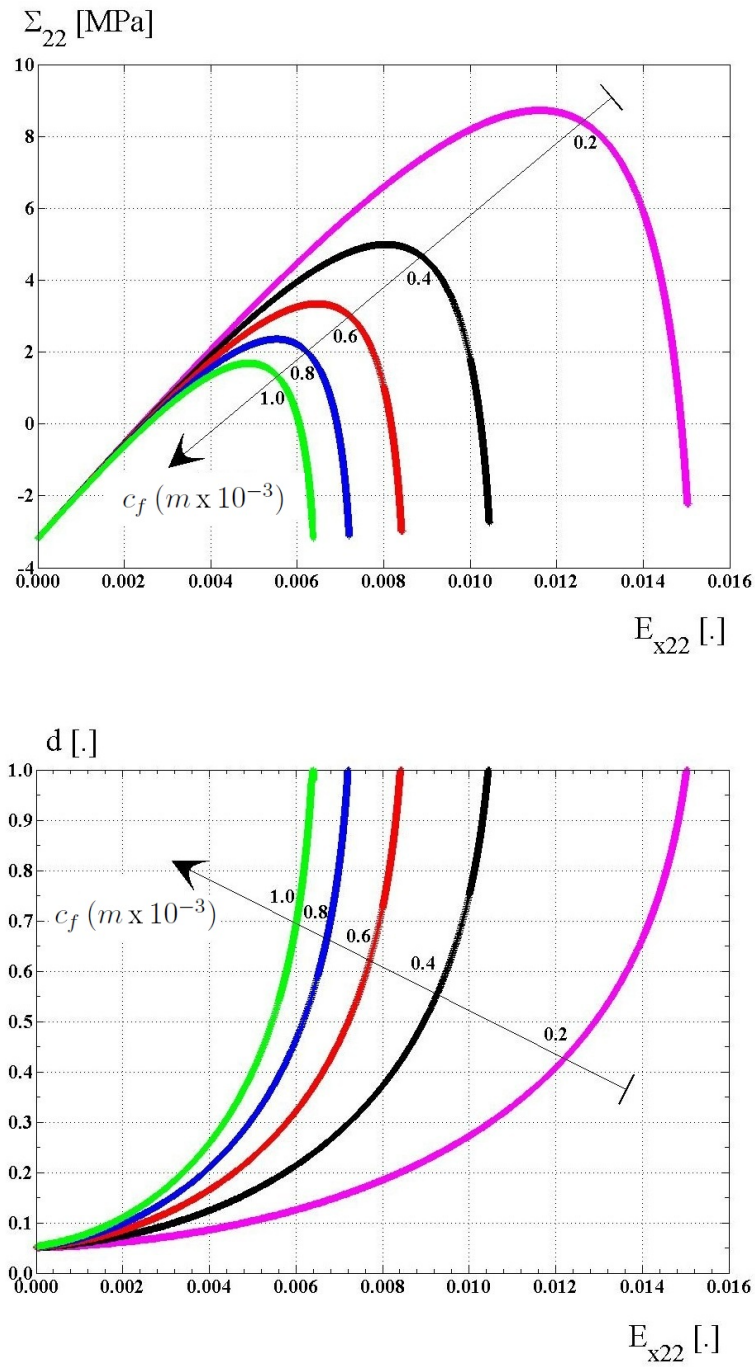


Figure 4.8: Quasi-brittle damage (Test 2): stress Σ_{22} (top) and damage variable d (bottom) as functions of imposed macroscopic strain E_{x22} and for different values of the size of fracture process zone: $c_f = 1.0 \cdot 10^{-3}m$ (green), $c_f = 0.8 \cdot 10^{-3}m$ (blue), $c_f = 0.6 \cdot 10^{-3}m$ (red), $c_f = 0.4 \cdot 10^{-3}m$ (black), $c_f = 0.2 \cdot 10^{-3}m$ (magenta)

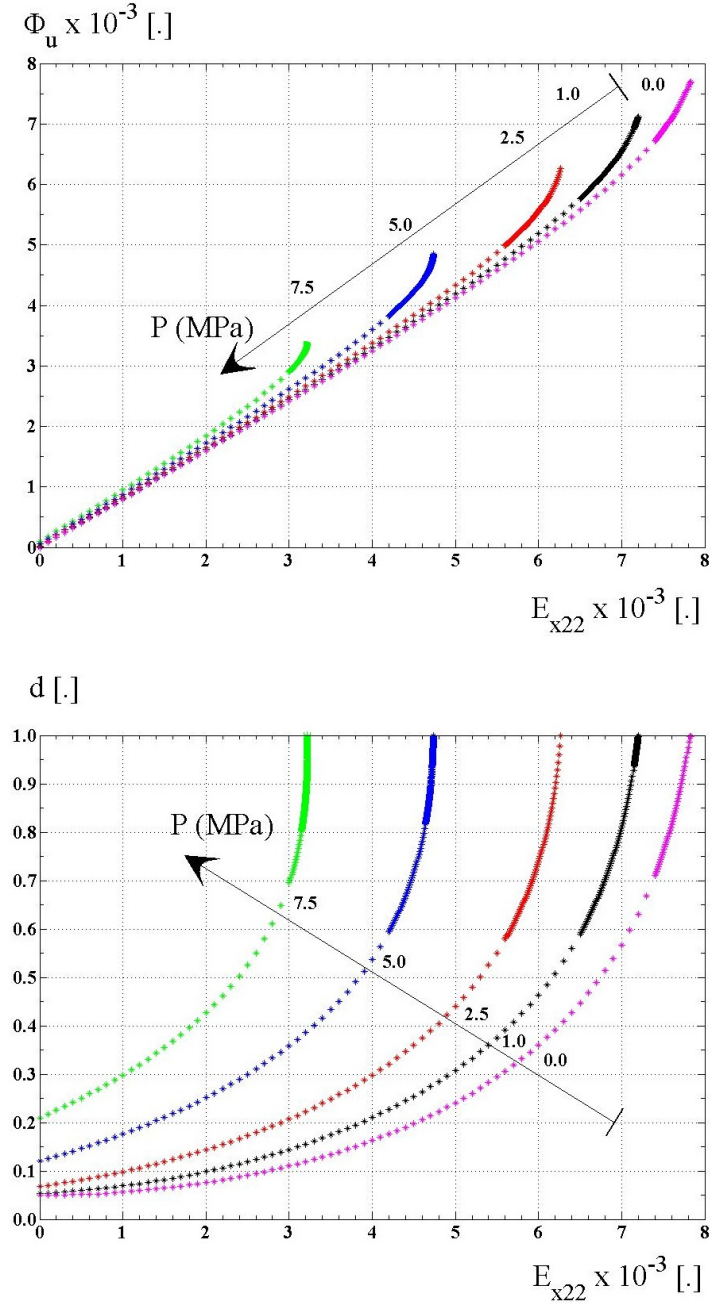


Figure 4.9: Quasi-brittle damage (Test 2): porosity variation Φ_u (top) and damage variable d (bottom) as functions of imposed macroscopic strain E_{x22} and for different values of constant pressure: $P = 0.0$ MPa (magenta), $P = 1$ MPa (black), $P = 2.5$ MPa (red), $P = 5$ MPa (blue) and $P = 7.5$ MPa (green).

Chapter 5

Conclusions and perspectives

5.1 General conclusions

In this dissertation the constitutive modeling of damage evolution in a geomaterial consisting of a deformable and saturated porous solid with a (quasi-)periodic distribution of fluid-filled cavities (cracks) has been presented.

The objective of this thesis was the development of a macroscopic damage evolution law based only on an explicit description of the mesoscopic scale level which could be successfully employed to describe damage behavior and to assess long-term safety of underground storage facilities and of civil engineering works. With this aim, a homogenization-based approach was used in both the two main parts composing this work.

The first part was concentrated on the upscaling of the finely heterogeneous mesoscopic structure to an equivalent continuum. In order to get this goal, three steps were developed:

- A multiscale study of the porosity was developed, both in the framework of large and small deformations, with the aim of understanding how the porosity, at different scales of observation, is varying in reason of the motion of the surrounding porous solid. So, the first chapter presents different relations governing mesoscopic and macroscopic porosities in Eulerian and Lagrangian descriptions. They were developed by means of Taylor developments and, at an intermediate step, they are consistent with relations already available in the literature, e. g. in Callari and Abati (2011).
- A description of the mesoscopic body has been investigated by referring to the original poroelastic model deduced by means of a phenomenological approach by Biot (1941), and reobtained by (Auriault 2004; Auriault and Sanchez-Palencia 1977) using homogenization by asymptotic developments. Then, it has been proposed a set of governing equations for the mesoscopic structure which can be seen as a modified version of that one proposed by Auriault and Sanchez-Palencia: actually, the fluid mass balance for the porous solid is presented separated from the Biot's constitutive law for the fluid content; moreover a different definition of average fluid flow is chosen.

- Homogenization of a solid with periodic mesoscale structure characterized by a saturated porous matrix including fluid-filled cracks. Among the results of this step there was a realistic description of the effects of crack-length variation on macroscopic poroelastic parameters, that is, the numerical evaluation of homogenized elasticity tensor, Biot's coupling tensor and Biot modulus (i.e. mechanical and capacity properties). It was done for different mesoscopic cavity lengths, considered as the damage parameter; then, by means of polynomial interpolation, continuous functions of the damage have been obtained.

The second part of the work is dedicated to the construction of the poroelastic damage model. We considered a quasi-periodic family of fluid-filled cavities that may propagate under the action of the external loading. Then, the objective is to write a damage evolution law deduced from the meso-structural fracture phenomena. This was done in the following steps:

- An energy analysis for the poro-mechanical solid with a large number of cavity allowed us to determine the exact (before homogenization) expression of the hydro-mechanical energy release rate during mesoscopic fracture and to interpret the different terms contributing to the energy balance.
- A combination of asymptotic homogenization and energy analysis allowed us to deduce a macroscopic damage evolution law. This result extends previous developments concerning the case of a fractured non porous solid without fluid coupling (Dascalu, Bilbie and Agiasofitou 2008). A mesostructural length is present in the damage law and this allows for the prediction of size effects. We showed that, under some approximation, the obtained damage law is similar in form with the model based on phenomenological and thermodynamic arguments proposed by Dormieux, Kondo and Ulm (2006a) for a non porous solid with fluid-filled cracks.
- By means of numerical time-integration analysis of the local macroscopic hydro-mechanical damage behaviour, we have evaluated the proposed model predictions for particular paths of macroscopic strain and fluid pressure. The obtained results show that damage significantly increases for imposed increasing values of macroscopic fluid pressure. This response is qualitatively consistent with experimental results of drained tests (e.g. see references cited by Bart, Shao and Lydzba (2000)). Moreover, we deduce that the model is capable to predict also other physical behaviours like the presence of size effects related to failure of the solid.

5.2 Perspectives

A natural continuation of the present study are the numerical simulations, by finite elements, of macroscopic structures phenomena like localization of damage and strains and the influence of the fluid on such behaviours would be of much interest for the complete understanding of the model. So, we plan to perform further investigations for a complete

calibration of the model, considering the analysis of BVPs with hydromechanical coupling, such as laboratory tests and underground works.

To this aim, we will extend existing finite element formulations for porous media (e.g. Callari and Abati (2009)) to include the laws presented herein for the modeling of damage.

Possible extensions of the proposed mesoscale model to better describe the effects of damage on transport parameters (e.g. the macroscopic permeability) could be devised, for example by means of the following alternative approaches:

1. The consideration of a new periodic cell, with connected cracks saturated by viscous fluid.
2. The modeling of damage effects on transport only at the macroscale. In fact, the attainment of fully damaged conditions ($d=1$) often leads to the coalescence of cracks in macroscopic discontinuities (e.g. see Souley, Homand, Pepa and Hoxha (2001)), which could be treated by means of strong discontinuities, following Callari and Armero (2002); Callari, Armero and Abati (2010).

Lastly, a more realistic model, which could be a generalisation of the one presented in this dissertation, would be a 3D model obtained by homogenization starting from 3D mesostructural aspects. The differences of geometry of the mesostructure may essentially influence the effective 3D response as compared with the 2D one.

Appendix A

Porosity rate and volumetric strain

In this appendix, some relations from Callari and Abati (2011) are reported for a comparison with the relation (1.26) proposed herein.

A.1 Definitions

With reference to , the Jacobian J^α , with $\alpha = pm, s$, of the deformation function φ^α is defined as:

$$J^\alpha := \frac{V^\alpha}{V_r^\alpha} \quad (\text{A.1})$$

The volumetric strain E_v^α of the α -phase is defined as:

$$E_v^\alpha := \frac{\Delta V^\alpha}{V_r^\alpha} \quad (\text{A.2})$$

where the notation $\Delta(\cdot)$ indicates a finite increment, that is to say the difference between the values in the current and in the reference configuration of (\cdot) . Then, the corresponding strain rate is defined as:

$$\dot{E}_v^\alpha = \dot{J}^\alpha \quad (\text{A.3})$$

The logarithmic volumetric strain λ^α and its rate $\dot{\lambda}^\alpha$ are defined as:

$$\lambda^\alpha := \ln J^\alpha \quad \dot{\lambda}^\alpha := \frac{\dot{J}^\alpha}{J^\alpha} \quad (\text{A.4})$$

The symmetric part of the displacement gradient \mathbf{e}^α of the α -phase is defined as:

$$\mathbf{e}^\alpha := \nabla_X^{sym} \mathbf{u}^\alpha(\mathbf{X}, t) \quad (\text{A.5})$$

and its trace ε_v^α reads:

$$\varepsilon_v^\alpha := \mathbf{e}^\alpha : \mathbf{1} = \text{div}_X \mathbf{u}^\alpha \quad (\text{A.6})$$

The spatial strain rate tensor \mathbf{D}^α of the α -phase is defined as:

$$\mathbf{D}^\alpha := \nabla_x^{sym} \mathbf{v}^\alpha(\mathbf{x}, t) \quad (\text{A.7})$$

where $\mathbf{v}^\alpha(\mathbf{x}, t)$ is the Eulerian velocity field. And its trace d_v^α reads:

$$d_v^\alpha := \mathbf{D}^\alpha : \mathbf{1} = \text{div}_x \mathbf{v} = \frac{\dot{J}^\alpha}{J^\alpha} \quad (\text{A.8})$$

A.2 Useful relations

From the comparison between the relations (A.3) and (A.8), the following relation between the rates of the volumetric strain and of trace of the spatial strain is deduced:

$$\dot{E}_v^\alpha = J^\alpha d_v^\alpha \quad (\text{A.9})$$

By using the relations (A.4) and (A.8), the Eulerian microscopic porosity rate $\dot{\eta}$ reads:

$$\dot{\eta} := \frac{d}{dt} \left(\frac{V^{pm} - V^s}{V^{pm}} \right) = (1 - \eta)(d_v^{pm} - \dot{\lambda}^s) \quad (\text{A.10})$$

By using the definition (A.1) of the J^α and by means of a simple manipulation, the increment of the Eulerian microscopic porosity $\Delta\eta$ reads:

$$\Delta\eta = (1 - \eta_r) \left(1 - \frac{J^s}{J^{pm}} \right) \quad (\text{A.11})$$

where η_r is the value of the microscopic porosity in the reference configuration, as already written in the (1.23a).

A.3 Small transformations framework

In the framework of the small transformations, the symmetric part of the displacement gradient \mathbf{e}^α (A.5) acquires a physical meaning: it is the infinitesimal strain tensor. Then, the exact volumetric strain E_v^α can be approximated with the trace of \mathbf{e}^α :

$$E_v^\alpha = \varepsilon_v^\alpha + \dots \quad (\text{A.12})$$

Moreover, the Lagrangian and the Eulerian system are almost identical and it follows that:

$$\mathbf{v}^\alpha(\mathbf{x}, t) = \dot{\mathbf{u}}^\alpha(\mathbf{X}, t) + \dots \quad (\text{A.13})$$

and it yields a further approximation:

$$\dot{\varepsilon}_v^\alpha = d_v^\alpha + \dots \quad (\text{A.14})$$

Also the exact logarithmic volumetric strain rate of the solid phase $\dot{\lambda}^\alpha$ (A.4b), and the Jacobian of the deformation J^α (A.1) can be approximated by means of the Taylor's development (C.6) as follows:

$$\dot{\lambda}^s = \frac{\dot{\varepsilon}_v^s + \dots}{1 + \varepsilon_v^{pm} + \dots} = (\dot{\varepsilon}_v^s + \dots)(1 - \varepsilon_v^{pm} + \dots) = \dot{\varepsilon}_v^s + \dots \quad (\text{A.15})$$

and

$$J^\alpha = 1 + \text{div } \mathbf{u}^\alpha + \dots = 1 + \varepsilon_v^\alpha + \dots \quad (\text{A.16})$$

In the same way, the microscopic porosity increment $\Delta\eta$ is rewritten as:

$$\begin{aligned} \Delta\eta &= (1 - \eta_r) \left(1 - \frac{1 + \varepsilon_v^s + \dots}{1 + \varepsilon_v^{pm} + \dots} \right) = (1 - \eta_r) [1 - (1 + \varepsilon_v^s + \dots)(1 - \varepsilon_v^{pm} + \dots)] \\ &= (1 - \eta_r)(\varepsilon_v^{pm} - \varepsilon_v^s) + \dots \end{aligned} \quad (\text{A.17})$$

Lastly, in order to evaluate the microscopic porosity rate, the relation (A.17) is useful to show the presence of second-order terms in the product between the current microscopic porosity and an infinitesimal strain measure:

$$\eta \dot{\varepsilon}_v^\alpha = \eta_r \dot{\varepsilon}_v^\alpha + (1 - \eta_r)(\varepsilon_v^{pm} - \varepsilon_v^s) \dot{\varepsilon}_v^\alpha = \eta_r \dot{\varepsilon}_v^\alpha + \dots \quad (\text{A.18})$$

so, the (A.10) becomes:

$$\dot{\eta} = (1 - \eta_r)(\dot{\varepsilon}_v^{pm} - \dot{\varepsilon}_v^s) \quad (\text{A.19})$$

Appendix B

From microscale to mesoscale

In this appendix, it is proposed a recall of the work presented in (Auriault 2004; Auriault and Sanchez-Palencia 1977) which are the main references of this thesis project for what concerns the homogenization of porous media by asymptotic homogenization.

A porous saturated solid is upscaled and the obtained “mesoscopic” description is equivalent to the model proposed by Biot (1941) which was deduced by means of a phenomenological approach. Notwithstanding that, in their formulation, the fluid mass balance equation and the Biot’s constitutive law for the fluid mass content are merged in a single equation, while for this thesis it was decided to split in (2.20, 2.33) in order to start from the classical form of the Biot’s model. Moreover, the (2.33) is written in term of Lagrangian porosity which is equivalent to the fluid mass content used in the original version of the consolidation equations proposed in (Biot 1941). Lastly, also the average value of the pore fluid velocity used in the thesis (3.11) is different from the one presented below (3.13).

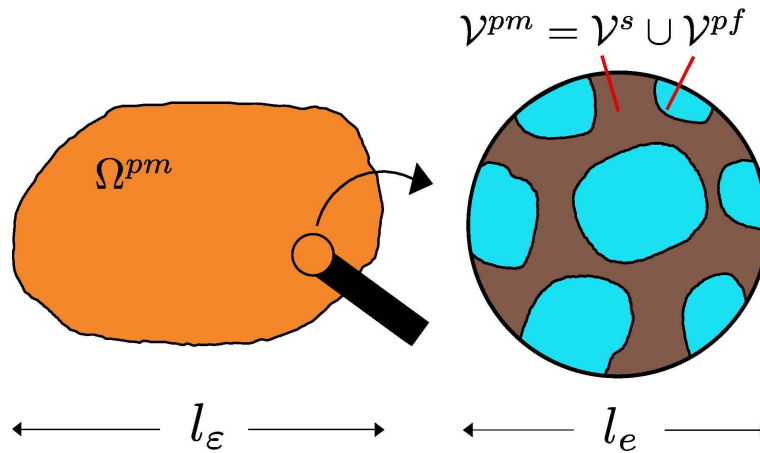


Figure B.1: Mesoscopic and microscopic scales of observation. Condition of scale separation satisfied: $l_\epsilon \gg l_e$. Random distributions of saturated microscopic pores.

B.0.1 Microscopic description

The porous saturated solid Ω is the union of two disjoint subdomains: the solid subdomain Ω^s and the set of fluid-saturated pores Ω^{pf} , that is, $\Omega = \Omega^s \cup \Omega^{pf}$ and $\emptyset = \Omega^s \cap \Omega^{pf}$. And $\partial\Omega^{s-pf}$ denotes the set of interfaces between the pores and the surrounding solid phase. The governing equations which describes the microscopic hydro-mechanical problem read:

$$\mathbf{0} = \text{div}_x \boldsymbol{\sigma} \quad \text{linear momentum balance in } \Omega^{pm} \quad (\text{B.1a})$$

$$0 = \text{div}_x \mathbf{v}^{pf} \quad \text{fluid incompressibility in } \Omega^{pf} \quad (\text{B.1b})$$

$$\boldsymbol{\sigma}^s = \mathbf{a} @ \mathbf{e}_x(\mathbf{u}^s) \quad \text{solid elastic matrix in } \Omega^s \quad (\text{B.1c})$$

$$\boldsymbol{\sigma}^{pf} = 2\mu \mathbf{D}_x - p^{pf} \mathbf{I} \quad \text{viscous Newtonian fluid in } \Omega^{pf} \quad (\text{B.1d})$$

$$\boldsymbol{\sigma}^s @ \mathbf{n} = \boldsymbol{\sigma}^{pf} @ \mathbf{n} \quad \text{stress continuity on } \partial\Omega^{s-pf} \quad (\text{B.1e})$$

$$\mathbf{v}^{pf} = \dot{\mathbf{u}}^s \quad \text{no-slip condition on } \partial\Omega^{s-pf} \quad (\text{B.1f})$$

where \mathbf{a} is the elastic tensor, \mathbf{n} is the normal vector to the solid-fluid interface $\partial\Omega^{s-pf}$ outward oriented with respect to the solid phase, and \mathbf{D}_x is the strain rate tensor defined as

$$\mathbf{D}_x(\mathbf{v}^{pf}) = \frac{1}{2} \left(\nabla_x \mathbf{v}^{pf} + \nabla_x^t \mathbf{v}^{pf} \right) \quad (\text{B.2})$$

B.0.1.1 Assumptions and useful asymptotic expansions

It is assumed that the heterogeneities, that is, the saturated pores are periodically distributed. Then a periodic cell \mathcal{B}_e of size e is identified and then resized by means of e in the unit cell Z (fig. B.2). A series of saturated porous solid of period e with $e \rightarrow 0$ are considered, then, all the fields depend on this scale parameter and the all notation changes from \mathbf{u}^s to $\mathbf{u}^{s(e)}$, for instance.

Moreover, by means of an heuristic reasoning, it is assumed that the symmetrical part of the strain rate tensor $\mathbf{D}_x^{(e)}$ of the fluid velocity is of order two with respect to the scale

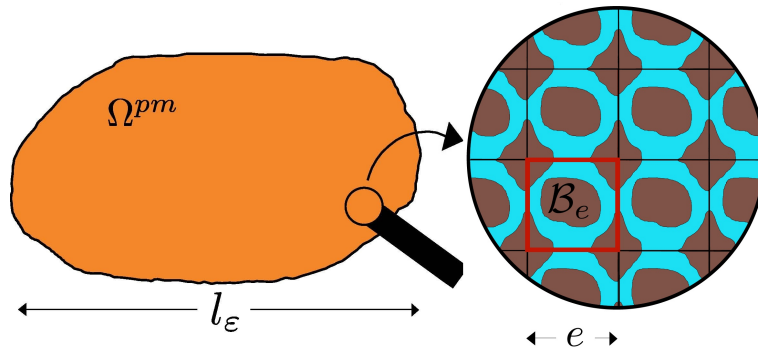


Figure B.2: Periodic distributions of saturated microscopic pores. Periodic cell \mathcal{B}_e of size e .

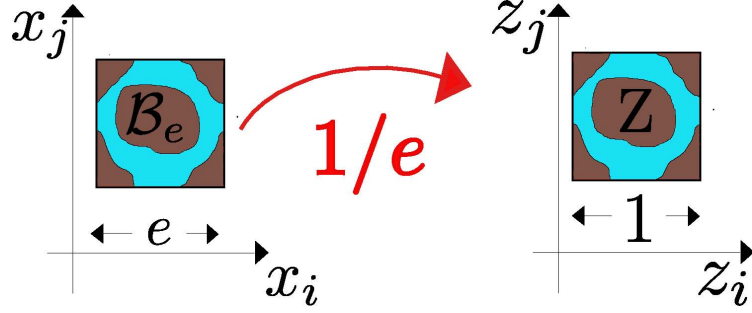


Figure B.3: Microscopic periodic cell \mathcal{B}_e and corresponding resized unit cell Z .

parameter e :

$$\mathbf{D}_x^{(e)} := \mathbf{D}_x(\mathbf{v}^{pf(e)}, e) = e^2 \mathbf{D}_x(\mathbf{v}^{pf(e)}) \quad (\text{B.3})$$

then, the viscosity of the fluid can be neglected at the order zero. The homogenization method based on the double-scale asymptotic expansions is applied to the microscopic description and the main expansions are listed below.

The primary microscopic variables $\mathbf{u}^{s(e)}$ and $p^{f(e)}$ are searched for in the form:

$$\mathbf{u}^{s(e)}(\mathbf{x}) = \mathbf{u}^{s(0)}(\mathbf{x}, \mathbf{x}/e) + e \mathbf{u}^{s(1)}(\mathbf{x}, \mathbf{x}/e) + \dots \quad \text{in } Z^s \quad (\text{B.4a})$$

$$p^{pf(e)}(\mathbf{x}) = p^{pf(0)}(\mathbf{x}, \mathbf{x}/e) + e p^{pf(1)}(\mathbf{x}, \mathbf{x}/e) + \dots \quad \text{in } Z^{pf} \quad (\text{B.4b})$$

where \mathbf{z} is the microscopic or fast space variable. Then, the governing equations of the microscopic problem (B.1) are expanded by using the (B.4) and the most useful expansions are the following:

$$\text{div}_x \boldsymbol{\sigma}^{(0)} + \text{div}_z \boldsymbol{\sigma}^{(1)} = 0 \quad \text{in } Z^{pm} = Z^s \cup Z^{pf} \quad (\text{B.5a})$$

$$\text{div}_z \mathbf{v}^{pf(0)} = 0 \quad \text{in } Z^{pf} \quad (\text{B.5b})$$

$$\text{div}_x \mathbf{v}^{pf(0)} + \text{div}_z \mathbf{v}^{pf(1)} = 0 \quad \text{in } Z^{pf} \quad (\text{B.5c})$$

$$\mathbf{e}_x^{(0)}(\mathbf{u}^s) = \mathbf{e}_x(\mathbf{u}^{s(0)}) + \mathbf{e}_z(\mathbf{u}^{s(1)}) \quad \text{in } Z^s \quad (\text{B.5d})$$

$$\boldsymbol{\sigma}^{s(0)} = \mathbf{a}_@(\mathbf{e}_x(\mathbf{u}^{s(0)}) + \mathbf{e}_z(\mathbf{u}^{s(1)})) \quad \text{in } Z^s \quad (\text{B.5e})$$

$$\mathbf{D}_x^{(1)}(\mathbf{v}^{pf}) = \mathbf{D}_z(\mathbf{v}^{pf(0)}) \quad \text{in } Z^{pf} \quad (\text{B.5f})$$

$$\boldsymbol{\sigma}^{pf(0)} = -p^{pf(0)} \mathbf{I} \quad \text{in } Z^{pf} \quad (\text{B.5g})$$

$$\boldsymbol{\sigma}^{pf(1)} = 2\mu \mathbf{D}_z(\mathbf{v}^{pf(0)}) - p^{pf(1)} \mathbf{I} \quad \text{in } Z^{pf} \quad (\text{B.5h})$$

$$\boldsymbol{\sigma}^{s(0)} @ \mathbf{n} = -p^{pf(0)} \mathbf{n} \quad \text{on } \Gamma^{s-pf} \quad (\text{B.5i})$$

$$\mathbf{v}^{pf(0)} = \dot{\mathbf{u}}^{s(0)} \quad \text{on } \Gamma^{s-pf} \quad (\text{B.5j})$$

$$\mathbf{v}^{pf(1)} = \dot{\mathbf{u}}^{s(1)} \quad \text{on } \Gamma^{s-pf} \quad (\text{B.5k})$$

B.0.2 Mesoscopic description

At the end of this work, the following homogenized equations are obtained:

$$\mathbf{0} = \operatorname{div}_x \boldsymbol{\sigma}^{pm} \quad \text{in } Z^{pm} \quad (\text{B.6a})$$

$$\boldsymbol{\sigma}^{pm} = \mathbf{c} @ \mathbf{e}_x(\mathbf{u}^{pm}) - \mathbf{b} p^{pm} \quad \text{in } Z^{pm} \quad (\text{B.6b})$$

$$-\operatorname{div}_x \mathbf{q}_{Aur}^{pm} = \mathbf{b} : \mathbf{e}_x(\dot{\mathbf{u}}^{pm}) + s \dot{p}^{pm} \quad \text{in } Z^{pm} \quad (\text{B.6c})$$

$$\mathbf{q}_{Aur}^{pm} = -\mathbf{k} @ \nabla_x p^{pm} \quad \text{in } Z^{pm} \quad (\text{B.6d})$$

with

$$\mathbf{q}_{Aur}^{pm} := \mathbf{v}_{Aur}^{pm(\varepsilon)} - \eta_r \dot{\mathbf{u}}^{pm(\varepsilon)} \quad (\text{B.7})$$

where

$$\mathbf{v}_{Aur}^{pm} := \frac{1}{|Z|} \int_{Z^{pf}} \mathbf{v}^{pf(0)} dv \quad (\text{B.8})$$

Remark B.0.1. *On the contrary in this work, the (3.12, 3.11) are used and they read as follows:*

$$\mathbf{q}^{pm} = \eta_r (\mathbf{v}^{pm} - \dot{\mathbf{u}}^{pm}) \quad (\text{B.9})$$

with

$$\mathbf{v}^{pm} := \frac{1}{|Z^{pf}|} \int_{Z^{pf}} \mathbf{v}^{pf(0)} dv \quad (\text{B.10})$$

Appendix C

Useful Taylor developments

In this appendix, the Taylor developments used in the chapter 1 are shown and proved.

C.1 Taylor formula

A real-valued function $f(x)$ of one variable and N times differentiable at a point x can be represented by means of the Taylor formula as the sum of the Taylor polynomial $P_N(x, dx)$ of degree N and of a remainder term $R_N(x, dx)$ (Abramowitz and Stegun 1970):

$$f(x + dx) = P_N(x, dx) + R_N(x, dx) \quad (\text{C.1})$$

with

$$P_N(x, dx) = \sum_{n=0}^N \frac{f^{(n)}(x)}{n!} dx^n = f(x) + f'(x) dx + \frac{f''(x)}{2!} dx^2 + \dots + \frac{f^{(N)}(x)}{N!} dx^N \quad (\text{C.2})$$

and

$$R_N(x, dx) = dx^{N+1} \varepsilon(x, dx) \quad \text{for } dx \rightarrow 0 \quad (\text{C.3})$$

In the following developments proposed in this appendix, it is useful the case of a function $f(x, y)$ of two variables and N times differentiable at a point (x, y) ; in such a case the Taylor formula reads:

$$\begin{aligned} f(x + dx, y + dy) = & f(x, y) + \frac{\partial f}{\partial x} dx + \frac{\partial f}{\partial y} dy + \frac{1}{2} \left(\frac{\partial^2 f}{\partial x^2} (dx)^2 + 2 \frac{\partial^2 f}{\partial x \partial y} dx dy + \frac{\partial^2 f}{\partial y^2} (dy)^2 \right) \\ & + \dots + \frac{1}{N!} \left(\sum_{p=0}^N C_N^p \frac{\partial^p f}{\partial x^p} \frac{\partial^{N-p} f}{\partial y^{N-p}} \frac{\partial^{N-p} f}{\partial y^{N-p}} (dx)^p (dy)^{N-p} \right) + (dx^2 + dy^2)^{(N+1)/2} \varepsilon(x, y, dx, dy) \end{aligned} \quad (\text{C.4})$$

with:

$$\varepsilon(x, y, dx, dy) \rightarrow 0 \quad \text{for } (dx^2 + dy^2)^{1/2} \rightarrow 0 \quad (\text{C.5})$$

A basic but useful Taylor development is the following one:

$$\frac{1}{1-x} = 1 + x + \dots \quad (\text{C.6})$$

C.2

Let $\mathbf{a}_1, \mathbf{a}_2, \mathbf{a}_3$ be three elements of the vector space \mathcal{V} , let $\mathbf{A} \in \mathcal{L}(\mathcal{V})$ be a linear transformation and let $(\mathbf{a}_1, \mathbf{a}_2, \mathbf{a}_3)$ denote the mixed product. Then, the definition of the determinant implies that:

$$\forall \mathbf{a}_1, \mathbf{a}_2, \mathbf{a}_3 \in \mathcal{V}, \quad \det(\mathbb{I} + \delta \mathbf{A})(\mathbf{a}_1, \mathbf{a}_2, \mathbf{a}_3) = \left((\mathbb{I} + \delta A) @ \mathbf{a}_1, (\mathbb{I} + \delta A) @ \mathbf{a}_2, (\mathbb{I} + \delta A) @ \mathbf{a}_3 \right) \quad (\text{C.7})$$

that is:

$$\det(\mathbb{I} + \delta \mathbf{A})(\mathbf{a}_1, \mathbf{a}_2, \mathbf{a}_3) = (\mathbf{a}_1 + \delta \mathbf{A} @ \mathbf{a}_1, \mathbf{a}_2 + \delta \mathbf{A} @ \mathbf{a}_2, \mathbf{a}_3 + \delta \mathbf{A} @ \mathbf{a}_3) \quad (\text{C.8})$$

Given the trilinearity of the mixed product, it follows that:

$$\begin{aligned} \det(\mathbb{I} + \delta \mathbf{A})(\mathbf{a}_1, \mathbf{a}_2, \mathbf{a}_3) &= (\mathbf{a}_1, \mathbf{a}_2, \mathbf{a}_3) \\ &+ \delta \left((\mathbf{A} @ \mathbf{a}_1, \mathbf{a}_2, \mathbf{a}_3), (\mathbf{a}_1, \mathbf{A} @ \mathbf{a}_2, \mathbf{a}_3), (\mathbf{a}_1, \mathbf{a}_2, \mathbf{A} @ \mathbf{a}_3) \right) + \delta^2(\dots) \end{aligned} \quad (\text{C.9})$$

which, for three linear independent vectors $\mathbf{a}_1, \mathbf{a}_2, \mathbf{a}_3$, becomes:

$$\det(\mathbb{I} + \delta \mathbf{A})(\mathbf{a}_1, \mathbf{a}_2, \mathbf{a}_3) = (\mathbf{a}_1, \mathbf{a}_2, \mathbf{a}_3) + \delta \text{tr} \mathbf{A} (\mathbf{a}_1, \mathbf{a}_2, \mathbf{a}_3) + \delta^2(\dots) \quad (\text{C.10})$$

By dividing for a non zero $(\mathbf{a}_1, \mathbf{a}_2, \mathbf{a}_3)$, it finally reads:

$$\det(\mathbb{I} + \delta A) = 1 + \delta \text{tr} A + \dots \quad (\text{C.11})$$

C.3

By using the Taylor formula (C.4), the Jacobian $J(\mathbf{X}, t)$ can be written as a Taylor development for $dt \rightarrow 0$:

$$J(\mathbf{X}, t + dt) = J(\mathbf{X}, t) + \dot{J}(\mathbf{X}, t) dt + \dots \quad (\text{C.12})$$

By definition the Jacobian is defined as the determinant of the gradient \mathbf{F} of the deformation function, then it reads:

$$J(\mathbf{X}, t + dt) = \det[\mathbf{F}(\mathbf{X}, t + dt)] = \det[\mathbf{F} + \dot{\mathbf{F}} dt + \dots] = \det[(\mathbb{I} + \dot{\mathbf{F}} \circ \mathbf{F}^{-1} dt + \dots) \circ \mathbf{F}] \quad (\text{C.13})$$

and, given that the determinant of the product of functions is equal to the product of the determinants, it follows that:

$$J(\mathbf{X}, t + dt) = \det[(\mathbb{I} + \dot{\mathbf{F}} \circ \mathbf{F}^{-1} dt + \dots) \circ \mathbf{F}] = \det \mathbf{F} \det(\mathbb{I} + \dot{\mathbf{F}} \circ \mathbf{F}^{-1} dt + \dots) \quad (\text{C.14})$$

By using the (C.11) and the (C.13), then the (C.14) becomes:

$$J(\mathbf{X}, t + dt) = J [1 + \text{tr}(\dot{\mathbf{F}} \circ \mathbf{F}^{-1}) dt + \dots] \quad (\text{C.15})$$

In the end, by comparison with the (C.12), it is deduced that:

$$\dot{J} = J \text{tr}(\dot{\mathbf{F}} \circ \mathbf{F}^{-1}) \quad (\text{C.16})$$

C.4

Given the hypothesis of small transformation, it can be searched for \mathbf{F}^{-1} in the following form:

$$\mathbf{F}^{-1} = \mathbf{F}^{(0)} + \delta \mathbf{F}^{(1)} + \dots \quad (\text{C.17})$$

The identity tensor \mathbb{I} can be written in a special form:

$$\mathbb{I} = \mathbf{F} \circ \mathbf{F}^{-1} = (\mathbb{I} + \nabla_X \mathbf{u}) \circ (\mathbf{A}^{(0)} + \delta \mathbf{A}^{(1)} + \dots) = \mathbf{A}^{(0)} \circ \mathbb{I} + \mathbf{A}^{(0)} \circ \nabla_X \mathbf{u} + \delta \mathbf{A}^{(1)} \circ \mathbb{I} \quad (\text{C.18})$$

Then, by identifying the terms of the same order and by comparison with the (C.17), it is deduced that:

$$\mathbf{F}^{-1} = \mathbb{I} - \nabla_X \mathbf{u} + \dots \quad (\text{C.19})$$

Appendix D

Reynolds transport theorem

This theorem was presented in Reynolds, Brightmore and H.Moorby (1903) and it can be find also in many books of Continuum Mechanics (e. g. (Gurtin 1981; Truesdell and Toupin 1960)).

It is worth remarking that it was proved for a domain which is moving with time. On the contrary, in this thesis, the domain is not only moving but also evolving with time in reason of the evolution of the mesoscopic fluid-filled cavities. Then, in order to verify the applicability of the theorem to the studied case, an original proof is presented below.

The theorem considers that, during the motion, the volume of the part may change with respect to its volume in the reference configuration; then, it is a generalization of the Transport Theorem which is true only for rigid motions.

THEOREM: let Φ be a smooth spatial field, either scalar valued or vector valued, then for any time t and part Ω

$$\frac{d}{dt} \int_{\Omega_t^{pm}} \Phi dV = \int_{\Omega_t^{pm}} \frac{\partial \Phi}{\partial t} dV + \int_{\partial \Omega_t} \Phi \mathbf{v} \cdot \mathbf{n} da \quad (\text{D.1})$$

where \mathbf{v} is the velocity and \mathbf{n} the outward normal to the boundary of Ω_t , $\partial \Omega_t$.

PROOF:

to be added, case of evolvinig domain!

Remark D.0.1.

$$\int_{\Omega_t} \frac{\partial \Phi}{\partial t} dV = \left[\frac{d}{dt} \int_{\Omega_t} \Phi dV \right]_{\tau=t} \quad (\text{D.2})$$

Then, it is clearly evident that the (D.1) asserts that the rate at which the integral of Φ over Ω_t is changing is equal to the rate computed as if Ω_t was fixed in its current position plus the rate at which Φ is carried out of this region across its boundary.

References

- Abramowitz, M. and I. A. Stegun (1970). *Handbook of Mathematical Functions with Formulas, Graphs, and Mathematical Tables*. Ed. by Dover Publications. New York.
- Auriault, J.-L. (1991). “Heterogeneous medium. Is an equivalent macroscopic description possible?” In: *International Journal of Engineering and Science* 29(7), pp. 785–795.
- (2002). “Upscaling heterogeneous media by asymptotic expansions”. In: *Journal of Engineering Mechanics* 128, pp. 817–822.
- (2004). *Transport in Porous Media: Upscaling by Multiscale Asymptotic Expansions*. Lecture notes. Udine: International Centre for Mechanical Sciences (CISM).
- Auriault, J.-L. and C. Boutin (1992). “Deformable porous media with double porosity. Quasistatics: I Coupling effects”. In: *Transport in Porous Media* 128, pp. 63–82.
- (1993). “Deformable porous media with double porosity. Quasistatics: II Memory effects”. In: *Transport in Porous Media* 10, pp. 153–169.
- Auriault, J.-L. and J. Lewandowska (2001). “Upscaling: Cell Symmetries and Scale Separation.” In: *Transport in Porous Media* 43, pp. 473–485.
- Auriault, J.-L. and E. Sanchez-Palencia (1977). “Etude du comportement macroscopique dun milieu poreux saturé déformable.” In: *Journal de Mécanique* 16(4), pp. 575–603.
- Bacigalupo, A. and L. Gambarotta (2012). “Computational two-scale homogenization of periodic masonry: Characteristic lengths and dispersive waves.” In: *Computer Methods in Applied Mechanics and Engineering* 16-28, pp. 213–216.
- Bakhvalov, N. and G. Panasenko (1989). *Homogenization: averaging processes in periodic media*. Ed. by Kluwer Academic Publishers Group. Dordrecht.
- Bart, M., J. F. Shao and D. Lydzba (2000). “Poroelastic behaviour of saturated brittle rock with anisotropic damage.” In: *International Journal for Numerical and Analytical Methods in Geomechanics* 24, pp. 1139–1154.
- Bazant, Z.P. and J. Planas (1997). *Fracture and Size Effect in Concrete and Other Quasibrittle Materials*. Ed. by CRC Press. Boca Raton, FL.
- Beavers, G. S. and D. D. Joseph (1967). “Boundary conditions at a naturally permeable wall”. In: *Journal of Fluid Mechanics* 30 (1), pp. 197–207.
- Bensoussan, A., J.-L. Lions and G. Papanicolaou (1978). *Asymptotic analysis for periodic structures*. Ed. by North-Holland. Amsterdam.
- Biot, M. A. (1941). “General theory of three-dimensional consolidation”. In: *Journal of Applied Physics* 12, pp. 155–164.
- Böhm, H. J. (2006). *A short introduction to basic aspects of continuum micromechanics*. Lecture notes. Vienna University of Technology.

- Bui, H. D., A. Erlacher and Q. S. Nguyen (1980). "Propagation de fissure en thermoélasticité dynamique." In: *Journal de Mécanique* 19, pp. 697–725.
- Caillerie, D. (1990). "Homogenization of periodic media". In: *Geomaterials*. Ed. by Elsevier Applies Science F. Darve.
- (2011). *Mécanique des milieux continus*. Grenoble INP, pp. 5–10.
- Caillerie, D. (2012). *Homogénéisation des matériaux à structure périodique*. Quiberon.
- Callari, C. (2007). *Appunti del corso di Meccanica dei Mezzi Porosi*. Lecture Notes. Università di Roma Tor Vergata, pp. 125–176.
- Callari, C. and A. Abati (2009). "Finite element methods for unsaturated porous solids and their application to dam engineering problems". In: *Computers and Structures* 87, pp. 485–501. URL: <http://dx.doi.org/10.1016/j.compstruc.2008.12.012>.
- (2011). "Hyperelastic Multiphase Porous Media with Strain-Dependent Retention Laws". In: *Transport in Porous Media* 86, pp. 155–176.
- Callari, C. and F. Armero (2002). "Finite Element Methods for the Analysis of Strong Discontinuities in Coupled Poroplastic Media". In: *Computer Methods in Applied Mechanics and Engineering* 191, pp. 4371–4400. URL: [http://dx.doi.org/10.1016/S0045-7825\(02\)00374-2](http://dx.doi.org/10.1016/S0045-7825(02)00374-2).
- Callari, C., F. Armero and A. Abati (2010). "Strong discontinuities in partially-saturated poroplastic solids". In: *Computer Methods in Applied Mechanics and Engineering* 199, pp. 1513–1535. URL: <http://dx.doi.org/10.1016/j.cma.2010.01.002>.
- Christensen, R. M. and K. H. Lo (1979). "Solutions for effective shear properties in three phase sphere and cylinder models". In: *Journal of Mechanics and Physics of Solids* 27, pp. 315–330.
- Coussy, O. (2004). *Poromechanics*. Ed. by John Wiley and Sons. Chichester.
- Dascalu, C. (2005). "An Introduction to Fracture Mechanics in Linear Elastic Materials". In: *L'objet* 2, pp. 1–15.
- (2009). "A two-scale damage model with material length." In: *Comptes-Rendus Mécanique* 337, pp. 645–652.
- Dascalu, C., G. Bilbie and E. K. Agiasofitou (2008). "Damage and size effects in solids: a homogenization approach". In: *International Journal of Solids and Structures* 45, pp. 409–430.
- Dascalu, C., B. François and O. Keita (2010). "A two-scale model for subcritical damage propagation." In: *International Journal of Solids and Structures* 47, pp. 493–502.
- de Boer, R., R.L. Schiffman and R.E. Gibson (1996). "The origins of the theory of consolidation - the Terzaghi/Fillunger dispute". In: *Géotechnique* 46, pp. 175–186.
- De Giorgi, E. and S. Spagnolo (1973). "Sulla convergenza degli integrali dell'energia per operatori ellittici del secondo ordine". In: *Bollettino dell'Unione Matematica Italiana* 8(4), pp. 391–411.
- Deudé, V., L. Dormieux, D. Kondo and S. Maghous (2002). "Micromechanical approach to nonlinear poroelasticity : application to cracked rocks". In: *Journal of Engineering and Mechanics* 128. Ed. by ASCE Library, pp. 848–855.
- Dormieux, L. and D. Kondo (2005). *Poroelasticity and damage theory for saturated cracked media*. Lecture notes. International Centre for Mechanical Sciences (CISM).

- Dormieux, L., D. Kondo and F.-J. Ulm (2006a). “A micromechanical analysis of damage propagation in fluid-saturated cracked media”. In: *Comptes rendus de Mécanique* 334. Ed. by Elsevier SAS, pp. 440–446.
- (2006b). *Microporomechanics*. Ed. by John Wiley and Sons. Chichester.
- Einstein, A. (1952). “Letter to Carl Seelig”. Einstein Archives.
- Eshelby, J. D. (1957). “The determination of the field of an ellipsoidal inclusion and related problems”. In: *Proceedings of the Royal Society A* 241, pp. 376–396.
- François, B. and C. Dascalu (2010). “A two-scale time-dependent damage model based on non-planar growth of micro-cracks.” In: *Journal of the Mechanics and Physics of Solids* 58(11), pp. 1928–1946.
- Frey, J. (2010). “Modélisation multi-échelle de l’endommagement hydro-mécanique des roches argileuses”. PhD Thesis. Grenoble INP.
- Frey, J., R. Chambon and C. Dascalu (2012). “A two-scale poromechanical model for cohesive rocks.” In: *Acta Geotechnica*, Doi: 10.1007/s11440-012-0173-8, published online.
- Gdoutos, E. E. (2005). *Fracture Mechanics*. Ed. by Springer. Vol. 123. Solid Mechanics and its Applications. Dordrecht.
- Geers, M.G.D., V. Kouznetsova and W.A.M. Brekelmans (2001). “Gradient-enhanced computational homogenization for the micro-macro scale transition”. In: *Journal de Physique IV France* 11, pp. 145–152.
- Giraud, A., Q. V. Huynh, D. Hoxha and D. Kondo (2007). “Effective poroelastic properties of transversely isotropic rock-like composites with arbitrarily oriented ellipsoidal inclusions”. In: *Mechanics of Materials* 39. Ed. by Elsevier, pp. 1006–1024.
- Griffith, A. A. (1921). “The phenomena of rupture and flow in solids”. In: *M. Acad. R. Sci. Series A, Containing Papers of a Mathematical or Physical Character* 221, pp. 163–198.
- Guedes, J. M. and N. Kikuchi (1990). “Pre-processing and postprocessing for materials based on the homogenization method with adaptive finite element methods”. In: *Computer Methods in Applied Mechanics and Engineering* 83, pp. 143–198.
- Guery, A. (2007). “Contributions à la modélisation micromécanique du comportement non linéaire de l’argilite du callovao- oxfordien”. PhD Thesis. Laboratoire de mécanique de Lille.
- Gurtin, M. E. (1979a). “On the energy release rate in quasi-static elastic crack propagation.” In: *Journal of Elasticity* 9(2), pp. 187–195.
- (1979b). “Thermodynamics and the Griffith criterion for brittle fracture.” In: *International Journal of Solids and Structures* 15, pp. 553–560.
- (1981). *An Introduction to Continuum Mechanics*. Ed. by INC. Academic Press. Vol. 158. Mathematics in Science and Engineering. United States of America.
- Hill, R. (1950). *The Mathematical Theory of Plasticity*. Ed. by Oxford University Press. Oxford.
- (1965). “A self-consistent mechanics of composite materials”. In: *Journal of Mechanics and Physics of Solids* 13, pp. 213–222.
- (1967). “The Essential Structure of Constitutive Laws for Metal Composites and Polycrystals”. In: *Journal of Mechanics and Physics of Solids* 15, pp. 79–95.

- Hori, M. and S. Nemat-Nasser (1993). "Double-inclusion model and overall moduli of multi-phase composites". In: *Mechanics of Materials* 5. Ed. by Elsevier, pp. 149–171.
- Inglis, C. E. (1913). "Stresses in a plate due to the presence of cracks and sharp corners". In: *Transactions of the Institute of Naval Architects* 55, pp. 219–241.
- Irwin, G. R. (1957). "Analysis of stresses and strains near the end of a crack traversing a plate". In: *Journal of Applied Mechanics* 24, pp. 361–364.
- Jouhari, M. and A. Ehrlacher (1996). "Fissuration des milieux poreux saturés : intégrale invariante". In: *Comptes-Rendus Mécanique* 323, pp. 9–14.
- (1997). "Thermodynamic analysis of a propagating crack in saturated porous media." In: *European Journal of Mechanics, A/Solids* 16(2), pp. 235–253.
- Karami, M. (1998). "Experimental investigation of poroelastic behaviour of a brittle rock." Doctoral Thesis. University of Lille.
- Keller, J. B. (1977). *Effective behaviour of heterogeneous media*. Ed. by Plenum Press U. Landman. New York, pp. 631–644.
- Koiter, W. T. (1960). "General theorems for elastic-plastic solids". In: *Progress in Solid Mechanics* 1. Ed. by Sneddon I.N. Hill R. eds., pp. 165–221.
- Kostrov, B. V. and L. V. Nikitin (1970). "Some general problems of mechanics of brittle fracture." In: *Archive Mechanics* 22, pp. 749–776.
- Kröner, E. (1986). *Statistical modeling*. Ed. by J. Gittus and Elsevier J. Zarka eds. Vol. 8.229-8.291. Modeling small deformations of polycrystals. London.
- Lemaitre, J. and R. Desmorat (2005). *Engineering Damage Mechanics*. Ed. by Springer. Vol. 123. Berlin.
- Lubliner, J. (1990). *Plasticity Theory*. Ed. by Macmillan Publishing Company.
- Lydzba, D. and J. F. Shao (2000). "Study of poroelasticity material coefficients as response of microstructure". In: *Mechanics of Cohesive-Frictional Materials* 5. Ed. by John Wiley and Sons, pp. 149–171.
- Maier, G. (1970). "A matrix structural theory of piecewise linear elasto-plasticity with interacting yield planes". In: *Meccanica*, pp. 54–66.
- Markenscoff, X. and C. Dascalu (2012). "Asymptotic homogenization analysis for damage amplification due to singular interaction of micro-cracks." In: *Journal of the Mechanics and Physics of Solids* 60(8), pp. 1478–1485.
- Mori, T. and K. Tanaka (1973). "Average stress in the matrix and average elastic energy of materials with misfitting inclusions". In: *Acta Metallurgica* 21, pp. 571–574.
- Nemat-Nasser, S. and M. Hori (1999). *Micromechanics : overall properties of heterogeneous materials*. Ed. by Elsevier. Amsterdam-Lausanne-New York.
- Orowan, E. (1952). "Fundamentals of brittle behavior in metals". In: *Fatigue and Fracture of Metals*. Ed. by John Wiley W.M. Murray, pp. 139–154.
- Pensée, V., L. Dormieux, D. Kondo and V. Deudé (2002). "Poroélasticité d'un milieu mésolfissuré : analyse micromécanique". In: *Comptes rendus de Mécanique* 330. Ed. by Elsevier SAS, pp. 147–152.
- Quintard, M. and S. Whitaker (1987). "Ecoulement monophasique en milieu poreux: Effet des hétérogénéités locales." In: *Journal de Mécanique Théorique et Appliquée* 6(5), pp. 691–726.

- Reynolds, O., A. W. Brightmore and W. H. Moorby (1903). *Papers on mechanical and physical subjects*. Ed. by Cambridge University Press Warehouse. Vol. 3, The sub-mechanics of the Universe. Collected Work. London. URL: <http://archive.org/details/papersonmechanic03reynrich>.
- Royer, P., J.-L. Auriault, J. Lewandowska and C. Serres (2002). "Continuum Modelling of Contaminant Transport in Fractured Porous Media." In: *Transport in Porous Media* 49, pp. 333–359.
- S., Ghosh, K. Lee and S. Moorthy (1995). "Multiple scale analysis of heterogeneous elastic structures using homogenisation theory and Voronoi cell finite element method". In: *International Journal of Solids and Structures* 32(1), pp. 27–62.
- Sacco, E. (2009). "A nonlinear homogenization procedure for periodic masonry." In: *European Journal of Mechanics A/Solids* 28, pp. 209–222.
- Sanchez-Hubert, J. and E. Sanchez-Palencia (1992). *Introduction aux méthodes asymptotiques et à l'homogénéisation*. Ed. by Masson. Vol. Collection Mathématiques Appliquées pour la Maîtrise. Paris.
- (1993). *Exercices sur les méthodes asymptotiques et à l'homogénéisation*. Ed. by Masson. Vol. Collection Mathématiques Appliquées pour la Maîtrise. Paris.
- Sanchez-Palencia, E. (1974). "Comportement local et macroscopique d'un type de milieux physiques hétérogènes." In: *International Journal of Engineering Science* 12, pp. 331–351.
- (1980). *Non-homogeneous media and vibration theory*. Ed. by Springer. Vol. Lecture notes in physics. 127. Berlin.
- (1983). *Homogenization method for the study of composite media*. Asymptotic analysis II – Lecture notes in mathematics 985. Université Paris VI, pp. 192–214.
- Shao, J. F. and D. Lydzba (1999). "Un modèle d'endommagement poroélastique pour milieux poreux saturés". In: *Comptes rendus de l'Académie des Sciences* 327, Série II b. Ed. by Editions scientifiques et médicales Elsevier SAS, pp. 1305–1310.
- Simo, J. C. and T. J. R. Hughes (1998). *Computational Inelasticity*. Ed. by Springer Verlag. New York.
- Souley, M., F. Homand, S. Pepa and D. Hoxha (2001). "Damage-induced permeability changes in granite: a case example at the URL in Canada." In: *International Journal of Rock Mechanics and Mining Sciences* 38, pp. 297–310.
- Suquet, P. (1982). "Plasticité et homogénéisation". Thèse en sciences mathématiques (mécanique théorique). Université Pierre et Marie Curie (Paris).
- Terada, K. and N. Kikuchi (1995). "Nonlinear homogenization method for practical applications". In: *Computational Methods in Micromechanics* AMD-212 / MD-62. Ed. by ASME, pp. 1–16.
- Truesdell, C.A. and R.A. Toupin (1960). *Principles of Classical Mechanics and Field Theory*. Ed. by Springer-Verlag. Vol. 3.1. Encyclopedia of Physics. Berlin, Germany.
- Zaoui, A. (1987). *Approximate statistical modelling and applications. Homogenization techniques for composite media*. Ed. by Springer. Vol. Lecture notes in physics. 272. Berlin, pp. 338–397.

Abstract

This work presents the constitutive modeling of a geomaterial consisting of a deformable and saturated porous matrix including a periodic distribution of evolving fluid-filled cavities. The homogenization method based on two-scale asymptotic developments is used in order to deduce a model able to describe the macroscopic hydro-mechanical coupling. By taking into account the cavity growth and without any phenomenological assumption, it is proposed a mesoscopic energy analysis coupled with the homogenization scheme which provides a damage evolution law. In this way, a direct link between the meso-structural fracture phenomena and the corresponding macroscopic damage is established. Lastly, a numerical study of the local macroscopic hydro-mechanical damage behaviour is presented.

Keywords: homogenization; meso-fracture; damage; porous media; hydro-mechanical coupling.

Resumé

Le présent travail montre la modélisation constitutive d'un géomatériau composé d'une matrice poreuse saturée et déformable contenant une distribution périodique de fissures évolutives remplies de fluide. La méthode d'homogénéisation des développements asymptotiques est utilisée afin de déduire un modèle capable de décrire le couplage hydro-mécanique macroscopique. Prenant en considération l'évolution de fissures et sans faire des hypothèses phénoménologiques, une analyse énergétique mésoscopique couplée avec un schéma d'homogénéisation a été développée et elle fournit une loi d'évolution d'endommagement macroscopique. De cette façon, un lien direct entre les phénomènes de rupture de la structure mésoscopique et l'endommagement macroscopique correspondant est établie. Finalement, on présente une étude numérique du comportement macroscopique d'endommagement hydro-mécanique.

Mots clés: homogénéisation; méso-fissuration; endommagement; milieux poreux; couplage hydro-mécanique.

Sommario

In questa tesi si presenta la modellazione costitutiva di un geomateriale composto da una matrice porosa satura e deformabile contenente una distribuzione periodica di cavità riempite da fluido che si propagano. Il metodo di omogeneizzazione basato sugli sviluppi asintotici a doppia scala viene utilizzato con l'obiettivo di dedurre un modello capace di descrivere l'accoppiamento idro-meccanico macroscopico. Prendendo in considerazione la propagazione delle cavità e senza nessuna ipotesi fenomenologica, si propone un'analisi energetica mesoscopica accoppiata ad uno schema di omogeneizzazione che fornisce una legge di evoluzione del danno. In questo modo, una relazione diretta tra i fenomeni di frattura meso-strutturali ed il corrispondente danno macroscopico viene stabilita. Infine, uno studio numerico del comportamento macroscopico locale di danno idro-meccanico viene presentato.

Parole chiave: omogeneizzazione; meso-frattura; danno; mezzi porosi; accoppiamento idromeccanico.